

2015

# Functional MRI investigations of path integration and goal-directed navigation in humans

---

<https://hdl.handle.net/2144/15179>

*Boston University*

BOSTON UNIVERSITY  
GRADUATE SCHOOL OF ARTS AND SCIENCES

Dissertation

**FUNCTIONAL MRI INVESTIGATIONS OF  
PATH INTEGRATION AND  
GOAL-DIRECTED NAVIGATION IN HUMANS**

by

**KATHERINE R.M. SHERRILL**

B.A., Texas A&M University, 2005

M.A., Boston University, 2009

Submitted in partial fulfillment of the  
requirements for the degree of  
Doctor of Philosophy

2015

© 2015 by  
KATHERINE R.M. SHERRILL  
All rights reserved

Approved by

First Reader

---

Chantal Stern, D. Phil.  
Professor of Psychological and Brain Sciences

Second Reader

---

Michael Hasselmo, D.Phil.  
Professor of Psychological and Brain Sciences

Third Reader

---

Marc Howard, Ph.D.  
Associate Professor of Psychological and Brain Sciences

## **ACKNOWLEDGMENTS**

Many people have been supportive and influential to the development and completion of my doctoral dissertation. I am incredibly appreciative of my advisor Dr. Chantal Stern for her valuable encouragement, support, and guidance over my years in the Cognitive Neuroimaging Laboratory. She has given generously of her time and vast knowledge, and her input has molded my ability to think as a scientist. I would also like to thank Drs. Michael Hasselmo, Marc Howard, Sam Ling, and David Somers for their guidance in the development of this thesis and for being members of my dissertation committee. I would like to thank Dr. Robert Ross for his passion as a teacher and encouragement from the very beginning of graduate school, and Dr. Liz Chrastil for her valuable advice and enthusiasm for studying human navigation. I would like to thank Dr. Thackery Brown, Dr. Randall Newmark, Justine Cohen, Deepti Putcha, Dr. Yakeel Quiroz, Dr. Kishan Gupta, Dr. U. Murat Erdem, Andrew Whiteman, Rachel Nauer, and Allen Chang for their friendship, support, and collaboration over the years.

On a personal note, I would like to thank my parents Tom and Susan for their unfaltering love, encouragement, and support over the many decades I have been a student, especially through graduate school. Finally, I want to thank Colin Kelly Sherrill, my husband, who has been a source of love and motivation over the years. Without the support of my family, this dissertation would not have been possible.

**FUNCTIONAL MRI INVESTIGATIONS OF  
PATH INTEGRATION AND  
GOAL-DIRECTED NAVIGATION IN HUMANS**

(Order No.            )

**KATHERINE R.M. SHERRILL**

Boston University Graduate School of Arts and Sciences, 2015

Major Professor: Chantal Stern, Professor of Psychological and Brain Sciences

**ABSTRACT**

Path integration is a navigational process that humans and animals use to track changes in their position and orientation. Animal and computational studies suggest that a spatially-tuned navigation system supports path integration, yet this system is not well understood in humans. Here, the prediction was tested that path integration mechanisms and goal-directed navigation in humans would recruit the same key brain regions within the parietal cortex and medial temporal lobes as predicted by animal and computational models. The three experiments described in this dissertation used behavioral and functional magnetic resonance imaging methods in 131 adults (18-35 years) to examine behavioral and brain correlates of navigation.

In a landmark-free environment, path integration mechanisms are utilized to update position and orientation to a goal. Experiment 1 examined neural correlates of these mechanisms in the human brain. The results demonstrated that successful first and third person perspective navigation recruited the anterior hippocampus. The posterior hippocampus was found to track distance and temporal proximity to a goal location. The retrosplenial and posterior parietal

cortices were additionally recruited for successful goal-directed navigation.

In a landmark-rich environment, humans utilize route-based strategies to triangulate between their position, landmarks, and navigational goal. Experiment 2 contrasted path integration and landmark-based strategies by adding a solitary landmark to a sparse environment. The results demonstrated that successful navigation with and without an orienting landmark recruited the anterior hippocampus. Activity in the bilateral posterior hippocampus was modulated by larger triangulation between current position, landmark, and goal location during first person perspective navigation. The caudate nucleus was additionally recruited for landmark-based navigation.

Experiment 3 used functional connectivity methods coupled with two fMRI tasks to determine whether areas responsive to optic flow, specifically V3A, V6, and the human motion complex (hMT+), are functionally connected to brain regions recruited during first person perspective navigation. The results demonstrated a functional relationship between optic flow areas and navigationally responsive regions, including the hippocampus, retrosplenial, posterior parietal, and medial prefrontal cortices.

These studies demonstrate that goal-directed navigation is reliant upon a navigational system supported by hippocampal position computations and orientation calculations from the retrosplenial and posterior parietal cortices.

## TABLE OF CONTENTS

<b>CHAPTER 1: Introduction .....</b>	<b>1</b>
1.1 How is navigational space represented in the human brain? .....	2
1.2 What is path integration and how is it used in navigation?.....	3
1.3 How is distance to goals coded during navigation? .....	4
1.4 How does the brain calculate heading and orientation in an environment?...	5
1.5 How are landmarks used during goal-directed navigation?.....	7
1.6 How are optic flow signals used for spatial navigation? .....	9
1.7 Experiments in the dissertation.....	10
<b>CHAPTER 2: Hippocampus and retrosplenial cortex combine path integration signals for successful navigation .....</b>	<b>14</b>
2.1 Introduction .....	15
2.2 Materials and Methods .....	17
2.2.1 Participants .....	17
2.2.2 Virtual environment .....	18
2.2.3 Pre-scan training .....	20
2.2.4 Image acquisition .....	22
2.2.5 fMRI preprocessing .....	23
2.2.6 Data analysis.....	24
2.3 Results .....	29
2.3.1 Behavioral data .....	29
2.3.2 fMRI data.....	30
2.4 Discussion .....	34
2.4.1 Successful navigation recruits the anterior hippocampus .....	35
2.4.2 The posterior hippocampus tracks linear distance to the goal location.....	35
2.4.3 Navigation requiring path integration mechanisms update perceived location and orientation towards a goal location.....	38
2.4.4 Encoding of large-scale environment required for goal-directed navigation ..	40
2.5 Chapter 2 Figures.....	42
2.6 Chapter 2 Tables .....	49
<b>CHAPTER 3: Neural correlates highlight interactions between path integration and landmark-based strategies during goal-directed navigation .....</b>	<b>53</b>
3.1 Introduction .....	54
3.2 Materials and Methods .....	56
3.2.1 Participants .....	56
3.2.2 Virtual environment .....	57
3.2.3 Experimental training .....	59
3.2.4 Image acquisition .....	61
3.2.5 fMRI preprocessing .....	62
3.2.6 Data analysis.....	63
3.3 Results .....	68



3.3.1 Behavioral data .....	68
3.3.2 fMRI data.....	69
<b>3.4 Discussion .....</b>	<b>72</b>
3.4.1 The role of the hippocampus and caudate nucleus during successful goal-directed navigation .....	74
3.4.2 The hippocampus tracks Euclidean distance to a goal location.....	75
3.4.3 The posterior hippocampus triangulates between a goal location and landmark distance .....	76
3.4.4 Comparisons of FPP navigation requiring path integration mechanisms and landmark-based navigational strategies.....	78
<b>3.5 Chapter 3 Figures.....</b>	<b>80</b>
<b>3.6 Chapter 3 Tables .....</b>	<b>88</b>

**CHAPTER 4: Functional connections between optic flow areas and navigationally responsive brain regions during goal-directed navigation .. 93**

<b>4.1 Introduction .....</b>	<b>94</b>
<b>4.2 Materials and Methods .....</b>	<b>96</b>
4.2.1 Participants .....	96
4.2.2 Virtual navigation task environment .....	97
4.2.3 Training procedures .....	98
4.2.4 Experimental tasks.....	99
4.2.5 Image acquisition .....	101
4.2.6 fMRI pre-processing.....	102
4.2.7 Data analysis.....	103
<b>4.3 Results .....</b>	<b>110</b>
4.3.1 Behavioral data .....	110
4.3.2 fMRI connectivity data .....	111
<b>4.4 Discussion .....</b>	<b>115</b>
4.4.1 The role of optic flow responsive areas in processing egocentric movement .....	115
4.4.2 Optic flow processing regions are functionally connected with brain regions supporting first person perspective navigation.....	116
4.4.3 Functional connections with optic flow regions and motor cortex regions during Survey perspective navigation .....	120
<b>4.5 Chapter 4 Figures.....</b>	<b>122</b>
<b>4.6 Chapter 4 Tables .....</b>	<b>129</b>

**CHAPTER 5: Summary and Discussion .....** **132**

<b>5.1 Summary of results.....</b>	<b>133</b>
5.1.1 Restatement of original goals.....	133
5.1.2 Summary of results from Experiment 1 .....	134
5.1.3 Summary of results from Experiment 2.....	135
5.1.4 Summary of results from Experiment 3.....	137
<b>5.2 Discussion .....</b>	<b>138</b>
5.2.1 Path integration signals for successful goal-directed navigation.....	138
5.2.2 The hippocampus tracks distance and time during navigation .....	140

5.2.3 Orientation towards a goal location is supported by the parietal cortex.....	142
5.2.4 Optic flow processing regions are functionally connected with brain regions supporting navigation .....	143
<b>5.3 Conclusions.....</b>	<b>144</b>
 <b>BIBLIOGRAPHY .....</b>	 <b>146</b>
 <b>CURRICULUM VITAE.....</b>	 <b>157</b>

## LIST OF TABLES

<b>Table 2.1</b>	Brain regions significantly activated for first person perspective (FPP) and third person perspective (TPP) navigation phases in which participants successfully navigated to the goal location	49
<b>Table 2.2</b>	Brain regions exhibiting significant activity modulated with the participants' distance to the goal location at time points sampled throughout the FPP navigation phase	50
<b>Table 2.3</b>	Brain regions exhibiting significant activity from paired t-tests during the navigation phase	51
<b>Table 2.4</b>	Brain regions exhibiting significant activity from paired t-tests during the map presentation phase	52
<b>Table 3.1</b>	Brain regions significantly activated for FPP and Survey navigation phases in which participants successfully navigated to the goal location with or without presence of a landmark	88
<b>Table 3.2</b>	Brain regions exhibiting significant activity modulated with the participants' distance to the goal location at time points sampled throughout the FPP navigation phase with or without the presence of an orienting landmark	89
<b>Table 3.3</b>	Brain regions exhibiting significant activity modulated with the participants' navigational precision relative to landmark distance from the goal location during FPP navigation	91
<b>Table 3.4</b>	Brain regions exhibiting significant activity when contrasting the Landmark and No Landmark conditions during the FPP navigation phase	92
<b>Table 4.1</b>	Brain regions functionally connected with left and right V3A seed regions during navigation from the FPP and Survey perspective	129
<b>Table 4.2</b>	Brain regions functionally connected with left and	130

right V6 seed regions during navigation from the  
FPP and Survey perspective

<b>Table 4.3</b>	Brain regions functionally connected with right human motion complex seed region during navigation from the FPP and Survey perspective	131
------------------	--	-----

## LIST OF FIGURES

<b>Figure 2.1</b>	Task paradigm	42
<b>Figure 2.2</b>	Scanning day behavioral performance	43
<b>Figure 2.3</b>	Successful first person perspective (FPP) and third person perspective (TPP) navigation recruits the anterior hippocampus	44
<b>Figure 2.4</b>	Parametric modulation of linear distance to the goal location	45
<b>Figure 2.5</b>	Activations for navigation trial phase	46
<b>Figure 2.6</b>	Activations for map presentation trial phase	47
<b>Figure 3.1</b>	Task paradigm	80
<b>Figure 3.2</b>	Scanning day behavioral performance	82
<b>Figure 3.3</b>	Successful FPP and Survey perspective navigation with the absence and presence of an orienting landmark recruits the hippocampus	83
<b>Figure 3.4</b>	Parametric modulation of linear distance to the goal location	84
<b>Figure 3.5</b>	Navigational precision relative to landmark distance from the goal location recruits the posterior hippocampus	85
<b>Figure 3.6</b>	Activations for successful FPP navigation trial phases	87
<b>Figure 4.1</b>	Adapted computational model	122
<b>Figure 4.2</b>	Navigation task paradigm	123
<b>Figure 4.3</b>	Optic flow stimuli depiction	124

<b>Figure 4.4</b>	Connectivity seed regions	125
<b>Figure 4.5</b>	First person perspective (FPP) navigation: Optic flow processing regions are functionally connected with brain regions supporting FPP navigation	126
<b>Figure 4.6</b>	Survey perspective navigation: Optic flow processing regions are functionally connected with the primary motor cortex during Survey perspective navigation	128

## LIST OF ABBREVIATIONS

<b>BOLD</b>	Blood oxygen level-dependent
<b>DARTEL</b>	Diffeomorphic Anatomical Registration using Exponential Lie algebra
<b>EPI</b>	Echo planar imaging
<b>FDR</b>	False discovery rate
<b>fMRI</b>	Functional magnetic resonance imaging
<b>FPP</b>	First person perspective
<b>GLM</b>	General linear model
<b>GRAPPA</b>	Generalized autocalibrating partially parallel acquisitions
<b>Hipp</b>	Hippocampus
<b>ITI</b>	Intertrial interval
<b>MNI</b>	Montreal Neurological Institute
<b>mPFC</b>	Medial prefrontal cortex
<b>MP-RAGE</b>	Multiplanar rapidly acquired gradient echo
<b>PHC</b>	Parahippocampal cortex
<b>PPC</b>	Posterior parietal cortex
<b>ROI</b>	Region of interest
<b>RSC</b>	Retrosplenial cortex
<b>RT</b>	Reaction timeSD Standard deviation
<b>SEM</b>	Standard error of the mean
<b>SPM</b>	Statistical parametric map
<b>Survey</b>	Survey perspective
<b>TE</b>	Echo time

<b>TPP</b>	Third person perspective
<b>TR</b>	Repetition time
<b>WFU</b>	Wake Forest University



## **CHAPTER 1: Introduction**

Goal-directed navigation is a fundamental process used in our everyday lives. A large portion of human navigation encompasses navigating to and from locations, or goals, in our environment. How the brain supports navigation, specifically to intended goal locations, has been a major focus of psychological and neuroscientific research. Memory for specific locations in an environment and navigation based on these encoded spatial representations are thought to rely on brain structures within the medial temporal lobe and parietal cortex, focusing on the hippocampus, retrosplenial cortex, and posterior parietal cortex.

### **1.1 How is navigational space represented in the human brain?**

Human spatial navigation studies often target navigation from the first person perspective in familiar, landmark-rich environments (Hartley et al., 2003; Wolbers et al., 2005; Ekstrom and Bookheimer, 2007; Brown et al., 2010; Zhang and Ekstrom, 2013, Brown et al., 2013). The focus of this dissertation was to examine mechanisms for accurate navigation in sparse environments, which requires the integration of encoded spatial representations and self-motion cues. By studying brain regions that support these navigational mechanisms in environments that provide little or no landmark cues, we can better understand how humans orient themselves during navigation towards a goal location.

Current understanding of human navigation has been built by connecting varying levels of neuroscientific investigation, from membrane potentials to individual neurons, from neuronal networks to complex behavior. Cells in the

rodent hippocampal formation have been found to represent location and orientation during navigation. These cells increase their firing rates during movement in specific locations in their environment (“place cells”; O’Keefe and Dostrovsky, 1971), code arrays of locations via a triangular coordinate system (“grid cells”; Hafting et al., 2005), code timing of events in space (“time cells”; MacDonald et al., 2011), and are tuned to specific heading directions (“head direction cells”; Taube et al., 1990). Studies of human navigation have started to establish that these same spatially tuned regions are present in the human and are activated when coding location (Ekstrom et al., 2003), arrays of locations (Doeller et al., 2010; Jacobs et al., 2013), and perceived heading direction (Baumann and Mattingley, 2010). Therefore, a spatial system may support goal-directed navigation in humans; however, it is not established how these neural mechanisms interact to reach our navigational goals.

## **1.2 What is path integration and how is it used in navigation?**

Navigating in a sparse environment requires self-localization to reach an intended goal when environmental cues are not available. Path integration is a navigational strategy in which self-motion cues are used to track adjustments in location and orientation (Gallistel, 1990; Diekmann et al., 2009; Chrastil, 2013). A human neuroimaging study suggests that path integration may be supported by the hippocampus (Wolbers et al., 2007). In rodents, place cells in the hippocampus provide spatial tuning through structured responses that code

current position in an environment (O'Keefe and Dostrovsky, 1971; Ekstrom et al., 2003). The increased firing of these cells as an animal traverses specific regions builds a spatial representation of the environment. Persistent spiking of head direction cells, which represent the direction and speed of a trajectory, are thought to update grid cell responses, and, thus, update hippocampal place cell activity giving more accurate knowledge of location in the environment (Burgess et al., 2007; Hasselmo, 2008; Hasselmo, 2009). Animal models indicate a convergence of self-motion and external cues in the hippocampus is essential for path integration and spatial memory processes (Leutgeb et al., 2000). These studies suggest the hippocampus has a sustained role supporting successful navigation in the absence of landmarks, where there is an increasing reliance on self-motion cues. Research in rodents has also demonstrated that hippocampal place cells can track current location relative to a goal location (Johnson and Redish, 2007; Pfeiffer and Foster, 2013). Therefore, accurate navigation to a goal location may recruit the hippocampus to update spatial representations along a planned route.

### **1.3 How is distance to goals coded during navigation?**

Spatially tuned neurons of the hippocampus may track proximity to goal locations through navigational episodes (Johnson and Redish, 2007; Dupret et al., 2010; Viard et al., 2011). The spatial tuning of the hippocampus through integration of current location and goal proximity provides essential mapping mechanisms

required for path integration. The presence of place-goal conjunctive cells in the human hippocampus, which increased their firing rate when a specific goal was viewed from a specific location, may be indicative of a hippocampal role in associating goal-related contextual inputs with place (Ekstrom et al., 2003). Yet, little is known about whether the hippocampus supports a mechanism for actively tracking progress to goal locations. A recent computational model suggests that a reward signal propagates through a place cell map of the environment originating from goal locations (Erdem and Hasselmo, 2012; Erdem et al., 2014). Place cells in the hippocampus then activate based on the highest associated reward signal to guide behavior towards the goal location. The hippocampus may be responsive to the shortest linear distance between participants' current location and the goal location from moment-to-moment as they navigate through the environment. This online guidance system in the hippocampus may provide accurate signals of proximity to goals as navigators are moving within the environment.

#### **1.4 How does the brain calculate heading and orientation in an environment?**

Positional and directional spatial information are essential components of self-motion to accurately know one's location in an environment. In rodents, specialized cells, termed "head direction cells", fire as a function of the animal's current heading, independent of location, and are modulated by self-motion cues

(Taube, 2007). These cells complement other neurons that underlie navigational behavior, in particular place cells and grid cells, which are spatially tuned to represent locations and distances (O'Keefe, 1976; Hafting et al., 2005). Positional and directional information may be integrated within the rodent navigational network by neurons with conjunctive place and directional properties (Sargolini et al., 2006; McNaughton et al., 2006). In humans, several cortical regions in addition to the medial temporal lobe guide navigation through the integration of spatial representations and self-motion cues to update goal-directed behavior (Aguirre and D'Esposito, 1999; Epstein, 2008; Save and Poucet, 2009; Vann et al., 2009; Whitlock et al., 2012). Studies in primates (Sato et al., 2006) and humans (Rosenbaum et al., 2004; Spiers and Maguire, 2006; Epstein et al., 2007; Ekstrom and Bookheimer, 2007; Rodriguez, 2010) suggest the retrosplenial and posterior parietal cortices support the transformation of world coordinate-based spatial information into self-motion cues to guide movements from a ground-level perspective. Animal models demonstrate that the posterior parietal cortex supports representations of space for movements within an egocentric coordinate frame (Snyder et al., 1997, 2000; Sato et al., 2006; Save and Poucet, 2009; Whitlock et al., 2012). In humans, previous studies suggest the retrosplenial cortex integrates route-based spatial information with self-motion cues (Wolbers and Buchel, 2005) and computes perceived heading (Baumann and Mattingley, 2010; Chrastil et al., under review). These studies suggest that the retrosplenial cortex, posterior parietal cortex, and

hippocampus support path integration by providing signals to self-localize in an environment. The retrosplenial and posterior parietal cortices support orientation towards the goal location, and these orientation signals are integrated with distance and direction calculations to the goal as represented by the hippocampus.

### **1.5 How are landmarks used during goal-directed navigation?**

Landmarks are useful during navigation because they are fixed in space; therefore, humans and animals may use landmarks during wayfinding to determine their position and orientation in their environment. An experiment in this dissertation examined navigational strategies used if a single landmark was present in an environment to orient navigation towards a goal. During path integration, self-motion cues are used to determine displacement relative from a starting position (Gallistel, 1990; Byrne et al., 2007; Wolbers et al., 2007).

Navigation using a landmark may require additional brain regions to support different types of navigational strategies from path integration due to the fixed landmark cue. Path integration tracks position and orientation in the environment and landmark-based navigation strategies update these quantities based on visual cues in the environment (Epstein and Vass, 2013). In rodents, place cells in the hippocampus have been found to encode the bearing and distance of environmental landmarks (McNaughton et al., 1995). These findings have been supported by studies indicating that place cells can be controlled by the location

of visual cues (Gothard et al., 1996; Knierim, 2002; Knierim and Rao, 2003), and that a type of place cell called “landmark-vector” cells encode spatial locations as a vector relationship to local landmarks (Deshmukh and Knierim, 2013).

Representations of orientation to a goal location could be updated based on calculations of current location relative to a visible landmark. Research in this dissertation examines the role of the hippocampus in coding proximity to the goal location relative to landmark distance to the goal location during ground-level navigation.

Landmark-based navigation utilizing path integration mechanisms may be supported by parallel systems in the hippocampus and striatum. The caudate nucleus of the striatum supports behavioral flexibility in humans (Monchi et al., 2006; Jankowski et al., 2009; Ross et al., 2009) and works in conjunction with the hippocampus for decision-making during route-based navigation (Johnson et al., 2007; Brown et al., 2012; Brown & Stern, 2013). Landmarks can also be used as part of an egocentric, or body-centered, navigational strategy along an encoded route (Iaria et al., 2003; Doeller et al., 2008). The caudate nucleus is associated with navigation relying on egocentric strategies to orient position in an environment relative to landmark cues (Iaria et al., 2003; Hartley et al., 2003; Igoli et al., 2010; Etchamendy and Bohbot, 2007). Taken together, the caudate nucleus may be recruited to update egocentric positioning relative to an orienting landmark during navigation to a goal location as represented by the hippocampus.



## **1.6 How are optic flow signals used for spatial navigation?**

Path integration relies heavily on the accurate perception of optic flow, the pattern of relative motion between the observer and environment (Gallistel, 1990). Self-motion cues from optic flow may be used to track changes in position and orientation within one's environment (Mittelstaedt and Mittelstaedt, 1980). Computational models suggest that visual input from optic flow provides information about egocentric motion and influences firing patterns in cells that are critical for rodent navigation (Raudies et al., 2012; Raudies & Hasselmo, 2012). Human functional magnetic resonance imaging (fMRI) studies have identified cortical regions that are responsive to optic flow motion processing, specifically visual cortical areas V3A and V6 and hMT+. Area V3A, located inferior to the parieto-occipital sulcus, is highly selective for processing visual motion (Tootell et al., 1997; Seiffert et al., 2003; Pitzalis et al., 2010). Area V6, located in the dorsal parieto-occipital sulcus, has been described as selectively responding to expanding egocentric flow field visual motion information in humans, which simulates forward motion (Pitzalis et al., 2006; Cardin and Smith, 2010; Pitzalis et al., 2010). Macaque studies have established that the medial superior temporal (MST) area accounts for heading information derived from optic flow, suggesting a role in self-motion processing based on visual cues (Logan and Duffy, 2006; Bremmer et al., 2010). The human motion complex (hMT+), a homolog of macaque area MST (Dukelow et al., 2001; Huk et al., 2002), is located in the posterior region of the middle temporal gyrus and is activated

making estimations of heading (Peuskens et al., 2001) and has been characterized as extracting coherent motion cues selective for self-motion (Rust et al., 2006; Cardin and Smith, 2010; Pitzalis et al., 2010; Cardin and Smith, 2011). Perception of egocentric flow motion is a critical aspect of visuospatial cognition, as humans rely on processing of visual input continuously as they navigate through their environment. Research in this dissertation examines a functional link between brain regions known to process optic flow, specifically visual cortical areas V3A, V6, and hMT+, and navigational brain regions in humans. Establishing functional connections between path integration and regions known for visual motion processing could further our understanding of how neural systems interact during goal-directed navigation.

### **1.7 Experiments in the dissertation**

The experiments described in Chapters 2-4 used current functional magnetic resonance imaging (fMRI) techniques to study brain activity in healthy, young adults. Participants were trained outside the scanner to navigate in sparse virtual environments. The virtual navigation environments used in these experiments were based on the open field environments used in rodent studies of path integration (O'Keefe, 1976; Morris, 1981; McNaughton et al., 1983; Steele and Morris, 1999; O'Keefe and Burgess, 2005). The studies were designed to test predictions based on these animal studies and computational model simulations of medial temporal lobe function (Hasselmo, 2009; Raudies et al., 2012; Erdem

and Hasselmo, 2012; Erdem et al., 2014; Howard et al., 2014; Hasselmo and Stern, 2014), which provide the conceptual framework of this thesis. The experiments described in this dissertation provide a characterization of the brain regions involved in the encoding and retrieval of spatial representations in humans and extend our knowledge about the neural basis of path integration and spatial memory in rodents to the human brain.

Experiment 1, described in Chapter 2, examines brain regions that support the integration of encoded spatial representations with path integration mechanisms for successful goal-directed navigation in humans. Furthermore, Experiment 1 examines whether regions of the human brain are important for tracking distance to the goal location during ground-level navigation relying on the integration of survey representations and self-motion cues. To address these questions, the first experiment used a task in which participants viewed a map of a landmark-deprived environment indicating the start and goal locations then utilized these survey-level spatial representations to actively navigate the environment. Navigation occurred from first person, third person or survey perspectives. Results demonstrate significantly greater activity in the retrosplenial cortex and posterior parietal cortex for successful navigation in both the first person perspective (FPP) and third person perspective (TPP). The hippocampus was recruited during successful FPP navigation utilizing self-motion cues and orientation towards a goal location. Experiment 1 also provides a novel demonstration that the posterior hippocampus activation is correlated

with coding proximity to a goal location during active navigation.

If a single landmark was present in an environment in which path integration mechanisms are necessary to navigate, humans may utilize the landmark in a more egocentric positioning strategy to triangulate their position and guide navigation to a goal (Hartley et al., 2003; Baumann et al., 2010; Epstein and Vass, 2013). Experiment 2, described in Chapter 3, examines brain regions that support goal-directed navigation in an open field environment with either the presence or absence of an orienting landmark. Participants viewed a map of the environment indicating their start and goal locations then utilized these survey-level spatial representations to actively navigate the environment. Navigation occurred from the first person or survey perspectives, and on half the trials, a landmark was present as an orientating cue in the environment. Results demonstrate that the hippocampus and caudate are more strongly recruited for successful FPP and Survey navigation trials with a landmark present than trials when participants were unsuccessful in utilizing an orienting landmark during navigation. The hippocampus was recruited for first person perspective navigation when monitoring self-motion would be integral to navigation success since a landmark was not present in the environment to help with self-localization. Furthermore, the hippocampus was important for tracking distance to the goal location during first person perspective navigation both with and without an orienting landmark in the environment. Critically, larger location computations when triangulating position between a landmark and encoded goal

increased hippocampal activation.

Visual information about one's own movement in relation to the environment, or egocentric motion, is essential to tracking changes in orientation and location during FPP navigation. Experiment 3, described in Chapter 4, examines the functional network supporting the integration of processing visual self-motion cues with brain regions recruited for successful goal-directed navigation. Chapter 4 localized brain regions sensitive to optic flow and examined whether these regions are functionally connected with brain regions recruited during navigation. Visual cortical areas V3A, V6 and hMT+ were responsive to coherent and egocentric flow field visual motion processing during our optic flow task. Functional connections were then analyzed between optic flow seed regions (V3A, V6 and hMT+) and functional activity collected during first person perspective navigation. The navigation task corresponds to the tasks described in Experiment 1 (Chapter 2). Results demonstrate that regions responsive to processing optic flow (V3A, V6 and hMT+) are functionally connected with the retrosplenial cortex, posterior parietal cortex, hippocampus, and medial prefrontal cortex for active FPP navigation. Data presented in Chapter 4 establish functional connections between regions sensitive to optic flow, specifically visual cortical areas V3A, V6 and hMT+, and areas that are active during navigation.

**CHAPTER 2: Hippocampus and retrosplenial cortex combine path  
integration signals for successful navigation**

## 2.1 Introduction<sup>1</sup>

Path integration uses self-motion cues to track adjustments in orientation and location (Wolbers et al., 2007). Research in rodents has demonstrated that hippocampal place cells can track current location related to a goal location (Johnson and Redish, 2007; Pfeiffer and Foster, 2013). In humans, several cortical regions in addition to the hippocampus guide navigation through the integration of spatial representations and self-motion cues to update goal-directed behavior (Aguirre and D'Esposito, 1999; Epstein, 2008; Save and Poucet, 2009; Vann et al., 2009; Whitlock et al., 2012). Studies in primates (Sato et al., 2006) and humans (Rosenbaum et al., 2004; Spiers and Maguire, 2006; Epstein et al., 2007; Ekstrom and Bookheimer, 2007; Rodriguez, 2010) suggest the retrosplenial and posterior parietal cortices support the transformation of world coordinate-based spatial information into self-motion cues to guide movements from a ground-level perspective. Specifically, it has been suggested that the retrosplenial cortex integrates route-based spatial information with self-motion cues (Wolbers and Buchel, 2005) and computes perceived heading (Baumann and Mattingley, 2010). These studies suggest that regions within the retrosplenial and posterior parietal cortices integrate current orientation with distance and direction towards the goal location as represented by the hippocampus.

---

<sup>1</sup> This work has been previously published as Sherrill KR, Erdem UM, Ross RS, Brown TI, Hasselmo ME, Stern CE (2013). Hippocampus and retrosplenial cortex combine path integration signals for successful navigation. *The Journal of Neuroscience*, 33:19304-19313. Reprinted here with permission.

Human spatial memory studies often target navigation from the first person perspective in familiar, landmark-rich environments (Hartley et al., 2003; Wolbers et al., 2005; Ekstrom and Bookheimer, 2007; Brown et al., 2010; Zhang and Ekstrom, 2013, Brown et al., 2013). The focus of this study was to examine path integration mechanisms for accurate navigation through the integration of orientation and self-motion cues in the absence of landmark cues. When landmark information is not available, path integration can be used to build a metric representation of position. Place cells in the hippocampus provide spatial tuning through structured responses that code current position in an environment (O'Keefe and Dostrovsky, 1971; Ekstrom et al., 2003). Spatially tuned neurons of the hippocampus may track proximity to goal locations through navigational episodes (Johnson and Redish, 2007; Dupret et al., 2010; Viard et al., 2011). The integration of current location and goal proximity by the hippocampus may provide essential mapping mechanisms required for path integration.

The present study provides novel insight into the encoding of survey-level spatial information required for ground-level, goal-directed navigation and the integration of these encoded spatial representations with path integration mechanisms for successful navigation. On each trial, participants viewed a map of a landmark-deprived environment indicating the start and goal locations then utilized these survey-level spatial representations to actively navigate the environment. Navigation occurred from first person, third person or survey perspectives. We predicted the posterior parietal and retrosplenial cortices



would encode survey-level representations of the environment and recruit these spatial representations for active, ground-level navigation. We predicted the hippocampus would be uniquely recruited for first person perspective navigation when monitoring self-motion would be integral to navigation success. Critically, we predicted the hippocampus would be important for tracking distance to the goal location during ground-level navigation relying on the integration of survey representations and self-motion cues.

## **2.2 Materials and Methods**

### **2.2.1 Participants**

Thirty-four participants were recruited for this study from the Boston University community. All participants were right-handed and had self-reported experience playing video games. Written informed consent was obtained from each participant prior to enrollment in accordance with the experimental protocol approved by both the Partners Human Research Committee and the Boston University Charles River Campus Institutional Review Board.

Four participants were eliminated from the final analysis due to excessive motion during functional magnetic resonance imaging (fMRI) scanning and six additional participants were eliminated due to technical issues during the scanning sessions. Twenty-three participants were included in the final parametric data analysis (mean age  $22.461 \pm 3.49$  (SD); 13 males, 10 females). A subset of participants was included in a whole-brain analysis of navigators who

scored at least 50% correct on all trials in each perspective (18 participants; mean age  $22.801 \pm 3.50$  (SD); 12 males, 6 females). The number of correct trials was not large enough to include participants with less than 50% correct trials in each perspective in the whole-brain analysis. However, participants who did not score at least 50% correct on all trials in each perspective but had little movement in the scanner were included in the linear regression analysis (parametric).

### **2.2.2 Virtual environment**

We developed a navigation task in which participants encoded a start and goal location from a survey-level map perspective and subsequently translated this spatial representation into accurate, goal-directed navigation in a first person perspective (FPP), third person perspective (TPP), or Survey perspective. Critically, the environment contained no distinguishing landmarks, distal cues, or goal location markers. Panda3D Software (Entertainment Technology Center, Carnegie Mellon University, PA) was used to create a virtual environment consisting of an open field extending in all directions towards the horizon and sky (Figure 1B). Within the virtual environment, one virtual unit represented one meter. Short circular columns (radius six virtual units, height 0.15 virtual units) were placed upon the floor of the open field environment in a sixty-degree hexagonal pattern. While moving through the virtual space, a participant could not traverse across any column. This prevented participants from moving directly

to the goal location in a straight line, encouraging active computation and maintenance of orientation as their route arced around the columns.

We varied the initial heading direction across trials (facing North, East, West, South). We also varied the position of the goal location relative to the start location (30°, 60°, 90°, 120°, or 150° angles). Heading direction and goal location bearing at the start location was counterbalanced across trial conditions and runs. Participants were informed that their heading direction at the start of the navigation phase would always be facing the cardinal direction indicated by an arrow on the map presentation (Figure 1A).

Participants navigated through the environment using a button response box. Movement was simulated using three button responses corresponding to the left, forward, and right directions. Participants could not navigate in a reverse direction. Button presses could occur simultaneously (i.e. left and forward), allowing for a smooth range of simulated motion. Navigation occurred in one of three visual perspectives: first person perspective (FPP), third person perspective (TPP), or a Survey perspective (Figure 1B). In all three visual perspectives, movement speed was held constant at five virtual units per hour, the equivalent of a five kilometers per hour (km/h) walking speed. In the FPP, the participant's perspective was set at a height of two virtual units to represent a two meter tall person walking through the virtual environment. The field of view during FPP navigation was restricted to the scene in front of the participant, consistent with the definition of first person perspective. Optic flow was

representative of what a person walking through the environment would experience. In the TPP, the participant's perspective was set at a height of seven virtual units, and a vehicle was guided by the participant to the goal location while the participant remained stationary in the environment (i.e. the camera did not translate with the vehicle). The field of view from the TPP encompassed a larger portion of the environment. During TPP guided navigation, the vehicle always remained at the center of the participant's field of view. In the Survey perspective, the participant steered a vehicle to the goal location from a fixed, survey-level perspective looking directly down at the 0,0,0 coordinate (Figure 1B).

### **2.2.3 Pre-scan training**

One day prior to scanning, participants became familiarized with the button box controls and the three different navigation perspectives of the virtual environment (FPP, TPP, and Survey perspective). Participants spent twelve minutes practicing navigating in each visual perspective the virtual environment with no goal location. Participants then completed five practice runs with 50% accuracy to ensure their ease with the navigational controls and their understanding of the task design. Three practice runs included trials with the navigation phase unique to one perspective (i.e. all four trials in one run had FPP navigation phases). Lastly, two practice runs were composed of twelve trials randomly counterbalanced to include navigation phases in all three perspectives (FPP,

TPP, and Survey). Participants had to complete the last two practice runs with at least 60% accuracy to take part in fMRI scanning.

### *Experimental Testing during fMRI Scanning*

Scanning data was collected the day after training. Participants were given a practice run to refamiliarize themselves with the task and keyboard controls prior to being placed in the scanner. During scanning, participants performed ten runs composed of twelve trials per run. Each trial consisted of map presentation, delay, and navigation phases, followed by an inter-trial interval (ITI). Trials of the FPP, TPP and Survey perspective conditions were presented in an interleaved, randomized order. During the two-second map presentation, participants were shown a survey representation of the environment with their start location, heading direction, and goal location clearly marked. The two-second duration of the map presentation phase discouraged participants from merely counting columns to navigate to the goal location. Due to the short duration of the map presentation, route planning was based on orientation from the start location to the goal location. The map presentation phase was followed by a ten second delay, during which participants made no response. Following the delay was an eight second navigation phase requiring active navigation to the goal location. Participants were instructed to navigate to the precise location where they thought the encoded goal was located. The goal location was not visible during the navigation phase, and no feedback was given as to whether the participant

successfully reached the goal location. A trial was considered correct if participants' trajectories during the navigation phase came within a radius of three virtual units from the goal location. The distance between the start location and goal location was on average  $25.78 \pm 1.61$  (SD) virtual units across all trials. Therefore, three virtual units correspond to 11.6% of the average distance between the start and goal location. Critically, no distinguishing landmarks, distal cues, or goal location markers were present in the environment. This required participants to merge self-motion cues from optic flow with their planned route during ground-level navigation. Participants did not know trial type (FPP, TPP, or Survey perspective navigation) until the start of the navigation phase. The order of the trials was counterbalanced across runs, and the order of runs was randomized across participants. There were forty trials per experimental condition.

#### **2.2.4 Image acquisition**

Images were acquired at the Athinoula A. Martinos Center for Biomedical Imaging, Massachusetts General Hospital in Charlestown, MA using a 3 Tesla Siemens MAGNETOM TrioTim scanner with a 32-channel Tim Matrix head coil. A high-resolution T1-weighted multi-planar rapidly acquired gradient echo (MP-RAGE) structural scan was acquired using Generalized Autocalibrating Partially Parallel Acquisitions (GRAPPA) (TR = 2530 ms; TE = 3.31 ms; flip angle =  $7^\circ$ ; slices = 176; resolution = 1 mm isotropic). T2\*-weighted BOLD images were

acquired using an Echo Planar Imaging (EPI) sequence (TR = 2000 ms; TE = 30 ms; flip angle = 85°; slices = 33, resolution = 3.4x3.4x3.4 mm, interslice gap of 0.5 mm). Functional image slices were aligned parallel to the long axis of the hippocampus.

### **2.2.5 fMRI preprocessing**

Functional imaging data were preprocessed and statically analyzed using the SPM8 software package (Statistical Parametric Mapping, Wellcome Department of Cognitive Neurology, London, UK). All BOLD images were first reoriented so the origin (i.e. coordinate xyz = [0, 0, 0]) was at the anterior commissure. The images were then corrected for differences in slice timing and were realigned to the first image collected within a series. Motion correction was conducted next and included realigning and unwarping the BOLD images to the first image in the series in order to correct for image distortions caused by susceptibility-by-movement interactions (Andersson et al., 2001). Realignment was estimated using 2<sup>nd</sup> degree B-spline interpolation with no wrapping while unwarp reslicing was done using 4<sup>th</sup> degree B-spline interpolation with no wrapping. The high-resolution structural image was then coregistered to the mean BOLD image created during motion correction and segmented into white and gray matter images. The bias-corrected structural image and coregistered BOLD images were spatially normalized into standard Montreal Neurological Institute (MNI) space using the Diffeomorphic Anatomical Registration using Exponentiated Lie

algebra (DARTEL) algorithm (Ashburner, 2007) for improved inter-subject registration. BOLD images were resampled during normalization to 2 mm<sup>3</sup> isotropic voxels and smoothed using a 6 mm full-width at half-maximum Gaussian kernel. The normalized structural images of all 23 participants were averaged after normalization for displaying overlays of functional data.

## **2.2.6 Data analysis**

### **2.2.6.1 Behavioral analyses**

To compare overall performance between the FPP, TPP, and Survey perspective experimental conditions, an analysis of variance (ANOVA) was run comparing accuracy performance. Individual trials were considered correct if participants' trajectories during the navigation phase came within a radius of three virtual units from the goal location. Behavioral analyses were completed using PASW Statistics 18 (SPSS, Inc., Chicago, IL).

### **2.2.6.2 fMRI analysis**

#### *Whole brain analyses*

To model the data, separate regressors were created for the Map Presentation, Delay, Navigation Phase, and Intertrial Interval (ITI) for each condition (FPP, TPP, and Survey). Correct trials and incorrect trials were modeled separately for a total of twenty-four regressors. The six motion parameters calculated during



motion correction were added to the model as additional covariates of no interest. Regressors from the task were constructed as a series of square waves or “boxcars”. Boxcar onsets were defined by the onset of each event and extended for the duration of the event (two seconds for Map Presentation, ten seconds for the Delay, eight seconds for the Navigation Phase, and a four to twelve second variable duration for the ITI). These parameters were convolved with the canonical hemodynamic response function in SPM8.

The model was then analyzed using the general linear model (GLM) approach. Participant-specific parameter estimates pertaining to each regressor were calculated. The t-contrasts between the FPP, TPP, and Survey perspectives for the two task components of interest (Map Presentation and Navigation Phase) were constructed for each participant. Group-averaged statistical parametric maps (SPMs) were created by entering the FPP, TPP, and Survey conditions (FPP>Survey, TPP>Survey, FPP>TPP, TPP>FPP) contrast images from each participant into a one-sample t-test using participant as a random factor.

For each analysis, a voxel-wise statistical threshold of  $p < 0.01$  was applied to the whole brain contrast maps. To correct for multiple comparisons, we applied a cluster-extent threshold technique. The AlphaSim program in the AFNI software package (<http://afni.nimh.nih.gov/afni/>) was used to conduct a 10,000 iteration, 6 mm autocorrelation Monte Carlo simulation analysis on voxels within the group functional brain space using the ResMS header file (173,458

voxels). From this analysis, a minimum voxel extent of 144 was determined to maintain a family-wise error rate of  $p < 0.01$ .

#### *Correct versus incorrect navigation trials*

We examined successful versus unsuccessful ground-level navigation by comparing correct trials versus incorrect trials. Parameter estimates of the FPP and TPP successful navigation trials were combined and contrasted against the combined parameter estimates of FPP and TPP navigation trials where participants were unsuccessful in reaching the goal location. The contrast images were then entered into a one-sample t-test using participant as a random factor. There were not enough error trials to analyze FPP and TPP separately, yet by combining the two conditions we could more broadly examine navigational accuracy.

#### *Parametric modulation of linear distance to goal location*

To examine how successful ground-level navigation integrated with spatial representations encoded at the survey-level, we conducted a parametric modulation analysis testing whether hippocampal activation tracks linear distance to the goal location from moment to moment during the navigation phase. The parametric fMRI data analysis was conducted using a targeted region of interest (ROI) approach. We predicted the hippocampus would support goal-directed navigation by maintaining a guidance system to track linear distance to the goal

location. To test this hypothesis, we created an anatomical ROI mask with a dilation of zero from the anatomical boundaries of the left and right hemisphere hippocampi using the Wake Forest University (WFU) Pick-Atlas (Maldjian et al., 2003) available for SPM.

For the parametric analysis, the models from the previous analyses were modified into a new model such that the FPP and TPP navigation regressors were defined by stick functions sampled at each second of the trials. Parametric modulators for these regressors contained the normalized distance-to-goal values corresponding to each of these time points (Spiers and Maguire, 2007). Distance to the goal location was calculated as the shortest linear distance between the participant's current location and the goal location ( $d$ ). We rescaled the distance to goal to between 0 and 1, with a value of 1 indicating the participant was at the goal location and a value of 0 reflecting the farthest distance from the goal location on a given trial ( $1-d/d_{max}$  where  $d_{max}$  is the absolute distance from start location to goal location).

Separate one-sample t-tests for both the FPP and TPP conditions were conducted within our ROI volume. Similar to the whole brain analysis, we applied a voxel-wise statistical threshold of  $p < 0.01$  to the contrast maps. From a 10,000 iteration, 6 mm autocorrelation Monte Carlo simulation of the ROI volume (1878 voxels) in AlphaSim, a minimum voxel extent of 32 was determined to maintain a family-wise error rate of  $p < 0.01$ .

To examine the relative influence of time and distance to goal on

hippocampal activations during ground-level navigation, we conducted a second parametric modulation analysis testing the strength of the relationship between hippocampal activity and time during the navigation phase. The parametric fMRI data analysis was conducted using the same region of interest (ROI) approach as the distance to goal parametric analysis with FPP and TPP navigation regressors defined by stick functions sampled at each second of the trials. For the time analysis, the parametric modulators for these regressors were modified to contain time values (e.g. 1, 2, 3, etc.) corresponding to each second of the navigation phase.

Separate one-sample t-tests for both the FPP and TPP conditions were conducted within our ROI volume. We applied a voxel-wise statistical threshold of  $p < 0.01$  to the contrast maps. To compare the relative effect sizes of distance and time on hippocampal activity, parameter estimates were extracted from 5 mm spheres centered on peak coordinates in the hippocampus for FPP and TPP during the navigation phase. A paired sample t-test between extracted parameter estimates for the distance to goal and time analyses was conducted using PASW Statistics 18 (SPSS, Inc., Chicago, IL).

#### *Successful perspective specific analysis*

One-sample t-tests were constructed of contrast images comparing the FPP and TPP conditions with the Survey perspective (FPP > Survey, TPP > Survey). The Survey perspective presented a bird's eye view of the entire environment and

was visually identical to the map presentation. When navigating in the Survey perspective, participants had to simply navigate the vehicle to match the map information maintained in visual short-term memory. By comparing the FPP and TPP conditions with the Survey perspective during the navigation phase, we controlled for task components such as motor responses, isolating activity related to integrating map information into ground-level navigation and processing self-motion from optic flow. FPP > Survey and TPP > Survey contrasts were constructed for both the map presentation and navigation phases of the experimental task. We also directly contrasted activity for FPP and TPP (FPP > TPP; TPP > FPP) for the map presentation and navigation phases of the experimental task.

Parameter estimates were extracted from 5 mm spheres centered on peak coordinates in our regions of interest (hippocampus, retrosplenial cortex, posterior parietal cortex, and parahippocampal cortex) for contrasts between FPP, TPP, and Survey perspectives during the map presentation and navigation phases. Paired sample t-tests between conditions for the map presentation and navigation phases were conducted using PASW Statistics 18 (SPSS, Inc., Chicago, IL).

## **2.3 Results**

### **2.3.1 Behavioral data**

We examined navigation performance to determine whether there were any

differences in accuracy when navigating from FPP, TPP and Survey perspectives. Participants reached the goal with precision in the FPP in 71.25% of the trials (SEM 4.09), the TPP in 75.69% of the trials (SEM 2.53), and the Survey perspective in 81.81% of the trials (SEM 2.91) (Figure 2). A repeated-measures General Linear Model revealed a significant main effect of Perspective ( $F_{(1,17)} = 858.41, p < 0.001$ ). Follow up t-tests revealed the main effect of Perspective was driven by the Survey perspective, which had more correct trials than the FPP ( $p = 0.017$ ) and the TPP ( $p = 0.044$ ). Importantly, no significant differences in percent correct were found using paired sample t-tests between the FPP and TPP conditions during the navigation phase ( $p = 0.178$ ) indicating the two ground-level conditions were completed with comparable accuracy. Participants navigated to the goal location in  $6.32 \pm 0.06$  (SD) seconds on average across all trials.

## **2.3.2 fMRI data**

### **2.3.2.1 *Correct versus incorrect trials fMRI analysis***

To examine brain regions contributing to successful navigation, we contrasted successful FPP and TPP navigation trials with navigation trials in which the participant was unsuccessful in reaching the goal location. Our whole brain analysis demonstrated the anterior hippocampus was active for trials in which the participant successfully navigated to the goal location (Figure 3 and Table 1).

This finding suggests that the differential activity for successful navigation involves computation in the anterior hippocampus.

### **2.3.2.2 Parametric analysis of proximity to goal**

A primary goal of the experiment was to test whether the hippocampus actively tracks goal proximity (linear distance to goal location). Because the columns prevented direct (straight line) navigation to the goal, participants needed to integrate visual motion cues to accurately monitor the spatial relationship of their current location and the goal location while circumnavigating the obstacles. The left and right posterior hippocampus was modulated with the participants' distance to the goal location at time points sampled throughout the FPP navigation phase (Figure 4A). Right posterior hippocampal activity was also modulated with linear distance to the goal location during the TPP navigation phase; although, this activation was significant at a lower cluster extent threshold ( $p < 0.05$  cluster significance). For a summary of brain regions activated at the whole-brain level for the parametric analysis of proximity to the goal location in the FPP, see Table 2.

To further characterize the role of hippocampal activation during the navigation phase, we examined activations associated with the progression of time across the navigation phase. The left posterior hippocampus was modulated with time during the FPP navigation phase ( $t_{(23)} = 3.29$ ). Time was not correlated with navigation activity in the TPP, even at a lower statistical threshold

of  $p < 0.05$ . Parameter estimate extractions demonstrated that left posterior hippocampal beta weights were significantly greater for the distance to goal analysis than the time analysis ( $t_{(23)} = 2.118$ ,  $p = 0.046$ ) (Figure 4B). Furthermore, while activity in the right posterior hippocampus was significantly modulated by distance to goal, the linear effects of time did not reach statistical significance in this region. Together, these results indicate that distance to goal has a stronger influence on posterior hippocampal activity than a measure of time.

### ***2.3.2.3 Navigation requiring path integration mechanisms to update perceived location and orientation towards a goal location***

We examined activity during the navigation phase in which participants were at a ground-level (FPP and TPP) perspective and retrieved survey-level spatial information to successfully navigate to the goal location. The hippocampus, retrosplenial cortex, and posterior parietal cortex were more strongly recruited for FPP than Survey perspective during the navigation phase (Figure 5A and Table 3). The retrosplenial cortex and parahippocampal cortex were more strongly activated for TPP than Survey perspective during the navigation phase (Figure 5B and Table 3). Direct contrasts of the FPP and TPP conditions revealed a difference in the relative recruitment of retrosplenial and parahippocampal cortices during these two navigational perspectives. The retrosplenial cortex was active along with other brain regions when contrasting FPP against TPP navigation (Table 3). When contrasting TPP against FPP, the parahippocampal



cortex had significantly greater activation. Although the retrosplenial and parahippocampal cortices were both active when FPP and TPP were contrasted against the Survey perspective, retrosplenial function was more strongly recruited in the FPP, and navigation in the TPP more strongly recruited the parahippocampal cortex.

#### ***2.3.2.4 Encoding of survey-level spatial information required for goal-directed navigation***

Successful navigation in the task requires that participants encode the start location, initial orientation and goal location during the Map Presentation phase. Importantly, participants were unaware during the map presentation phase of the visual perspective in which they would subsequently be tested during the navigation phase. Regions activated during the map presentation support the encoding of survey-level spatial information required for successful navigation to the goal location. Therefore, comparison of map phase activation corresponding to correct FPP and TPP navigation trials against the map presentation for correct Survey navigation trials was analogous to subsequent memory paradigms. Several brain regions of interest were commonly activated for map encoding on successful subsequent FPP and TPP navigation trials (Table 4). These regions included the retrosplenial cortex, posterior parietal cortex, and parahippocampal cortex (Figure 6 A and B). These common activations during map presentation for successful FPP and TPP trials relative to correct Survey trials may facilitate

encoding of map information into a representation useful specifically for successful ground-level navigation. The results demonstrate that activation in the bilateral hippocampus at map presentation contributed to successful FPP navigation to the goal location (Figure 6A).

Direct contrast of map presentation for successful FPP versus successful TPP trials (FPP > TPP; TPP > FPP) revealed activation differences specific to the FPP. The brain regions active when contrasting encoding-related activity during map presentation of successful FPP navigation trials against the map presentation phase of successful TPP navigation trials were the retrosplenial cortex and parahippocampal cortex (Table 4). There were no significant TPP greater than FPP differences during map presentation.

## **2.4 Discussion**

We employed a task that required the encoding of survey-level map representations of the environment and subsequent navigation to a goal location in the first person perspective (FPP), third person perspective (TPP) or Survey perspective. Critically, no landmarks or distal cues were present in the environment. Our study found four main results: 1) anterior hippocampus activation when participants successfully navigated to the goal location 2) a novel demonstration that the posterior hippocampus plays a role in coding proximity to a goal location during active navigation 3) the retrosplenial cortex and posterior parietal cortex were recruited for successful navigation in both the FPP and TPP

4) path integration utilizing self-motion cues and orientation towards the goal location during successful FPP navigation recruited the hippocampus.

#### **2.4.1 Successful navigation recruits the anterior hippocampus**

Rodent models of navigation theorize place cell representations of location drive expectations of reward for goal locations (Foster et al., 2000; Johnson and Redish, 2007). In particular, the rodent ventral hippocampus, the analog for the human anterior hippocampus, has been associated with context and reward processing (Moser and Moser, 1998; Ferbinteanu and McDonald, 2001; Fanselow and Dong, 2010; Royer et al., 2010) suggesting goal locations may be represented by the anterior hippocampus. A recent fMRI study demonstrated that the anterior hippocampus activates during spatial planning and the relative distance between the start location and goal (Viard et al., 2011). In the present study, FPP and TPP successful navigation trials recruited the anterior hippocampus more than trials when the goal location was not precisely reached. The results demonstrate accurate ground-level navigation to the goal location recruits the anterior hippocampus. We suggest this recruitment may serve to successfully integrate orientation with a planned route.

#### **2.4.2 The posterior hippocampus tracks linear distance to the goal location**

Spatial coding for goal proximity within the hippocampus is relatively novel in

studies of human navigation. Previous studies have suggested goal-directed navigation relies upon the integration of spatial representations from the hippocampus with goal-related information from regions outside of the medial temporal lobe (MTL) (Spiers and Maguire, 2007). However, the presence of place-goal conjunctive cells in the human hippocampus, which increased their firing rate when a specific goal was viewed from a specific location, may be indicative of a hippocampal role in associating goal-related contextual inputs with place (Ekstrom et al., 2003). Yet, little is known about whether the hippocampus supports a mechanism for actively tracking progress to goal locations. A recent computational model suggests that a reward signal propagates through a place cell map of the environment originating from goal locations (Erdem and Hasselmo, 2012). Place cells in the hippocampus then activate based on the highest associated reward signal to guide behavior towards the goal location. Our study supports this model by demonstrating that the posterior hippocampus was responsive to the shortest linear distance between participants' current location and the goal location from moment-to-moment as they navigate through the environment. These results provide a novel demonstration that actively coding proximity to a goal location during ground-level navigation in the absence of landmarks recruits the posterior hippocampus.

Recent animal models have suggested that a small portion of cells in the hippocampus may have temporally tuned patterns of activity in addition to spatially specific behavior (Pastalkova et al., 2008; MacDonald et al., 2011;

Kraus et al., 2013). These “time cells” may represent a fundamental role of the hippocampus in providing an internal representation of elapsed time, supporting memory for the timing of discrete events. In the current study, participants used self-motion cues to track distance to an encoded goal location. Since time and distance are fundamentally linked during navigation, activations in the hippocampus correlated with proximity to the goal location may, in part, represent cells sensitive to elapsed time. The current task was not specifically designed to separate distance and time in the analyses, so results of our parametric analyses could reflect influences of both time and distance traveled in human navigation. Yet, some models that track distance can be modified to track time elapsed (Hasselmo and Stern, 2013). To further explore this possibility, we modeled two separate analyses to track proximity to the goal location and progression of time across the navigation phase. Our results indicate that activity in posterior left hippocampus, which significantly tracked distance to the goal, was also correlated with time across the FPP navigation phase; however, direct comparison of parameter estimates extracted from our distance to goal and time analyses demonstrate a significantly stronger modulation of activity by distance than time in the left hippocampus. Furthermore, activity in the posterior right hippocampus significantly tracked distance to goal but not the progression of time. Taken together, our results suggest that during FPP navigation, tracking distance to a goal location has a significant impact on bilateral signal in the hippocampus.

### **2.4.3 Navigation requiring path integration mechanisms update perceived location and orientation towards a goal location**

#### *FPP navigation recruits the hippocampus*

The hippocampus may support path integration (Wolbers et al., 2007), which is a mechanism for tracking distance and orientation using self-motion cues. In rodents, persistent spiking of head direction cells, which represent the direction and speed of a trajectory, are thought to update grid cell responses, and, thus, update hippocampal place cell activity giving more accurate knowledge of location in the environment (Burgess et al., 2007; Hasselmo, 2008; Hasselmo, 2009). Animal models indicate a convergence of self-motion and external cues in the hippocampus is essential for path integration and spatial memory processes (Leutgeb et al., 2000). These studies suggest the hippocampus has a sustained role supporting successful navigation in the absence of landmarks, where there is an increasing reliance on self-motion cues.

The present study targets processes related to integrating survey-level spatial information with ground-level active navigation based on optic flow through simple repeating geometric features. Consistent with its theorized role in path integration, the hippocampus was more active for the navigation phase for successful FPP than successful Survey perspective trials. Hippocampal recruitment for successful FPP navigation is consistent with a framework in which self-motion cues from optic flow support hippocampal position computations. Behavioral studies of patients with hippocampal lesions have generally not

supported the necessity of the hippocampus for path integration tasks (Shrager et al., 2008; Kim et al., 2013). In contrast, a recent fMRI study of path integration in healthy, young adults has shown hippocampal activation correlates with angular accuracy in a triangle completion task, wherein participants indicated the direction from their current location back to their start location (Wolbers et al., 2007). In the present study, participants did not need to track their relationship to the start location during FPP navigation; however, path integration may be essential to track current position relative to the goal location based on spatial information encoded at the map presentation.

#### *Regions commonly recruited for FPP and TPP navigation*

In the present study, successful navigation to a goal location from the FPP and TPP relied on self-motion cues to update orientation towards a goal location. During FPP and TPP navigation, the retrosplenial cortex (RSC) and posterior parietal cortex (PPC) were commonly recruited. The RSC and PPC have been associated with landmark-based navigation (Hartley et al., 2003; Rosenbaum et al., 2004; Spiers and Maguire, 2006; Byrne et al., 2007). In our study, the common recruitment of these brain regions in the absence of landmarks suggests they play a more basic role in spatial mapping and orientation through path integration. Previous studies suggest the RSC integrates route-based spatial information with self-motion cues (Wolbers and Buchel, 2005) to orient and direct movement to a goal location (Epstein, 2008; Baumann et al., 2010).

Data from Spiers and Maguire (2006) demonstrated that PPC was recruited during active navigation to a goal suggesting a role in the coding and monitoring of response-based spatial information concerning distant locations. Taken together, our results indicate PPC activity may support the integration of planned route actions with the spatial relationship between current location and orientation towards the goal location, as represented by the RSC.

Interestingly, the RSC and parahippocampal cortex (PHC) were commonly recruited for FPP and TPP navigation, yet contrasts of FPP and TPP navigation phases revealed a dissociation in relative activation for navigation in the two perspectives. Navigational demands in the FPP required additional recruitment of the RSC, and additional demands on the PHC were necessary during navigation in the TPP. FPP navigation may have required additional recruitment of the RSC to assist in the integration of self-motion cues with distance and direction towards goal locations. The PHC may have been recruited to process the changing spatial layout of the scene during TPP navigation. While the visual input in these perspectives is different, it is also an inherent part of our task design. We believe our contrasts primarily reflect the strategy differences necessary to navigate using self-motion cues in FPP and process changing spatial layout in TPP.

#### **2.4.4 Encoding of large-scale environment required for goal-directed navigation**

Recent studies show spiking activity in the rat hippocampus during sharp wave



ripples representing the trajectory the rat subsequently follows from its current location to a known goal location (Pfeiffer and Foster, 2013). Human neuroimaging studies suggest that regions within the MTL, including the hippocampus and parahippocampal cortex, may be important for navigating, and learning to navigate, environments from a ground-level perspective (Hartley et al., 2003; Wolbers and Buchel, 2005; Weniger et al., 2010; Brown et al., 2010, 2013). Our experiment characterizes an important facet of the MTL's role in active navigation by demonstrating recruitment of MTL regions during survey-level encoding when the encoded spatial representations were required for successful ground-level navigation. In particular, when navigation was tested in the FPP, bilateral hippocampal activation at map encoding related to successful navigation to the goal location. Our current study demonstrates that encoding of distance and directional measures required for successful FPP navigation recruited the bilateral hippocampus in humans.

## 2.5 Chapter 2 Figures

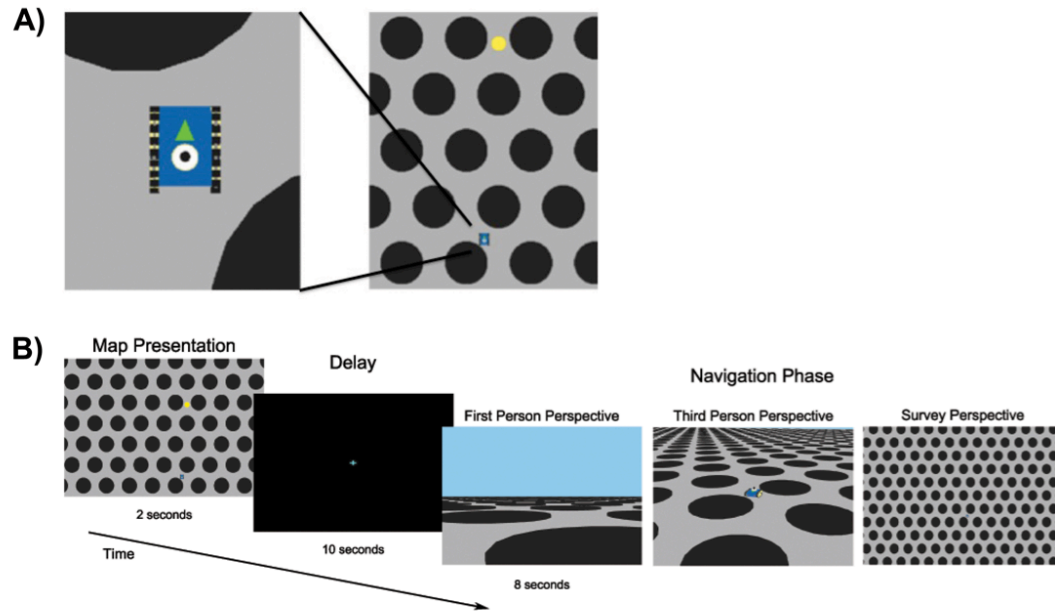


**Figure 2.1**

Task paradigm. A) Survey perspective of the vehicle (blue) that was guided by participants to the goal location (yellow dot). Expanded view displays the vehicle with green arrow showing orientation in the environment. B) During the two-second map presentation, participants were shown a survey representation of the environment with their start location, heading direction, and goal location clearly marked. Map presentation was followed by a ten second delay, during which participants made no response. Following the delay was an eight second navigation phase requiring active navigation to the goal location in which movement occurred in one of three visual perspectives: first person perspective (FPP), third person perspective (TPP), or a survey perspective.

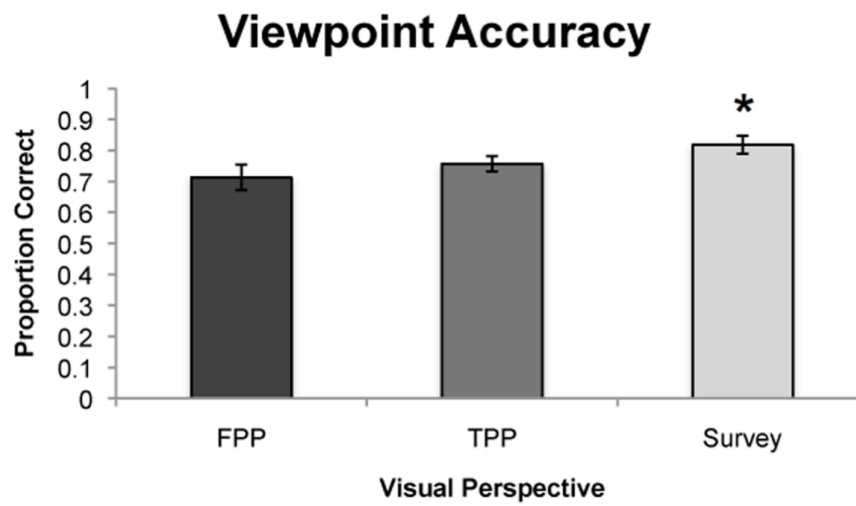


**Figure 2.2**

Scanning day behavioral performance. Error bars denote SEM. Significant differences are indicated with an asterisk. The chart depicts the proportion of correct trials for first person perspective (FPP), third person perspective (TPP), or a survey perspective.

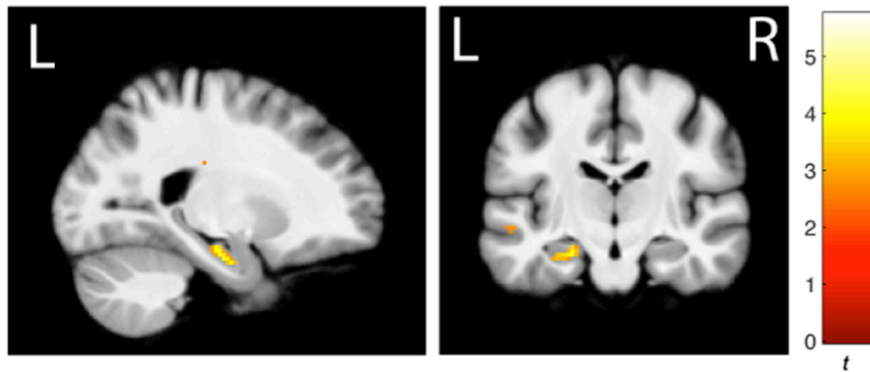


**Figure 2.3**

Successful FPP and TPP navigation recruits the anterior hippocampus. The whole-brain analyses image has a statistical threshold of  $p < 0.01$  corrected for multiple comparisons with a voxel extent of 144.

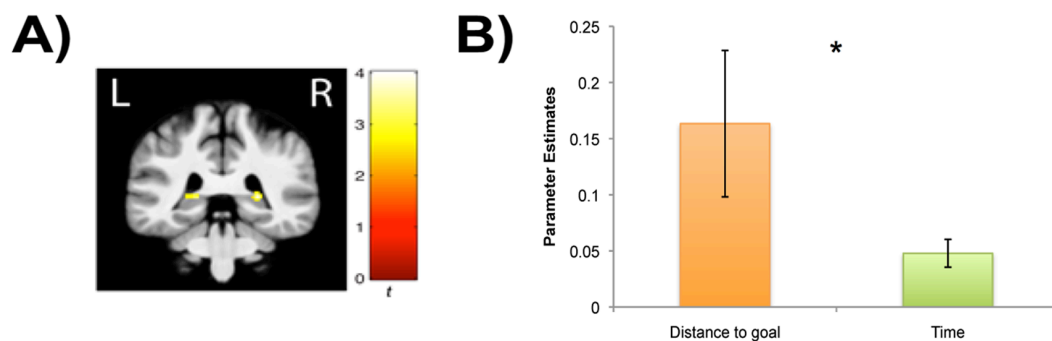


**Figure 2.4**

Parametric modulation of linear distance to the goal location. A) The posterior hippocampus tracks linear distance to the goal location in the FPP. The ROI analysis of the left and right hemisphere hippocampi has a statistical threshold of  $p < 0.01$  corrected for multiple comparisons with a voxel extent of 32. B) Parameter estimate extractions from the posterior left hippocampus in the distance to goal and time analyses. Error bars denote SEM. Significant differences are indicated with an asterisk. The chart depicts parameter estimates extracted from the left posterior hippocampus were significantly greater in the distance to goal analysis than the time analysis for first person perspective (FPP) navigation.

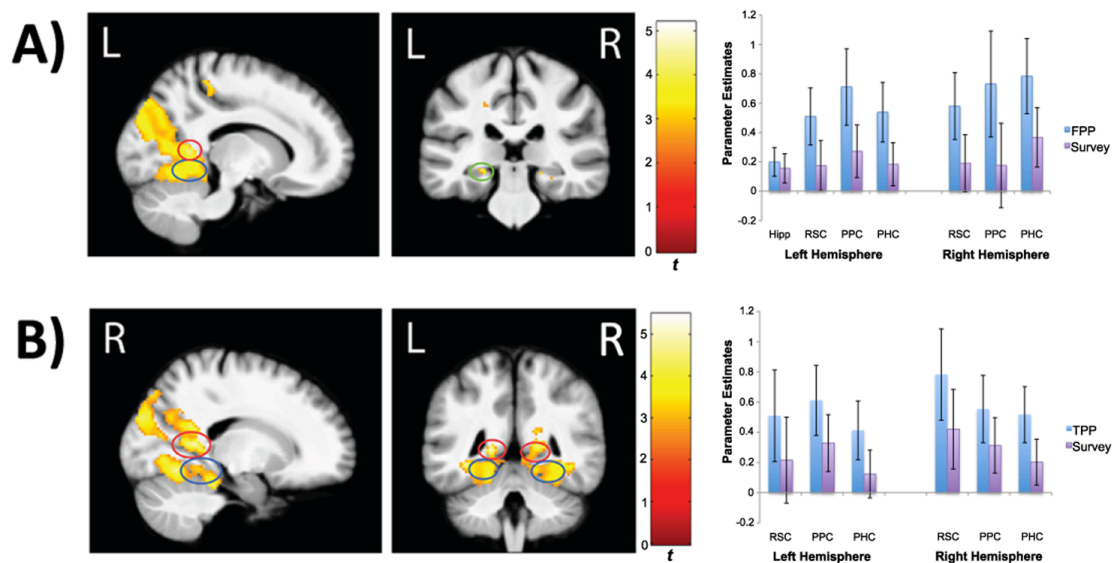


**Figure 2.5**

Activations for navigation trial phase. Both whole-brain analyses images have a statistical threshold of  $p < 0.01$  corrected for multiple comparisons with a voxel extent of 144. Green circles indicate hippocampal (Hipp) activations. Red circles indicate retrosplenial cortex (RSC) activations. Purple circles indicate posterior parietal cortex (PPC) activations. Blue circles indicate parahippocampal cortex (PHC) activations. A) Whole-brain image of activity significantly greater for FPP navigation against Survey navigation (FPP > Survey). Parameter estimate extractions from regions of interest are plotted on the right. Error bars denote SEM. B) Whole-brain image of activity significantly greater for TPP navigation than Survey navigation (TPP > Survey). Parameter estimate extractions from regions of interest are plotted on the right. Error bars denote SEM.

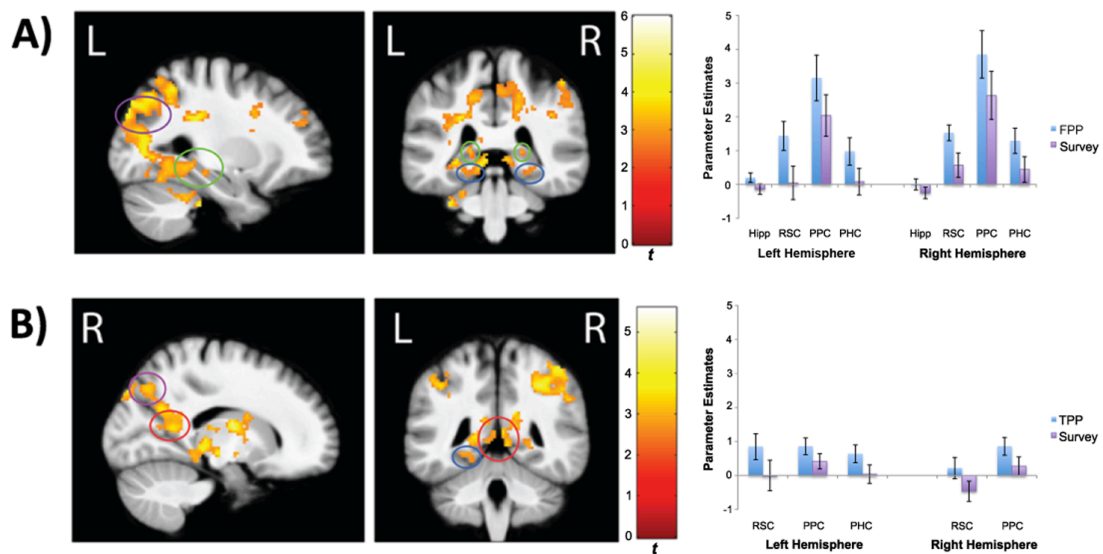


**Figure 2.6**

Activations for map presentation trial phase. Both whole-brain analyses images have a statistical threshold of  $p < 0.01$  corrected for multiple comparisons with a voxel extent of 144. Green circles indicate hippocampal (Hipp) activations. Red circles indicate retrosplenial cortex (RSC) activations. Purple circles indicate posterior parietal cortex (PPC) activations. Blue circles indicate parahippocampal cortex (PHC) activations. A) Whole-brain image of activity significantly greater for map presentation phase for subsequent successful FPP navigation against map presentation activation for successive Survey navigation (FPP > Survey). Parameter estimate extractions from regions of interest are plotted on the right. Error bars denote SEM. B) Whole-brain image of activity significantly greater for map presentation phase for subsequent successful TPP navigation against map presentation activation for successive Survey navigation

(TPP > Survey). Parameter estimate extractions from regions of interest are plotted on the right. Error bars denote SEM.



## 2.6 Chapter 2 Tables

		Left		Right	
Contrast	Area	T	MNI x,y,z	T	MNI x,y,z
Successful>Unsuccessful	Hippocampus (Head)	4.25	-26,-12,-22		
FPP&TPP navigation trials	Precuneus	4.20	-12,-56,34	3.26	4,-54,26
	Superior frontal gyrus	4.23	-16,-46,44		
	Angular gyrus	3.59	-46,-60,24		
	Middle temporal gyrus	5.46	-56,6,-24	5.73	64,-2,-18

**Table 2.1**

Brain regions significantly activated for FPP and TPP navigation phases in which participants successfully navigated to the goal location. MNI coordinates reflect cluster-center voxels. T-values reflect a statistical threshold of  $p < 0.01$ .

Activation clusters survived cluster-threshold correction for multiple comparisons to  $p < 0.01$  with a minimum cluster size of 144.

Contrast	Area	Left		Right	
		T	MNI x,y,z	T	MNI x,y,z
FPP Distance analysis	Hippocampus (Tail)	3.36	-18,-40,4	3.44	24,-40,4
	Precuneus	3.81	-4,-72,52	5.81	4,-62,60
	Superior parietal lobule	4.10	-18,-70,60	5.44	20,-72,58
	Dorsal lateral prefrontal cortex	3.50	-38,34,32	3.96	42,34,36
	Caudate (Dorsal)	2.56	12,4,12	2.93	-12,-2,16
	Superior marginal gyrus	6.05	-42,-54,46	7.10	44,-58,48
	Superior frontal gyrus	3.64	-4,24,40	3.55	8,24,46
	Middle temporal gyrus			3.69	62,-50,-8
	Insula	3.20	-42,10,6	3.90	44,16,-4
	Cuneus	2.93	-4,-80,26	2.79	4,-72,20
	Pons	4.41	-2,-30,-34	4.70	1,-30,-34
	Cerebellum	3.76	-20,-28,-34	4.00	24,-30,-30

**Table 2.2**

Brain regions exhibiting significant activity modulated with the participants' distance to the goal location at time points sampled throughout the FPP navigation phase. MNI coordinates reflect cluster-center voxels. T-values reflect a statistical threshold of  $p < 0.01$ . Activation clusters survived cluster-threshold correction for multiple comparisons to  $p < 0.01$  with a minimum cluster size of 144.

Contrast	Area	Left		Right	
		T	MNI x,y,z	T	MNI x,y,z
FPP>Survey	Hippocampus (Body)	4.09	-24,-30,-8		
	Retrosplenial cortex	4.25	-14,-50,8	3.30	14,-46,6
	Precuneus	3.53	-8,-80,42	3.27	12,-80,42
	Parahippocampal cortex	4.57	-18,-44,-4	4.65	14,-46,-10
	Cuneus	4.28	-4,-78,20	4.10	10,-76,20
	Fusiform gyrus	4.41	-18,-56,-12	4.31	12,-52,-8
	Lateral occipital gyrus	3.76	-38,-78,12	4.31	44,-78,10
	Postcentral gyrus	3.96	-14,-36,56		
TPP>Survey	Retrosplenial cortex	3.35	-12,-52,6	5.23	16,-52,8
	Precuneus	4.43	-8,-84,42	3.82	22,-76,46
	Parahippocampal cortex	3.26	-22,-40,12	3.75	28,-38,-12
	Cuneus	4.98	-24,-90,28	4.53	20,-90,26
	Lingual gyrus	3.87	-8,-68,-6	5.22	10,-66,-6
	Fusiform gyrus	3.82	-22,-64,-10	4.91	24,-64,-14
	Lateral occipital gyrus	4.19	-48,-78,8	4.71	44,-80,8
FPP>TPP	Retrosplenial cortex	3.22	-10,-44,0	3.41	10,-44,0
	Cuneus	3.56	-6,-70,16	3.24	14,-72,16
	Lingual gyrus	2.96	-10,-60,-6	2.71	12,-60,-6
	Posterior cingulate gyrus			3.88	10,-14,40
	Postcentral gyrus	2.63	-12,-40,46		
TPP>FPP	Parahippocampal cortex			4.86	34,-34,-18
	Superior parietal lobule	3.93	-42,-36,52		
	Dorsal lateral prefrontal cortex	4.48	-56,4,44	3.05	52,34,16
	Lateral occipital gyrus	6.03	-42,-66,-16	4.77	40,-64,-18
	Tempo-occipital gyrus	3.73	-34,-40,-24	4.76	34,-40,-24
	Angular gyrus			4.79	30,-70,24
	Postcentral gyrus	4.31	-40,-36,52		

**Table 2.3**

Brain regions exhibiting significant activity from paired t-tests during the navigation phase. MNI coordinates reflect cluster-center voxels. T-values reflect a statistical threshold of  $p < 0.01$ . Activation clusters survived cluster-threshold correction for multiple comparisons to  $p < 0.01$  with a minimum cluster size of 144.

Contrast	Area	Left		Right		
		T	MNI x,y,z	T	MNI x,y,z	
FPP>Survey	Hippocampus (Posterior)	3.85	-30,-38,-4	2.92	22,-38,4	
	Hippocampus (Body)	3.38	-22,-30,-12			
	Retrosplenial Cortex	2.69	-10,-46,2	3.90	10,-42,0	
	Precuneus	5.60	-6,-62,62	4.12	8,-60,56	
	Superior parietal lobule	5.34	-28,-86,34	3.87	18,-82,44	
	Supramarginal gyrus	4.80	-46,-46,46	3.60	48,-44,54	
	Parahippocampal cortex	3.65	-22,-44,-12	2.77	22,-44,-12	
	Dorsal lateral prefrontal cortex	5.99	-32,40,36	4.16	32,44,36	
	Superior frontal gyrus			5.40	30,2,68	
	Caudate (Dorsal)	3.00	-16,-2,24	2.65	16,2,22	
	Cuneus	3.55	-2,-88,26	5.01	4,-88,20	
	Angular gyrus	3.91	-40,-76,22	4.36	34,-74,16	
	Lingual gyrus	3.78	-18,-58,-2	3.47	10,-62,4	
	Cerebellum	5.95	-38,-44,-30	4.96	18,-48,-22	
	TPP>Survey	Retrosplenial cortex	2.99	-10,-44,2	2.88	6,-46,8
		Precuneus	3.83	-12,-70,50	3.32	22,-68,58
Superior parietal lobule		4.31	-36,-60,58	5.55	34,-60,44	
Supramarginal gyrus		3.52	-42,-44,44	5.28	52,-40,46	
Parahippocampal cortex		3.02	-20,-40,-12			
Medial prefrontal cortex (Dorsal)		4.41	-4,30,34	3.86	4,18,42	
Dorsal lateral prefrontal cortex		4.11	-52,8,38	5.21	50,16,22	
Caudate (Dorsal)		2.72	-14,2,18	2.75	16,4,18	
Angular gyrus		4.67	-30,-82,36	3.08	34,-72,42	
Cuneus		3.49	-18,-96,22	3.64	4,-90,20	
Cingulate gyrus		3.47	-2,4,34	4.65	6,12,26	
Lateral occipital gyrus				4.4	46,-58,-18	
Insula		4.35	-32,16,-2	5.58	40,20,-8	
FPP>TPP		Retrosplenial cortex	3.86	-14,-44,-6		
	Parahippocampal cortex			2.70	28,-44,-6	
	Cuneus	6.91	-10,-82,-32	8.24	16,-78,30	
	Lingual gyrus	4.90	-12,-68,2	5.58	10,-62,8	
	Lateral occipital gyrus			4.00	48,-68,16	
	Postcentral gyrus	3.32	-4,-16,56	3.47	8,-26,54	
TPP>FPP	No significant activations					

**Table 2.4**

Brain regions exhibiting significant activity from paired t-tests during the map presentation phase. MNI coordinates reflect cluster-center voxels. T-values reflect a statistical threshold of  $p < 0.01$ . Activation clusters survived cluster-threshold correction for multiple comparisons to  $p < 0.01$  with a minimum cluster size of 144.

**CHAPTER 3: Neural correlates highlight interactions between path  
integration and landmark-based strategies during goal-directed navigation**

### 3.1 Introduction

Goal-directed navigation is a fundamental process used in our everyday lives. Human navigators are able to successfully navigate in dense urban environments as well as in sparse environments. Human spatial memory studies often target navigation in landmark-rich environments (Hartley et al., 2003; Brown et al., 2010; Zhang and Ekstrom, 2013). However, humans are able to successfully navigate in a landmark-free environment by continuously tracking adjustments in orientation and location using self-motion cues (Wolbers et al., 2007; Sherrill et al., 2013). This process, known as path integration, allows humans to accurately update their spatial position. In a landmark-rich environment, humans utilize landmarks in a more route-based strategy to triangulate their position and guide navigation to a goal (Hartley et al., 2003; Baumann et al., 2010; Epstein and Vass, 2013). By adding a solitary landmark to our sparse environment, we contrasted navigation using path integration mechanisms with landmark-based navigational strategies.

An online guidance system is critical when navigating to a goal location in an environment with no distinguishing landmarks. Previous neuroimaging studies suggest that the retrosplenial cortex is recruited in determining one's position and orientation in a broader spatial environment (Rosenbaum et al., 2004; Epstein et al., 2007; Epstein and Vass, 2014). Patients with lesion damage to the retrosplenial cortex can identify landmarks, yet cannot use these landmarks to orient themselves within an environment (Aguirre and D'Esposito, 1999; Park

and Chun, 2009). These results suggest the retrosplenial cortex is important for orientation within an environment, and these orientation calculations need to be integrated with distance estimations for successful goal-directed navigation. Regions of the medial temporal lobe may support these distance computations. Human neuroimaging work has demonstrated that the hippocampus codes distances between familiar landmarks (Morgan et al., 2011) and supports goal-directed navigation through distance calculations in an environment (Sherrill et al., 2013; Howard et al., 2014). These findings suggest that spatial distance coding may be represented in the human hippocampus for locations in large-scale environments.

If a solitary landmark is present in a stark environment, route-based navigational strategies may utilize the landmark to navigate to the encoded goal. The caudate nucleus of the striatum supports behavioral flexibility in humans (Monchi et al., 2006; Jankowski et al., 2009; Ross et al., 2009) and works in conjunction with the hippocampus for decision-making during route-based navigation (Johnson et al., 2007; Brown et al., 2012; Brown & Stern, 2013). The caudate nucleus is often associated with navigation relying on place-action associations, or egocentric strategies (Iaria et al., 2003; Hartley et al., 2003; Igoli et al., 2010; Etchamendy and Bohbot, 2007). Taken together, the caudate nucleus may be recruited during guidance of route-based navigational behaviors based on an orienting landmark.

The current study examines goal-directed navigation in an open field

environment with either the presence or absence of an orienting landmark. In each trial, participants first viewed a map of the environment indicating their start and goal locations; on half of the trials, a landmark was present as an orienting cue in the environment. Then following a delay, participants utilized these survey-level spatial representations to actively navigate to the goal location. Navigation occurred from the first person or survey perspectives. We predicted the hippocampus would be recruited for first person perspective navigation in which monitoring self-motion was integral to navigation success, namely, when no landmark was present. The caudate nucleus was predicted to be recruited when using an orienting landmark to successfully navigate to an encoded goal location via route-based strategies. The hippocampus may also have an important role in tracking distance to the goal location during first person perspective navigation relying on the integration of position and orientation updates. Critically, we predicted that hippocampal activation would increase during first person perspective navigation, particularly when triangulating position between the landmark and an encoded goal involved greater computations.

## **3.2 Materials and Methods**

### **3.2.1 Participants**

Twenty-nine participants were recruited for this study from the Boston University community. All participants were right-handed and had self-reported experience playing video games. Written informed consent was obtained from each



participant prior to enrollment in accordance with the experimental protocol approved by both the Partners Human Research Committee and the Boston University Charles River Campus Institutional Review Board.

Four participants were eliminated from the final analysis due to excessive motion during functional magnetic resonance imaging (fMRI) scanning and two participants were eliminated due to claustrophobia. Twenty-three participants were included in the parametric data analyses (mean age  $22.574 \pm 4.34$  (SD); 10 males, 13 females). Participants who scored at least 50% correct on all trials in each navigation condition were included in the whole-brain analysis (18 participants; mean age  $23.223 \pm 4.67$  (SD); 9 males, 9 females). The number of trials was not large enough to include participants with less than 50% correct trials in each condition in the whole-brain analysis.

### **3.2.2 Virtual environment**

We used a navigation task in which participants encoded a start and goal location from a survey-level map perspective and subsequently translated this spatial representation into accurate, goal-directed navigation from either a first person perspective (FPP), or Survey perspective (Sherrill et al., 2013). Panda3D Software (Entertainment Technology Center, Carnegie Mellon University, PA) was used to create the virtual environment consisting of an open field extending in all directions towards the horizon and sky (Figure 1B). The environment contained no distinctive landmarks or distal cues. Within the virtual environment,

one virtual unit represented one meter. Short circular columns (radius six virtual units, height 0.15 virtual units) were placed upon the floor of the open field environment in a sixty-degree hexagonal pattern. While moving through the virtual space, a participant could not traverse across any column. This prevented participants from moving directly to the goal location in a straight line, encouraging active computation and maintenance of orientation as their route arced around the columns.

In this experiment, we modified the original paradigm (Sherrill et al., 2013) to include a landmark condition. This modification allowed us to examine successful navigation in the presence or absence of an orienting landmark. On half of the trials, a single distinguishing landmark was included in the environment, which participants could use as an orientation cue. The landmark was a single column colored blue that was included in both the map presentation and navigation phase on half of the trials (Figure 1C). The landmark was located either directly adjacent to the goal location, one ring of columns away from the goal location, or two rings of columns away from the goal location. The goal location marker was only presented during the map presentation (encoding) phase, but the landmark was visible in both map presentation and navigation phases.

Participants navigated through the environment using a button response box. Movement was simulated using three button responses corresponding to the left, forward, and right directions. Participants could not navigate in a reverse

direction. Button presses could occur simultaneously (i.e. left and forward), allowing for a smooth range of simulated motion. Navigation occurred from either the first person perspective (FPP), or a Survey perspective (Figure 1B). In the FPP, the participant's perspective was set at a height of two virtual units to represent a two meter tall person walking through the virtual environment. The field of view during FPP navigation was restricted to the scene in front of the participant, consistent with the definition of first person perspective. Optic flow was representative of what a person walking through the environment would experience. In the Survey perspective, the participant steered a vehicle to the goal location from a fixed, survey-level perspective looking directly down at the center of the environment (Figure 1B). Further description of the virtual environment can be found in Sherrill et al. (2013).

### **3.2.3 Experimental training**

#### **3.2.3.1 *Pre-scan training***

One day prior to scanning, participants became familiarized with the button box controls and the different navigation perspectives of the virtual environment (FPP and Survey perspective). Participants spent eight minutes practicing navigating in each visual perspective with no goal location. Participants then completed six training runs with 50% accuracy to ensure their ease with the navigational controls and their understanding of the task design. Four training runs included

trials with the navigation phase unique to one perspective (Survey or FPP) and with or without the presence of an orienting landmark (for example, training trials were blocked so that all four trials in one run were FPP navigation trials with a landmark present in the environment). The final two training runs were composed of sixteen trials randomly counterbalanced to include navigation phases in each visual perspective (FPP and Survey) and included trials with and without an orienting landmark (“landmark” condition and “no landmark” condition, respectively). Participants had to complete the last two training runs with at least 50% accuracy to take part in fMRI scanning.

### ***3.2.3.2 Experimental testing during fMRI scanning***

Scanning data was collected the day after training. Participants were given a single in-scanner practice run with the task and keyboard controls during the initial structural scan once they were placed in the scanner. During functional scanning, participants performed ten runs composed of sixteen trials per run. Each trial consisted of a map presentation, delay, and navigation phase, followed by an inter-trial interval (ITI). Trials containing FPP or Survey perspective navigation phases with or without a landmark (FPP without landmark present – “FPP”, FPP with landmark – “FPP Landmark”, Survey perspective without landmark present – “Survey”, Survey perspective with landmark – “Survey Landmark”) were presented in an interleaved, randomized order. During the two-second map presentation, participants were shown a survey representation of

the environment with their start location, heading direction, and goal location clearly marked. If a landmark was present in the trial, one of the columns was colored blue to act as an orienting landmark. The two-second duration of the map presentation phase discouraged participants from merely counting columns to navigate to the goal location. The map presentation phase was followed by a four second delay period. Following the delay was an eight second navigation phase allowing active navigation to the goal location. Participants were instructed to navigate to the precise location where they thought the encoded goal was located. The goal location was not visible during the navigation phase, but during the landmark condition, the landmark was visible in both map presentation and navigation phases. No feedback was given as to whether the participant successfully reached the goal location. A trial was considered correct if participants' trajectories during the navigation phase came within a radius of three virtual units to the goal location. Participants did not know the visual perspective of the navigation phase (FPP or Survey perspective) until the start of the navigation phase. The order of the trials was counterbalanced across runs, and the order of runs was randomized across participants. There were forty trials for each of the four experimental conditions (FPP, FPP Landmark, Survey, and Survey Landmark).

### **3.2.4 Image acquisition**

Images were acquired at the Athinoula A. Martinos Center for Biomedical

Imaging, Massachusetts General Hospital in Charlestown, MA using a 3 Tesla Siemens MAGNETOM TrioTim scanner with a 32-channel Tim Matrix head coil. High-resolution T1-weighted multi-planar rapidly acquired gradient echo (MP-RAGE) structural scans were acquired using Generalized Autocalibrating Partially Parallel Acquisitions (GRAPPA) (TR = 2530 ms; TE = 3.31 ms; flip angle = 7°; slices = 176; resolution = 1 mm isotropic). T2\*-weighted BOLD images were acquired using an Echo Planar Imaging (EPI) sequence (TR = 2000 ms; TE = 30 ms; flip angle = 85°; slices = 33, resolution = 3.4x3.4x3.4 mm, interslice gap of 0.5 mm). Functional image slices were aligned parallel to the long axis of the hippocampus.

### **3.2.5 fMRI preprocessing**

Functional imaging data were preprocessed and statically analyzed using the SPM8 software package (Statistical Parametric Mapping, Wellcome Department of Cognitive Neurology, London, UK). All BOLD images were first reoriented so the origin (i.e. coordinate xyz = [0, 0, 0]) was at the anterior commissure. The images were then corrected for differences in slice timing and were realigned to the first image collected within a series. Motion correction was conducted next and included realigning and unwarping the BOLD images to the first image in the series in order to correct for image distortions caused by susceptibility-by-movement interactions (Andersson et al., 2001). Realignment was estimated using 7<sup>th</sup> degree B-spline interpolation with no wrapping while unwarped reslicing

was done using 7<sup>th</sup> degree B-spline interpolation with no wrapping. The high-resolution structural image was then coregistered to the mean BOLD image created during motion correction and segmented into white and gray matter images. The bias-corrected structural image and coregistered BOLD images were spatially normalized into standard Montreal Neurological Institute (MNI) space using the Diffeomorphic Anatomical Registration using Exponentiated Lie algebra (DARTEL) algorithm (Ashburner, 2007) for improved inter-subject registration. BOLD images were resampled during normalization to 2 mm<sup>3</sup> isotropic voxels and smoothed using a 6 mm full-width at half-maximum Gaussian kernel. The normalized structural images of all 23 participants were averaged after normalization for displaying overlays of functional data.

### **3.2.6 Data analysis**

#### **3.2.6.1 Behavioral analysis**

To compare overall performance between the FPP and Survey perspective landmark and no landmark experimental conditions, an analysis of variance (ANOVA) was run comparing accuracy performance. Individual trials were considered correct if participants' trajectories during the navigation phase came within a radius of three virtual units from the goal location. Behavioral analyses were completed using PASW Statistics 18 (SPSS, Inc., Chicago, IL).

### **3.2.6.2 fMRI analysis**

#### *Whole brain analyses*

To model the data, separate regressors were created for the Map Presentation, Delay, Navigation Phase, and Intertrial Interval (ITI) for each of the four conditions (FPP, FPP Landmark, Survey, and Survey Landmark). Correct trials and incorrect trials were modeled separately for a total of thirty-two regressors. The six motion parameters calculated during motion correction were added to the model as additional covariates of no interest. Regressors from the task were constructed as a series of square waves or “boxcars”. Boxcar onsets were defined by the onset of each event and extended for the duration of the event (two seconds for Map Presentation, four seconds for the Delay, eight seconds for the Navigation Phase, and a six to ten second variable duration for the ITI). These parameters were convolved with the canonical hemodynamic response function in SPM8.

The model was then analyzed using the general linear model (GLM) approach. Participant-specific parameter estimates pertaining to each regressor of interest (the navigation phase of the FPP landmark and FPP no landmark trials) were calculated. The t-contrasts between the landmark and no landmark conditions in the FPP for the Navigation Phase were constructed for each participant. Group-averaged statistical parametric maps (SPMs) were created by entering the landmark and no landmark conditions for the FPP (FPP Landmark > FPP and FPP > FPP Landmark) beta images from each participant into a paired-



sample t-test using participant as a random factor.

For each analysis, a voxel-wise statistical threshold of  $p < 0.01$  was applied to the whole brain contrast maps. To correct for multiple comparisons, we applied a cluster-extent threshold technique. The 3dClustSim program in the AFNI software package (<http://afni.nimh.nih.gov/afni/>) was used to conduct a 10,000 iteration, 6 mm autocorrelation Monte Carlo simulation analysis on voxels within the group functional brain space using the ResMS header file (162,005 voxels). From this analysis, a minimum voxel extent of 146 was determined to maintain a family-wise error rate of  $p < 0.01$ .

#### *Correct versus incorrect navigation trials*

To examine successful versus unsuccessful navigation in both the landmark and no landmark conditions, we completed two separate analyses comparing correct trials versus incorrect trials. For these analyses, trials were separated into the Landmark and No Landmark conditions. For navigation phases when a landmark was present, parameter estimates of FPP and Survey successful navigation trials were combined and then contrasted against the combined parameter estimates of FPP and Survey navigation trials where participants were unsuccessful in reaching the goal location (FPP Landmark + Survey Landmark correct trials > FPP Landmark + Survey Landmark incorrect trials). The same contrast was completed for navigation phases without a landmark (FPP + Survey correct trials > FPP + Survey incorrect trials). The contrast images were entered into a one-

sample t-test using participant as a random factor. There were not enough error trials to analyze FPP and Survey perspective separately, yet by combining the two conditions we could more broadly examine navigational accuracy.

*Parametric analysis Euclidean distance to goal location*

We conducted a parametric modulation analysis testing whether hippocampal activation tracks linear distance to the goal location from moment to moment during the navigation phase. Previous work with a landmark-free version of this task (Sherrill et al., 2013) demonstrated that the hippocampus tracks linear distance (Euclidean) to the goal location. To replicate the previous findings for trials without a landmark present and to examine whether the hippocampus would also track Euclidean distance when an orienting landmark was present and utilized to track distance during FPP navigation, we conducted another parametric analysis in this study.

To examine whether the hippocampus tracks Euclidean distance, we modified the model from the previous analyses such that the FPP navigation regressors (FPP and FPP Landmark) were defined by stick functions sampled at each second of the trials. Parametric modulators for these regressors contained the normalized distance-to-goal values corresponding to each of these time points (Spiers and Maguire, 2007). Distance to the goal location was calculated as the shortest linear distance between the participant's current location and the goal location ( $d$ ). We rescaled the distance to goal to between 0 and 1, with a

value of 1 indicating that the participant was at the goal location and a value of 0 reflecting the farthest distance from the goal location on a given trial ( $1-d/d_{max}$  where  $d_{max}$  is the absolute distance from start location to goal location). Separate one-sample t-tests were conducted for both the FPP and FPP Landmark conditions.

*Navigational precision relative to distance between the landmark and goal location*

We also examined navigational precision relative to landmark proximity to the goal location by conducting a parametric modulation analysis. In addition to examining whether the hippocampus tracks Euclidean distance to the goal location during the navigation phase (see above), we also examined whether the hippocampus was recruited when triangulating location between a landmark and encoded goal location. To test this hypothesis, we modified the model from the previous analyses such that the FPP Landmark navigation regressor was given a precision score based on the participant's performance on each trial. The precision score was calculated by rescaling the ratio of the linear distance between the participant's final position during the navigation phase and goal location ( $d_1$ ) and the linear distance from the landmark to the goal location ( $d_2$ ). Distance to the goal location from the participant's end point of movement was calculated as the shortest linear distance between the participant's end location and the center of the goal location ( $d_1$ ). Distance between the landmark and the

goal location was calculated as the shortest Euclidean distance between the center of the landmark to the center coordinate of the goal location ( $d_2$ ). We rescaled the precision score to between 0 and 1, with a value of 1 indicating that the participant navigated with precision to the goal location and the landmark was a large distance from the goal location (maximum landmark distance from the goal location was two rows of columns away from the center coordinate of the goal location) ( $1 - d_1/d_2$ ).

A one-sample t-test for the FPP Landmark condition was conducted using participant as a random factor. Similar to the whole brain analysis, a voxel-wise statistical threshold of  $p < 0.01$  was applied to the whole brain contrast maps. To correct for multiple comparisons, we applied a voxel-wise statistical threshold of  $p < 0.01$  to the contrast maps. From a 10,000 iteration, 6 mm autocorrelation Monte Carlo simulation of the whole brain volume (162,005 voxels) in 3dClustSim, a minimum voxel extent of 146 was determined to maintain a family-wise error rate of  $p < 0.01$ .

### **3.3 Results**

#### **3.3.1 Behavioral data**

We examined navigation performance to determine whether there were any differences in accuracy when navigating from FPP and Survey perspectives with an orienting landmark present or absent in the environment. Participants reached the goal with precision in the FPP with no landmark (FPP) in 74.17% of

the trials (SEM 2.52), the FPP with a landmark (FPP Landmark) in 69.17% of the trials (SEM 3.03), the Survey perspective with no landmark (Survey) in 81.67% of the trials (SEM 2.36) and the Survey perspective with a landmark (Survey Landmark) in 81.39% of the trials (SEM 2.32) (Figure 2). A repeated-measures General Linear Model revealed a significant main effect of Perspective ( $F_{(1,17)} = 12.887, p = 0.002, \eta_p^2 = .431$ ). However, it's important to note that no significant differences in percent correct were found using a follow-up paired sample t-tests between the FPP and FPP Landmark conditions during the navigation phase ( $p = 0.092$ ).

### **3.3.2 fMRI data**

As a reminder, during the navigation phase, participants retrieved survey-level spatial information (map) and translated these spatial representations into the FPP in order to navigation to the goal location. On half of the trials, a single landmark was present and could be utilized as an orienting cue. On the other half of the trials, no landmark was present in the environment during the navigation phase.

#### **3.3.2.1 *Correct versus incorrect trials fMRI analysis***

To examine brain regions contributing to successful navigation, we contrasted successful FPP and Survey navigation trials with navigation trials in which the

participant was unsuccessful in reaching the goal location. This contrast was completed for Landmark and No Landmark trials. Our whole brain analysis demonstrated the hippocampus was active for trials in which the participant successfully navigated to the goal location when no orienting landmark was present during navigation (Figure 3A and Table 1). The hippocampus was also recruited for successful navigation with an orienting landmark present compared to unsuccessful navigation. In addition, the caudate nucleus was also recruited for successful navigation utilizing an orienting landmark (Figure 3B and Table 1). The results suggest that the hippocampus is active during successful navigation in conditions that include an orienting landmark. The caudate nucleus was only recruited for successful navigation utilizing an orienting landmark during FPP navigation.

### ***3.3.2.2 Parametric analysis of Euclidean distance to goal location***

We hypothesized that as found in our earlier work (Sherrill et al., 2013) the hippocampus would actively track goal proximity (Euclidean distance to goal location) across the navigation phase. Here, we wanted to test whether this activation would differ if an orienting landmark was present during navigation. Because the columns prevented direct (straight line) navigation to the goal, participants needed to integrate self-motion cues to accurately monitor the spatial relationship of their current location and the goal location while circumnavigating the obstacles. If a landmark was present in the environment, participants needed

to additionally triangulate between their current position, the landmark, and the goal location. We found that the left and right anterior hippocampal activity was modulated by participants' distance to the goal location throughout the FPP navigation phase with no landmark present in the environment (Figure 4A). We found that the anterior and posterior bilateral hippocampal activity was also modulated by linear distance to the goal location during FPP navigation utilizing an orienting landmark (Figure 4B). For a summary of brain regions activated at the whole-brain level for the parametric analysis of proximity to the goal location in the FPP, see Table 2.

### ***3.3.2.3 Parametric analysis of proximity to goal location relative to landmark distance***

In order to examine triangulation during navigation, we examined activations associated with the proximity of the participant's navigational route in relation to the landmark distance to the goal location. Each FPP navigation phase with a landmark was given a precision score (see Materials and Methods) to represent the ratio of the Euclidean distance from the participant's end location for the navigation phase to the goal location and the proximity of the landmark to the goal location. A high precision score indicates the participant was accurate in reaching the goal location while accounting for a larger distance between the landmark and goal location. Larger triangulations between landmark, current location and the encoded goal were required the farther the landmark was from

the goal location. The results demonstrate that the left and right posterior hippocampus were modulated with participants' proximity to the goal location relative to landmark distance to the goal location during FPP navigation phases with a landmark present (Figure 5B). Left anterior hippocampal activity was also modulated with proximity to the goal location during the FPP navigation phases with a landmark present in the environment. For a summary of brain regions activated for the parametric analysis of proximity to the goal location in the FPP, see Table 3.

#### ***3.3.2.4 First person perspective navigation with and without an orienting landmark***

Activity during the FPP navigation phase was compared between the Landmark and No Landmark conditions. The results demonstrate that the retrosplenial, posterior parietal, and parahippocampal cortices were more strongly recruited for FPP navigation with a landmark present than FPP navigation with no landmark present in the environment (Figure 6A and Table 4). Our results indicate that the medial prefrontal cortex was more strongly activated for FPP with no landmark present in the environment than FPP with a landmark present during the navigation phase (Figure 6B and Table 4).

### **3.4 Discussion**

The current fMRI study examined brain mechanisms recruited for successful



goal-directed navigation in an open field environment. We focused our analysis on navigational strategies based on the presence or absence of a landmark in the environment, tracking Euclidean distance to the goal location, and navigational precision based on a landmark's location. When a landmark was not present in the environment, participants used path integration mechanisms to update their position towards the encoded goal location. The hippocampus was recruited for successful navigation trials using path integration mechanisms compared to unsuccessful trials. If a landmark was present in the environment, the caudate nucleus, as well as the hippocampus, were recruited during successful navigation trials more than trials when the goal location was not successfully reached. The medial prefrontal cortex was recruited during successful first person perspective (FPP) goal-directed navigation without a landmark present compared to trials with a landmark in the environment. The retrosplenial, posterior parietal, and parahippocampal cortices were recruited during FPP goal-directed navigation with a landmark present compared to trials with no landmark in the environment. The hippocampus tracked distance to the goal location throughout the navigation phase regardless of the navigational strategies used to reach the goal location. Lastly, our results provide a novel demonstration that activity in the posterior hippocampus was more active on trials that required larger triangulations between the landmark, current location and the goal during FPP navigation.

### **3.4.1 The role of the hippocampus and caudate nucleus during successful goal-directed navigation**

Rodent models of navigation theorize place cell representations of location drive expectations of reward for goal locations (Foster et al., 2000; Johnson and Redish, 2007). In particular, the rodent ventral hippocampus, the analog for the human anterior hippocampus, has been associated with context and reward processing for locations (Moser and Moser, 1998; Ferbinteanu and McDonald, 2001; Fanselow and Dong, 2010; Royer et al., 2010) suggesting goal locations may be represented by the anterior hippocampus. Sherrill et al. (2013) demonstrated that successful navigation in humans recruited the anterior hippocampus more than trials when the goal location was not precisely reached. The current study indicates that the anterior hippocampus was recruited during successful navigation to a goal location both when using path integration strategies and landmark-based navigation. Participants do not receive feedback about whether they have successfully reached the goal location. Yet, our results indicate that the anterior hippocampus is recruited during successful trials than trials when the goal location was not successfully reached. Therefore, the anterior hippocampus may be representing the location of the goal during successful goal-directed navigation.

Route-based navigational strategies rely upon calculations of egocentric motion relative to objects in the environment (Hartley et al., 2003, Spiers and Maguire, 2007; Igoli et al., 2010). Previous human neuroimaging research

suggest that the caudate nucleus of the striatum supports behavioral flexibility in humans (Monchi et al., 2006; Jankowski et al., 2009; Ross et al., 2009) and is often associated with place-action, or egocentric, navigational strategies (Iaria et al., 2003; Hartley et al., 2003; Igoli et al., 2010; Etchamendy and Bohbot, 2007).

The results of the current study indicate that when an orienting landmark is present in the environment, the caudate nucleus is recruited in addition to the anterior hippocampus during successful navigation. Previous work from our lab indicates that the caudate nucleus works in conjunction with the hippocampus for decision-making during route-based navigation (Brown et al., 2012; Brown and Stern, 2013). Since the landmark may serve as a juncture along an encoded route (Epstein and Vass, 2013) or as an egocentric cue in the environment (Baumann et al., 2010; Wegman et al., 2014), the caudate nucleus may be recruited to incorporate these types of route-based navigational strategies with the goal location as represented by the hippocampus during successful goal-directed navigation.

#### **3.4.2 The hippocampus tracks Euclidean distance to a goal location**

A spatially-tuned rodent navigation system has been established through years of navigation research. Cells within this system increase their firing rates based on different aspects of movement in space (O'Keefe and Nadal, 1978; Fyhn et al., 2004; Hafting et al., 2005; Taube et al., 1990; Sargolini et al., 2006). This research has provided the foundation for spatial cognition research in mammals,

including humans. Studies of human navigation have started to establish that these spatially-tuned cells may be present during human navigation and modulate activation based on navigationally driven actions (Ekstrom et al., 2003; Doeller et al., 2010; Baumann and Mattingley, 2010; Jacobs et al., 2013).

Several human neuroimaging studies have shown that the hippocampus has a role in distance estimation (Spiers and Maguire, 2007; Morgan et al., 2011; Viard et al., 2011; Sherrill et al., 2013; Howard et al, 2014). In previous studies, distance estimations were made at decision points along a route, and hippocampal activity was associated with larger estimations of distance between position and a goal (Maguire and Spiers, 2007; Howard et al., 2014). In the present study, activation in the hippocampus is modulated across the entire navigation phase as the participant actively navigates closer to the goal location. Our results indicate that the hippocampus plays a role in tracking distance to a goal location and online tracking of distance estimations is activated for both the use path integration mechanisms or landmark-based navigational strategies.

### **3.4.3 The posterior hippocampus triangulates between a goal location and landmark distance**

Previous computational and rodent research demonstrated that hippocampal neurons, which increase their firing rates to form an ensemble code for location, termed “place” cells (O'Keefe and Dostrovsky, 1971; Wilson and McNaughton, 1993), also encode the bearing and distance of environmental landmarks

(Knierim et al., 1995). These findings have been supported by studies indicating that place cells can be controlled by the location of visual cues (Gothard et al., 1996; Gothard et al., 2001; Knierim, 2002; Knierim and Rao, 2003), and that a type of place cell called “landmark-vector” cells encode spatial locations as a vector relationship to local landmarks (Deshmukh and Knierim, 2013).

Representations of one’s orientation to the goal location in the current environment could be updated based on calculations of current location relative to the visible landmark. Our findings indicate that activity in the bilateral posterior hippocampus was modulated by precise navigation using larger triangulations between landmark and distance to the goal location during FPP navigation. Greater triangulation of position was necessary when distance between the landmark and goal location was larger. Precise navigation to the goal would indicate that the participant was very accurate in triangulating between their location during navigation, the landmark, and the encoded goal. Our results suggest that during FPP navigation triangulating distance to a goal location relative to a landmark in the environment has a significant impact on bilateral signal in the hippocampus.

Triangulating position in the current environment requires accurate perception of one's orientation and directional heading. Head direction cells within the thalamus of the mammalian brain are believed to encode the animal's perceived directional heading with respect to its environment (Taube et al, 1990; Taube, 1995). Head direction cells receive multimodal information about

landmarks and use this landmark information to update the directional heading signal (Taube, 2007). Consistent with rodent literature, thalamic activity in the current study was also modulated with navigational precision based on landmark distance to the goal location. Thalamic activity may be attributing to calculations of heading direction between the landmark and the goal location.

#### **3.4.4 Comparisons of FPP navigation requiring path integration mechanisms and landmark-based navigational strategies**

The presence or absence of an orienting landmark in the environment may influence the navigational strategies being used by participants in our navigation task. Not surprisingly, varying brain regions were recruited when directly contrasting FPP navigation with or without a landmark present in the environment. The retrosplenial, posterior parietal, and parahippocampal cortices were recruited during FPP navigation with an orienting landmark compared to trials with no landmark in the environment. The retrosplenial cortex (RSC) has been implicated in updating location and orientation information during navigation (Sherrill et al., 2013) and is sensitive to heading direction (Baumann and Mattingley, 2010) and orientation estimations (Epstein and Vass, 2013). The nearby posterior parietal cortex (PPC) is activated in human navigation tasks requiring in coordination of egocentric movements with allocentric information (Galati et al., 2010; Howard et al., 2014). Animal models have also shown PPC integrates representations of space for movements within an egocentric

coordinate frame (Snyder et al., 1997, 2000; Sato et al., 2006; Save and Poucet, 2009; Whitlock et al., 2012). The parahippocampal cortex (PHC) is recruited in landmark-based human navigation studies during recognition of locations (Epstein and Kanwisher, 1998; Epstein, 2008; Epstein and Vass, 2013) and navigational decision points in a new environment (Janzen and van Turennout, 2004; Janzen and Westeijn, 2007). The recruitment of the retrosplenial, posterior parietal, and parahippocampal cortices during FPP navigation with an orienting landmark support that these regions process egocentric heading signals based on the landmark location when successfully navigating to a goal location.

The medial prefrontal cortex was activated in a comparison of trials when no landmark was present during FPP navigation with trials with a landmark present. Medial prefrontal involvement in the current task is consistent with a theorized role in spatial working memory (Wolbers et al., 2007) and processing encoded routes (Spiers and Maguire, 2007). If no landmark was present in the environment, participants may have been more reliant upon spatial working memory of their encoded route to successfully reach the goal location, requiring additional recruitment of the medial prefrontal cortex.

### 3.5 Chapter 3 Figures

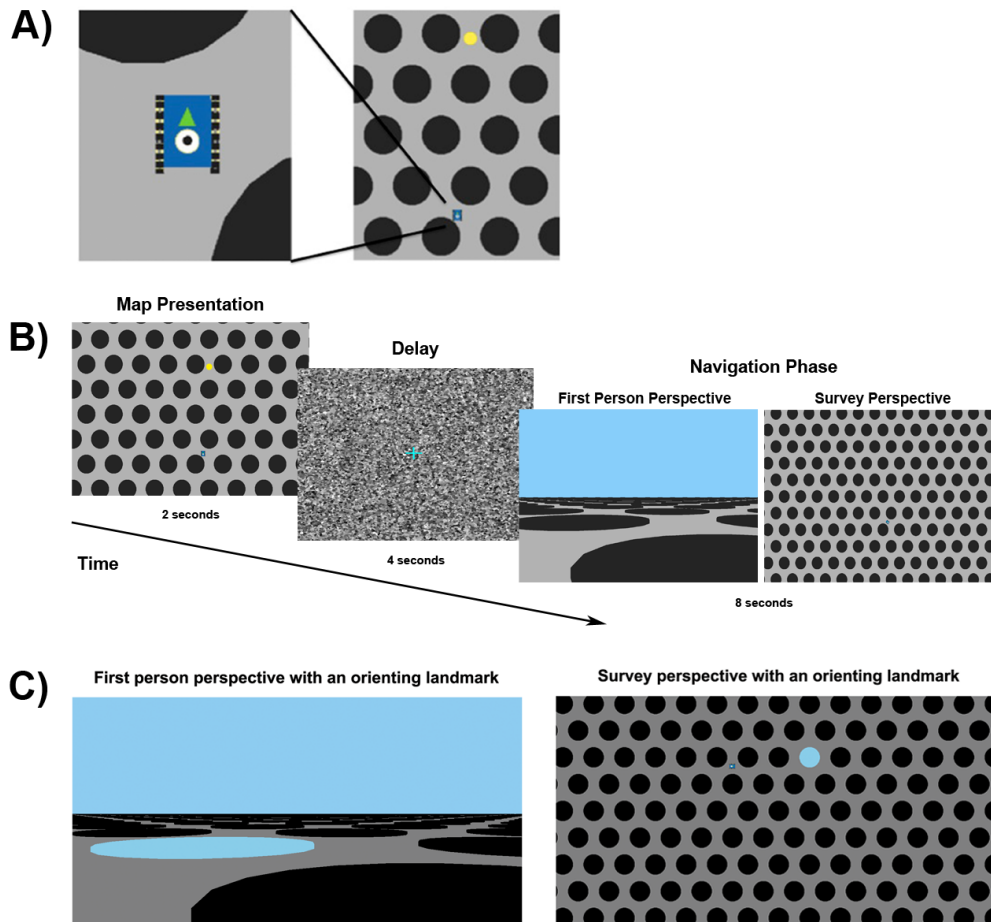


**Figure 3.1**

Task paradigm. A) Survey perspective of the vehicle (blue) that was guided by participants to the goal location (yellow dot). Expanded view displays the vehicle with green arrow showing orientation in the environment. B) Navigation took place in an open field environment (Sherrill et al., 2013) with or without an orienting landmark. Each trial included map presentation, delay, navigation phase and intertrial interval components. On half the trials, a single distinguishing



landmark was included in the environment, which participants could use as an orientation cue. Following the delay, participants actively navigated to the encoded goal location using a button box. Navigation occurred in either first person perspective (FPP) or Survey perspective. C) Displays of the landmark from FPP and Survey perspective. Critically, the goal location marker was only visible during map presentation, but the landmark was visible in both map presentation and navigation phases.

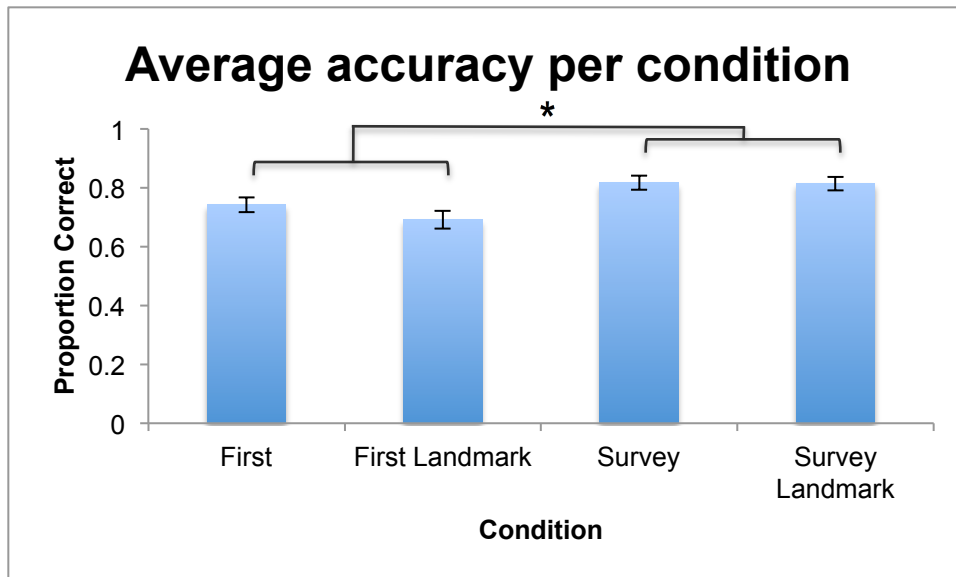


**Figure 3.2**

Scanning day behavioral performance. Error bars denote SEM. Significant differences are indicated with an asterisk. The chart depicts the proportion of correct trials for first person perspective with no landmark in the environment (FPP), first person perspective with a landmark present (FPP Landmark), Survey perspective with no landmark in the environment (Survey), or Survey perspective with a landmark present (Survey Landmark).

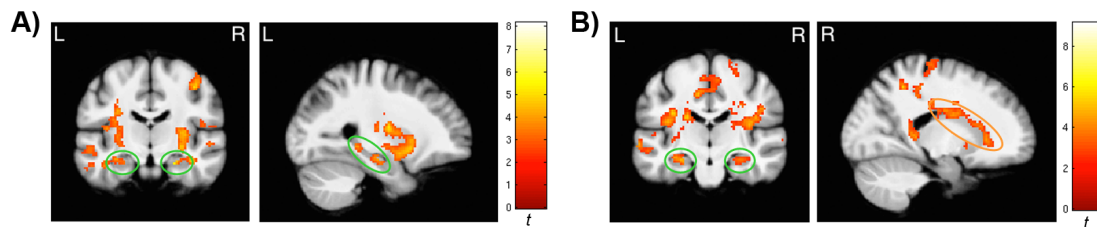


**Figure 3.3**

Successful FPP and Survey perspective navigation with and without an orienting landmark. The whole-brain analyses images have a statistical threshold of  $p < 0.01$  corrected for multiple comparisons with a voxel extent of 146. Green circles indicate hippocampal activations. Orange circles indicate caudate nucleus activations. A) Brain regions recruited during successful navigation without a landmark present in the environment. B) Brain regions recruited during successful navigation with an orienting landmark present in the environment.

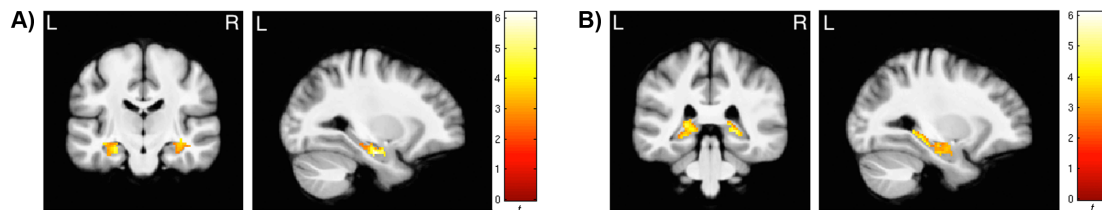


**Figure 3.4**

Parametric analysis of linear distance to the goal location. The ROI analysis of the left and right hemisphere hippocampi has a statistical threshold of  $p < 0.01$  corrected for multiple comparisons with a voxel extent of 42. A) The anterior hippocampus tracks linear distance to the goal location in the FPP with the absence of an orienting landmark in the environment. B) The anterior and posterior hippocampus tracks linear distance to the goal location in the FPP utilizing an orienting landmark in the environment.

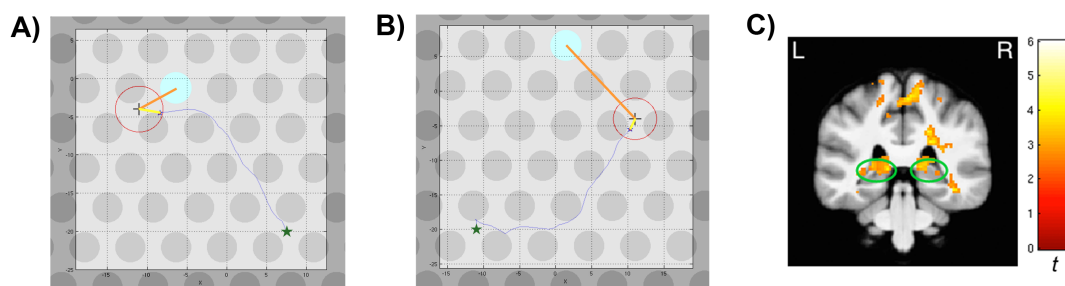


**Figure 3.5**

Navigational precision relative to landmark distance from the goal location. A) and B) Overlays of a representative participant's route (blue line) during a successful FPP trials with a landmark present in the environment. The green star indicates the participant's start location; the cross indicates the goal location for this trial. The red circle is represents a three unit virtual radius around the goal location, which the participant had to navigate within in order for the trial to be considered successful. The precision score was calculated by rescaling the ratio of the Euclidean distance from the participant's end location to the goal location ( $d_1$ ) (yellow line) and the Euclidean distance from the landmark to the goal location ( $d_2$ ) (orange line). A trial is weighted higher under this type of scoring when the participant was more accurate in navigating to the goal location yet had to make greater triangulations of position based on a larger distance between the landmark and goal location. A) A FPP navigation phase in which the landmark was located in an adjacent row of columns to the goal location. B) A FPP navigation phase in which the landmark was located two rows of columns away from the goal location. C) The posterior hippocampus triangulates accurate

navigation to the goal location in the FPP relative to an orienting landmark in the environment. The whole-brain analyses image has a statistical threshold of  $p < 0.01$  corrected for multiple comparisons with a voxel extent of 146. Green circles indicate hippocampal activations.

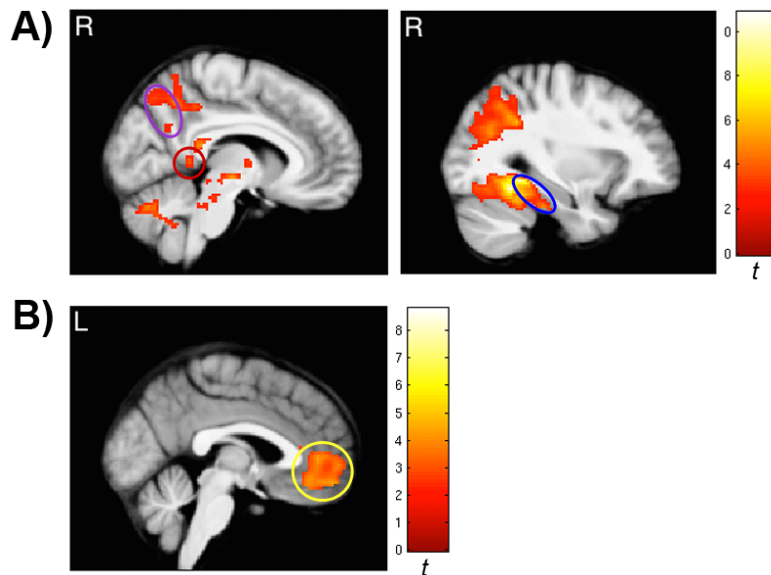


**Figure 3.6**

Whole brain activity for successful FPP navigation with and without a landmark. Both whole-brain analyses images have a statistical threshold of  $p < 0.01$  corrected for multiple comparisons with a voxel extent of 146. Red circles indicate retrosplenial cortex (RSC) activations. Purple circles indicate posterior parietal cortex (PPC) activations. Blue circles indicate parahippocampal cortex (PHC) activations. Yellow circles indicate medial prefrontal cortex (mPFC) activations. A) Whole-brain image of activity significantly greater for FPP Landmark navigation than FPP No Landmark navigation (FPP Landmark > FPP). B) Whole-brain image of activity significantly greater for FPP No Landmark navigation against FPP Landmark navigation (FPP > FPP Landmark).

### 3.6 Chapter 3 Tables

Condition	Contrast	Area	Left		Right	
			T	MNI x,y,z	T	MNI x,y,z
FPP No Landmark	Successful >	Hippocampus (Tail)	3.99	-26,-36,-4		
+ Survey No Landmark	Unsuccessful	Hippocampus (Body)	3.82	-28,-30,-8	3.37	34,-24,-12
trials	Navigation	Hippocampus (Head)	4.94	-30,-18,-14	5.20	22,-14,-20
		Retrosplenial cortex			2.77	6,-48,18
		Posterior parietal cortex	2.60	-2,-68,32	3.88	6,-62,30
		Precuneus	3.38	-2,-50,36	3.50	8,-48,32
		Medial prefrontal cortex	3.71	-4,56,-10		
		Parahippocampal gyrus	2.64	-34,-26,-22		
		Posterior cingulate gyrus	3.18	-2,-38,38		
		Angular gyrus	5.52	-46,-64,18	8.16	50,-70,22
		Insula			5.49	42,0,12
		Putamen	4.65	-22,6,-8	4.83	24,18,-4
		Postcentral gyrus			4.81	40,-14,50
		Fusiform gyrus	3.60	-34,-38,-26		
		Cuneus			2.92	6,-72,14
		Lateral occipital gyrus			3.93	40,-86,4
		Superior temporal gyrus	4.43	-52,-20,-2	5.35	58,-6,-6
		Middle temporal gyrus	4.57	-60,-48,-8	3.63	62,-54,2
FPP Landmark	Successful >	Hippocampus (Tail)	3.16	-22,-38,2	3.52	20,-38,4
+ Survey Landmark	Unsuccessful	Hippocampus (Body)	3.25	-28,-26,-16	4.27	30,-24,-14
trials	Navigation	Hippocampus (Head)	5.51	-24,-16,-18	5.52	36,-12,-20
		Caudate nucleus	3.14	-16,2,20	4.15	18,-2,24
		Retrosplenial cortex	3.61	-6,-50,14		
		Posterior parietal cortex	3.21	-4,-56,24	3.17	4,-50,28
		Medial prefrontal cortex	5.52	-4,64,2	2.82	2,46,-10
		Parahippocampal gyrus	3.11	-32,-28,-24		
		Posterior cingulate gyrus	4.84	-10,-18,44		
		Angular gyrus	4.19	-46,-64,22	5.97	42,-60,20
		Insula	8.82	-36,2,14	9.15	40,4,14
		Orbitofrontal cortex			3.91	28,34,-12
		Putamen	4.92	-24,10,-6	3.57	20,8,-8
		Precentral gyrus	3.71	-6,-22,58	3.82	16,-20,70
		Lateral occipital gyrus			3.32	52,-60,-6
		Superior temporal gyrus	4.89	-60,-12,-6	3.3	62,-4,2
		Middle temporal gyrus	3.31	-58,-2,-26	3.52	20,-38,4

**Table 3.1**

Brain regions significantly activated for FPP and Survey navigation phases in which participants successfully navigated to the goal location with or without a landmark. MNI coordinates reflect cluster-center voxels. T-values reflect a statistical threshold of  $p < 0.01$ . Activation clusters were corrected for multiple comparisons to  $p < 0.01$  with a minimum cluster size of 146.



Condition	Contrast	Area	Left		Right	
			T	MNI x,y,z	T	MNI x,y,z
FPP No Landmark	Distance analysis	Hippocampus (Tail)	4.62	-22,-40,-2	2.75	24,-36,-4
		Hippocampus (Body)	2.92	-24,-24,-16	2.85	28,-24,-16
		Hippocampus (Head)	5.20	-24,-16,-20	2.70	30,-16,-22
		Caudate nucleus	3.11	-10,4,14	3.70	16,-6,20
		Retrosplenial cortex	5.13	-4,-50,10	5.02	6,-48,10
		Posterior parietal cortex	5.73	-4,-58,30	5.56	6,-58,32
		Parahippocampal gyrus	3.76	-24,-28,-22		
		Medial prefrontal cortex	3.92	-6,52,4	4.50	8,56,2
		Orbitofrontal cortex	4.14	-36,38,-16	5.42	36,38,-16
		Dorsal lateral prefrontal cortex	4.21	-24,40,34	2.84	30,44,26
		Middle frontal gyrus (BA 9)	8.79	-36,20,46	4.08	42,20,44
		Middle frontal gyrus (BA 10)	3.80	-18,58,16	3.67	24,58,10
		Superior parietal lobule	3.10	-22,-58,60	5.75	18,-62,60
		Precuneus	2.69	-4,-54,54	4.21	6,-54,54
		Angular gyrus	6.16	-50,-60,28	8.03	48,-52,22
		Posterior cingulate gyrus	6.13	-2,-38,32	5.01	6,-28,36
		Insula	3.27	-36,4,8	3.54	36,8,6
		Lingual gyrus	3.24	-14,-50,-8	4.16	18,-52,-8
		Cuneus	4.45	-6,-76,12	7.01	8,-72,2
		Superior temporal gyrus	6.72	-58,-20,6	3.92	66,-20,4
	Middle temporal gyrus	3.49	-58,0,-22	3.14	56,0,-24	
	Paracentral gyrus	6.43	-2,-26,68	4.24	4,-24,68	
	Cerebellum	5.04	-28,-70,-36	3.81	22,-70,-24	
FPP Landmark	Distance analysis	Hippocampus (Tail)	5.25	-20,-40,2	4.58	22,-36,-2
		Hippocampus (Body)	5.32	-26,-30,-12		
		Hippocampus (Head)	3.48	-28,-14,-22	2.76	32,-14,-22
		Caudate nucleus	3.42	-12,0,16	4.81	18,6,20
		Retrosplenial cortex	4.22	-6,-50,10	5.30	6,-48,10
		Posterior parietal cortex	4.58	-6,-62,30	4.90	6,-58,32
		Medial prefrontal cortex	4.33	-6,52,-2	3.42	6,58,2
		Orbitofrontal cortex	4.77	-32,38,-18	4.92	34,36,-16
		Dorsal lateral prefrontal cortex	3.49	-26,48,26	3.00	28,46,22
		Ventral lateral prefrontal cortex	4.41	-52,24,2	4.88	52,30,6
		Middle frontal gyrus (BA 9)	7.69	-38,18,46	4.23	36,20,44
		Superior parietal lobule	3.73	-16,-58,60	6.29	20,-60,60
		Angular gyrus	8.08	-44,-68,30	5.95	52,-56,32
		Posterior cingulate gyrus	3.64	-4,-32,36	4.98	8,-30,36
		Precuneus	4.55	-8,-56,58	6.16	4,-54,56
		Cuneus	5.00	-8,-76,20	4.83	6,-74,24
		Lingual gyrus	3.68	-24,-28,-22	4.80	18,-54,-8
		Precentral gyrus	2.72	-10,-24,74	3.36	20,-30,70
		Postcentral gyrus	4.99	-20,-30,70	4.12	18,-40,68
		Paracentral gyrus	5.65	-2,-18,66	3.19	4,-16,64
	Cerebellum	5.61	-32,-68,-32	3.77	38,-66,-28	
	Superior temporal gyrus	3.64	-54,8,-16	2.97	54,10,-20	
	Middle temporal gyrus	7.88	-50,12,-34	4.39	36,14,-38	

Table 3.2

Brain regions exhibiting significant activity modulated with the participants'

distance to the goal location at time points sampled throughout the FPP navigation phase with or without an orienting landmark. MNI coordinates reflect cluster-center voxels. T-values reflect a statistical threshold of  $p < 0.01$ . Activation clusters survived cluster-threshold correction for multiple comparisons to  $p < 0.01$  with a minimum cluster size of 146.

Contrast	Area	Left		Right	
		T	MNI x,y,z	T	MNI x,y,z
FPP Landmark	Hippocampal (Tail)	2.87	-16,-38,2	2.78	26,-38,0
Precision analysis	Hippocampal (Head)	3.52	-26,-14,-18		
	Thalamus	3.81	-12,-34,4	2.71	14,-32,6
	Insula	3.61	-38,2,8	3.91	36,0,14
	Putamen	3.27	-24,6,-4		
	Amygdala	6.01	-24,-12,-16		
	Precentral gyrus	4.49	22,-22,66		
	Paracentral gyrus	5.27	-8,-28,54	4.31	4,-28,62
	Middle temporal gyrus	3.56	-66,-18,-12		
	Superior temporal gyrus	3.44	-60,-8,-2		

**Table 3.3**

Brain regions exhibiting significant activity modulated with the participants' navigational precision relative to landmark distance from the goal location during FPP navigation. MNI coordinates reflect cluster-center voxels. T-values reflect a statistical threshold of  $p < 0.01$ . Activation clusters survived cluster-threshold correction for multiple comparisons to  $p < 0.01$  with a minimum cluster size of 146.

Contrast	Area	Left		Right	
		T	MNI x,y,z	T	MNI x,y,z
FPP No Landmark >	Retrosplenial cortex			3.77	8,-44,4
FPP Landmark	Posterior parietal cortex			3.07	10,-58,28
	Parahippocampal gyrus	4.08	-30,-40,-12	4.13	28,-38,-12
	Precuneus	7.07	-10,-52,42	4.63	8,-54,46
	Superior parietal lobule	4.13	-34,-44,50		
	Angular gyrus	3.97	-28,-70,36	3.32	40,-54,38
	Thalamus	3.12	-16,-28,6	3.44	16,-28,8
	Caudate nucleus (ventral)	3.88	-6,8,0		
	Lingual gyrus	3.82	-18,-50,-10	4.32	22,-52,-10
	Fusiform gyrus	7.60	-32,-48,-16	10.85	32,-50,-14
	Middle frontal gyrus (BA 5)	3.60	-32,4,62		
	Cerebellum	4.75	-12,-70,-28	4.93	8,-72,-26
FPP Landmark >	Medial prefrontal cortex	3.20	-2,46,-6	3.26	4,48,-4
FPP No Landmark	Middle temporal gyrus	6.01	-60,-14,-14	4.36	56,2,-24

**Table 3.4**

Brain regions exhibiting significant activity when contrasting the Landmark and No Landmark conditions during the FPP navigation phase. MNI coordinates reflect cluster-center voxels. T-values reflect a statistical threshold of  $p < 0.01$ . Activation clusters survived cluster-threshold correction for multiple comparisons to  $p < 0.01$  with a minimum cluster size of 146.

**CHAPTER 4: Functional connections between optic flow areas and  
navigationally responsive brain regions during goal-directed navigation**

## 4.1 Introduction

Utilization of self-motion cues during first person perspective navigation to track changes in position and orientation relies heavily on the accurate perception of optic flow, the pattern of relative motion between the observer and environment. Humans and animals are able to spatially code their movement by monitoring self-motion to track changes in position and orientation, mechanisms that comprise a process known as path integration (McNaughton et al., 2006; Wolbers et al., 2007; Chrastil, 2013). It has been proposed that optic flow is important for path integration because it provides information about the navigator's movement through the environment (Kearns et al., 2002; Hasselmo, 2009; Tcheang et al., 2011; Raudies et al., 2012). fMRI and psychophysical experiments have used optic flow localizers to identify human cortical areas selective for processing flow motion, including areas V3A and V6 (Tootell et al., 1997; Seiffert et al., 2003; Cardin and Smith, 2010; Pitzalis et al., 2006; Pitzalis et al., 2010) and the human motion complex (hMT+) (Tootell et al., 1997; Seiffert et al., 2003; Duffy, 2009). Functional connections between brain regions sensitive to optic flow and navigationally responsive regions may support successful navigation in sparse environments, in which self-motion cues play an important role.

Spatially tuned cells in the rodent represent position and orientation during navigation. Hippocampal place cells increase their firing rates during movement in specific locations in their environment (O'Keefe and Dostrovsky, 1971),

entorhinal grid cells code arrays of locations (Hafting et al., 2005), and head direction cells are tuned to specific heading directions (Taube et al., 1990). Computational models suggest external cues from the environment drive persistent spiking of head direction cells, which update grid cell responses that, in turn, update hippocampal place cell activity (Hasselmo, 2009) (Figure 1). Recent models indicate that visual input from optic flow provides information about egocentric (navigator-centered) motion and influences firing patterns in these spatially tuned cells during rodent navigation (Raudies et al., 2012; Raudies & Hasselmo, 2012). Head direction cells have been found in the rodent retrosplenial cortex (Chen et al., 1994; Cho and Sharp, 2001). Since previous rodent research indicates that the hippocampus and retrosplenial cortex support position and orientation updating, these areas may be functionally connected with optic flow sensitive regions during navigation relying on self-motion cues. However, a functional link between brain regions sensitive to optic flow and navigationally responsive regions has not yet been established in animals or humans. Based on these animal and computational models, we predicted that in humans regions sensitive to optic flow, areas V3A, V6, and hMT+, would be functionally connected with navigationally responsive regions, including hippocampus and retrosplenial cortex, during first person navigation.

In the current fMRI study, we localized cortical brain regions responsive to flow motion and then determined whether these regions were functionally connected with navigationally responsive brain regions identified during first

person perspective (FPP) navigation. In our navigation task, participants viewed a map of a landmark-deprived environment indicating the start and goal locations and then utilized these survey-level spatial representations to actively navigate the environment in either FPP or Survey (Bird's eye) perspectives (Sherrill et al., 2013). The goal of this study was to examine functional connections between brain regions sensitive to optic flow (areas V3A, V6, and hMT+) and brain regions that support spatial navigation in humans, including the hippocampus and retrosplenial cortex, thus providing evidence for a link between empirical and computational models of navigation.

## **4.2 Materials and Methods**

### **4.2.1 Participants**

Twenty-three participants were recruited for this study from the Boston University community. All participants were right-handed and had self-reported experience playing video games. Written informed consent was obtained from each participant prior to enrollment in accordance with the experimental protocol approved by both the Partners Human Research Committee and the Boston University Charles River Campus Institutional Review Board.

Three participants were eliminated from the final analysis due to excessive motion during functional magnetic resonance imaging (fMRI) scanning while two additional participants were eliminated due to technical issues during the scanning sessions. Each participant completed a navigation task designed to



examine goal-directed navigation using path integration mechanisms (Sherrill et al., 2013) and an optic flow paradigm contrasting coherent and egocentric flow field visual motion with non-coherent, random motion processing (Seiffert et al., 2003, Pitzalis et al., 2010; Putcha et al., 2014). Our whole-brain analysis included participants who scored at least 50% correct on all trials in each perspective of the navigation task in order to maintain a minimum number of correct trials for analysis. Four participants were excluded due to poor performance on the navigation task. Fourteen participants were included in the final functional connectivity analysis (mean age  $23.214 \pm 3.26$  (SD); 9 males, 5 females).

#### **4.2.2 Virtual navigation task environment**

Detailed information about the navigation paradigm can be found in our earlier fMRI publication (Sherrill et al., 2013). Briefly, participants were shown a survey representation of their start location, heading direction, and a goal location. Following a delay, the participants actively navigated to the encoded goal location using a button box. Panda3D Software (Entertainment Technology Center, Carnegie Mellon University, PA) was used to create a virtual environment consisting of an open field extending in all directions towards the horizon and sky (Figure 2). Within the virtual environment, one virtual unit represented one meter. Short, circular columns (radius six virtual units, height 0.15 virtual units) were placed upon the floor of the open field environment to prevent participants from moving directly to the goal location. Thus, navigational routes arced around

the columns, encouraging active computation and maintenance of orientation.

Participants navigated through the environment using a button response box. Navigation occurred in one of three visual perspectives: first person perspective (FPP), third person perspective (TPP), or Survey perspective (Figure 2). For the current study, FPP and Survey perspectives were included in the analysis (see Sherrill et al., 2013 for univariate results for FPP vs. TPP navigation). In the FPP and Survey perspective, movement speed was held constant at five virtual units per second, the equivalent of a walking speed of five kilometers per hour (km/h). In the FPP, the participant's perspective was set at a height of two virtual units to represent a two meter tall person walking through the virtual environment. The field of view during FPP navigation was restricted to the scene in front of the participant, consistent with the definition of first person perspective. Optic flow was representative of what a person walking through the environment would experience. In the Survey perspective, the participant steered a vehicle to the goal location from a fixed, survey-level perspective looking directly down at the 0,0,0 coordinate (Figure 2). Thus, there was no optic flow representative of self-motion during Survey perspective navigation.

#### **4.2.3 Training procedures**

One day prior to scanning, participants were trained on the navigation task. In the task, they encoded start and goal locations from a survey-level map perspective and then translated this spatial representation into accurate, goal-directed

navigation from a FPP, TPP, or Survey perspective (Sherrill et al., 2013).

Participants were informed that following the navigation task they would complete an optic flow paradigm, but no pre-training on the optic flow paradigm was necessary. Scanning data was collected the day after initial training. Participants were given a practice run to refamiliarize themselves with the navigation task and keyboard controls prior to being placed in the scanner.

#### **4.2.4 Experimental tasks**

##### *Navigation Task*

Each trial consisted of map presentation, delay, and navigation phases, followed by an inter-trial interval (ITI). Trials of the FPP, TPP, and Survey perspective conditions were presented in an interleaved, randomized order. During the two-second map presentation, participants were shown a survey representation of the environment with their start location, heading direction, and goal location clearly marked. The map presentation phase was followed by a ten second delay, during which participants made no response. Following the delay was an eight second navigation phase requiring active navigation to the encoded goal location. Participants were instructed to recall the goal location and navigate to its precise position. The goal location was not visible during the navigation phase, and no feedback was given as to whether the participant successfully reached the goal location. A trial was considered correct if participants' trajectories during the navigation phase came within a radius of three virtual units

from the goal location. Critically, no distinguishing landmarks, distal cues, or goal location markers were present in the environment. This required participants to rely on stimuli such as self-motion cues from optic flow in order to execute their planned route during ground-level navigation. Participants did not know trial type (FPP, TPP, or Survey perspective navigation) until the start of the navigation phase. During scanning, participants performed ten runs of the navigation task composed of twelve trials per run. The order of the trials was counterbalanced across runs (run duration: 5 minutes and 52 seconds; TR = 2 seconds), and the order of runs was randomized across participants. There were forty trials per trial type.

#### *Optic Flow Localizer*

Following the navigation task, each scanning session included six runs of the functional optic flow localizer. Each functional run (run duration: 4 minutes and 24 seconds; TR = 2 seconds) consisted of 8 cycles of 16-second alternating blocks of flow motion (termed “Flow”) and random motion (termed “Random”) conditions. The order of the first presentation condition (Flow or Random) alternated across participants. Flow and random motion were created using two thousand moving white dots (each 2 arc-min x 2 arc-min; dot duration = 500ms) presented within a circular aperture of 10.5 degrees by 16.7 degrees (height x width). Dot density was 4.14 dots per cm<sup>2</sup>. Dot speed was scaled with the radial distance from the focus of expansion/contraction. In the flow condition, all dots

moved with a coherent expansion/contraction direction and/or consistent rotation direction about the central fixation cross. The expansion and contraction of optic flow changed several times per block of the Flow condition. Eight mini-blocks were included for each flow condition block, alternating between clockwise and counterclockwise flow during inward and outward contraction/expansion movement of dots (Figure 3A). In the random condition, the dot speed was equivalent to the flow condition, yet the direction of dot movement was random, without a coherent direction or center of expansion/contraction (Pitzalis et al., 2010) (Figure 3B). Participants were instructed for all conditions to maintain fixation on a small crosshair in the center of the screen. Visual stimuli were presented with VisionEgg (Straw, 2008) and were projected onto a rear-projection screen.

#### **4.2.5 Image acquisition**

Images were acquired at the Athinoula A. Martinos Center for Biomedical Imaging, Massachusetts General Hospital in Charlestown, MA using a 3 Tesla Siemens MAGNETOM TrioTim scanner with a 32-channel Tim Matrix head coil. A high-resolution T1-weighted multi-planar rapidly acquired gradient echo (MP-RAGE) structural scan was acquired using Generalized Autocalibrating Partially Parallel Acquisitions (GRAPPA) (TR = 2530 ms; TE = 3.31 ms; flip angle = 7°; slices = 176; resolution = 1 mm isotropic).

Images for the Navigation task were acquired first. T2\*-weighted BOLD

images were acquired using an Echo Planar Imaging (EPI) sequence (TR = 2000 ms; TE = 30 ms; flip angle = 85°; slices = 33, resolution = 3.4x3.4x3.4 mm, interslice gap of 0.5 mm). Functional image slices were aligned parallel to the long axis of the hippocampus.

Images for the optic flow paradigm were acquired immediately following the navigation task; participants were not taken out of the scanner between scans. T2\*-weighted BOLD fMRI data was acquired during visual stimuli presentation (TR = 2000 ms; TE = 30 ms; FA = 90°; slices = 32; resolution = 4x4x4 mm). Functional image slices were aligned parallel to the anterior-posterior commissural line.

#### **4.2.6 fMRI pre-processing**

Functional imaging data were preprocessed and statically analyzed using the SPM8 software package (Statistical Parametric Mapping, Wellcome Department of Cognitive Neurology, London, UK). All BOLD images were first reoriented so the origin (i.e. coordinate xyz = [0, 0, 0]) was at the anterior commissure. The images were then corrected for differences in slice timing and were realigned to the first image collected within a series. Motion correction was conducted next and included realigning and unwarping the BOLD images to the first image in the series in order to correct for image distortions caused by susceptibility-by-movement interactions (Andersson et al., 2001). Realignment was estimated using 7<sup>th</sup> degree B-spline interpolation with no wrapping while unwarped reslicing

was done using 7<sup>th</sup> degree B-spline interpolation with no wrapping. The high-resolution structural image was then coregistered to the mean BOLD image created during motion correction and segmented into white and gray matter images. The bias-corrected structural image and coregistered BOLD images were spatially normalized into standard Montreal Neurological Institute (MNI) space using the Diffeomorphic Anatomical Registration using Exponentiated Lie algebra (DARTEL) algorithm (Ashburner, 2007) for improved inter-subject registration. BOLD images were resampled during normalization to 2 mm<sup>3</sup> isotropic voxels and smoothed using a 6 mm full-width at half-maximum Gaussian kernel. The normalized structural images of all fourteen participants were averaged after normalization for displaying overlays of functional data.

#### **4.2.7 Data analysis**

##### **4.2.7.1 Behavioral data analysis**

To compare overall performance between the FPP and Survey perspective experimental conditions, a paired-samples t-test was run comparing accuracy in the two conditions. Individual trials were considered correct if participants' trajectories during the navigation phase came within a radius of three virtual units from the goal location. Behavioral analyses were completed using PASW Statistics 18 (SPSS, Inc., Chicago, IL). Only successful navigation trials were included in the subsequent analyses exploring functional connectivity between

optic flow sensitive and navigationally-responsive brain regions.

#### **4.2.7.2 fMRI analysis**

For the optic flow paradigm, trials were analyzed in a block design format.

Conditions were classified as either “flow” or “random”. Blocks for each condition were constructed as a series of square waves, termed “boxcars”. Each block was modeled as a 16-second boxcar defined by the onset of the condition.

Analysis was based on a mixed-effects general linear model in SPM8. To capture activation response to coherent flow motion that was not responsive to random motion, contrast images were created contrasting the Flow compared to Random conditions (Flow > Random) within each participant. Group-averaged statistical parametric maps (SPMs) were created by entering the Flow against Random conditions (Flow > Random) contrast images from each participant into a one-sample t-test using participant as a random factor.

For each analysis, a voxel-wise statistical threshold of  $p < 0.01$  was applied to the whole brain contrast maps. To correct for multiple comparisons, we applied a cluster-extent threshold technique. The AlphaSim program in the AFNI software package (<http://afni.nimh.nih.gov/afni/>) was used to conduct a 10,000 iteration, 6 mm autocorrelation Monte Carlo simulation analysis on voxels within the group functional brain space using the ResMS header file (172,761 voxels). From this analysis, a minimum voxel extent of 145 was determined to maintain a family-wise error rate of  $p < 0.01$ .



#### **4.2.7.3 *fMRI functional connectivity analysis***

##### **Region of interest (“seed” region) selection**

A group-averaged statistical parametric map of brain regions sensitive to optic flow was generated from the optic flow paradigm contrasting Flow and Random motion (see above). We used this optic flow activation map to localize seed regions for the functional connectivity analysis. Prior neuroimaging studies have identified human cortical areas that are responsive to optic flow motion processing, specifically visual cortical areas V3A and V6 and hMT+. Area V3A, located inferior to the parieto-occipital sulcus, is highly selective for processing visual motion (Tootell et al., 1997; Seiffert et al., 2003; Pitzalis et al., 2010). Human area V6, like macaque area V6, is located in the dorsal parieto-occipital sulcus (Pitzalis et al., 2006). Area V6 in humans has been described as selectively responding to expanding egocentric flow field visual motion information in humans, which simulates forward motion (Pitzalis et al., 2006; Cardin and Smith, 2010; Pitzalis et al., 2010). Macaque studies have established that the medial superior temporal (MST) area accounts for heading information derived from optic flow, suggesting a role in self-motion processing based on visual cues (Logan and Duffy, 2006; Bremmer et al., 2010). The human motion complex (hMT+), a homolog of macaque area MST (Dukelow et al., 2001; Huk et al., 2002), is located in the posterior region of the middle temporal gyrus and is activated by subjects making estimates of heading direction (Peuskens et al., 2001) and has been characterized as extracting coherent motion cues selective

for self-motion (Rust et al., 2006; Cardin and Smith, 2010; Pitzalis et al., 2010; Cardin and Smith, 2011).

Seed regions were drawn as 5 mm spherical ROIs centered on a peak activated voxel in the flow motion SPM (Flow > Random). The V3A seed region was centered on peak coordinates (Left: -16,-84,24; Right: 22,-84,20), and the V6 seed region was centered on peak coordinates (Left: -12,-80,32; Right: 22,-84,32), as shown in Figure 4. The hMT+ seed region was centered on peak coordinates (44,-62,2) from our whole brain activation map for flow motion (Flow > Random) (Figure 4). Our hMT+ seed region has similar coordinates to a human fMRI study in which hMT+ was activated during a triangle completion path integration task (Wolbers et al., 2007). Although our optic flow task significantly activated bilateral hMT+ regions at a lower statistical threshold ( $p < 0.05$ ), only the right hMT+ region survived our strict cluster correction of the Flow motion SPM (Flow > Random) ( $p < 0.01$  voxel extent with  $p < 0.01$  cluster significance); therefore, a right hemisphere seed region was specified in our analysis. Our seed regions were consistent in anatomical location with boundaries described in previous neuroimaging studies (Swisher et al., 2007; Tootell et al., 2007; Wandell et al., 2007; Wolbers et al., 2007; Pitzalis et al., 2010; Putcha et al., 2014).

### **Beta series correlation analysis**

Functional connectivity analyses were conducted using the beta series correlation analysis method (Rissman et al., 2004), which our lab has used

previously in memory and navigation studies (Ross et al., 2009; Brown et al, 2012). The beta series correlation method utilizes the univariate fMRI data analysis so that parameter estimates, or beta weights, reflecting the magnitude of the task-related blood oxygen level dependent (BOLD) responses are estimated for each trial. Therefore, the beta series correlation analysis requires that the individual trials of events examined in the functional connectivity analysis be modeled separately. Our functional connectivity analysis was restricted to two key phases of the task, the navigation phase and the intertrial interval (ITI) in order to compare the time period in which optic flow plays a key role in navigation. Our interest was in analyzing successful navigation, so only trials in which the participant successfully reached the goal location were included. The individual trials for the navigation phase and ITI for successful trials in each condition (FPP or Survey perspective) were modeled separately with their own regressor for inclusion in the functional connectivity analysis. The number of regressors in each participant's model varied based on the number of successful trials in each condition, but there were the same number of regressors for the navigation phase and ITI for a given condition. Because there were 40 trials per condition (FPP or Survey perspective navigation), a participant with 100% performance on the task would have 40 successful FPP navigation phase regressors, 40 ITI regressors from successful FPP navigation trials, 40 successful Survey navigation phase regressors, and 40 ITI regressors from successful Survey navigation trials.

To accurately capture variance within the task, all other covariates of non-interest were collapsed into regressors based on condition, task phase, and trial success, similar to modeling for a traditional univariate fMRI analysis. Trials in which the participant was unsuccessful in navigating to the goal location were modeled into 4 regressors to represent unsuccessful trials during the navigation phase and ITI for the FPP and Survey conditions. Two additional time periods of the task were modeled: the map presentation and the delay period. These two factors were each separately modeled with four regressors: successful trials in the FPP condition, unsuccessful trials in the FPP condition, successful trials in the Survey condition, and unsuccessful trials in the Survey condition. Data was also collected for trials in which navigation occurred from a third person perspective (TPP) (Sherrill et al., 2013). For the current study, FPP and Survey perspective were our conditions of interest in the analysis due to the consistency of their optic flow during the navigation phase. To accurately capture any variance due to the presence of TPP trials, 8 regressors were included for the successful and unsuccessful trials phases (Map Presentation, Delay, Navigation Phase, and ITI) for the TPP condition. Finally, the six motion parameters calculated during motion correction were added to the model as additional covariates of no interest. In total, a participant with 100% successful trials would have a design matrix containing 182 regressors (160 for the beta series correlation analysis of the navigation phase and ITI of FPP and Survey conditions, and 22 regressors for remaining task components and noise

sources). Regressors from the task were modeled as square waves, or “boxcars”. Boxcar onsets were defined by the onset of each event and extended for the duration of the event (eight seconds for the Navigation Phase and a four to twelve second variable duration for the ITI). These parameters were convolved with the canonical hemodynamic response function in SPM8.

Participant-specific parameter estimates were calculated for each regressor using the least squares solution of the general linear model (GLM) approach in SPM8. An SPM8 default 0.008 Hz high-pass filter was used during first level model specification to remove very slow drifts in signal over time. The parameter estimates for trials within each condition of interest were concatenated to form a “beta series”. The beta series functional connectivity method assumes that the degree of similarity (correlation strength) between the fluctuations of parameter estimates across trials between two voxels serves as a metric for the functional interaction between the voxels. Using a custom MATLAB (MathWorks, Natick, MA) script (Rissman et al., 2004), we determined correlations between the respective beta series for our seed regions of visual regions V3A and V6 and hMT+ and all other voxels in the brain during the navigation phase and ITI for the FPP and Survey conditions. Condition-specific whole brain correlation maps were obtained by calculating the correlation of the seed region’s beta series with that of all other voxels in the brain. The beta series correlation analysis generates raw correlation ( $r$ ) maps, which are then transformed into  $z$  maps using an arc-hyperbolic tangent transform to allow statistical comparisons

between correlation magnitudes.

Functional connectivity specifically related to successful navigation in either the FPP and Survey perspective was assessed by comparing the navigation phase z-transformed correlation maps to the ITI z-transformed correlation maps for each individual participant using paired *t*-tests in SPM8 (i.e. FPP navigation phase > FPP ITI). For each analysis, a voxel-wise statistical threshold of  $p < 0.01$  was applied to the whole brain contrast maps. To correct for multiple comparisons, we applied a cluster-extent threshold technique. The AlphaSim program in the AFNI software package (<http://afni.nimh.nih.gov/afni/>) was used to conduct a 10,000 iteration, 6 mm autocorrelation Monte Carlo simulation analysis on voxels within the group functional brain space using the ResMS header file (176,189 voxels). From this analysis, a minimum voxel extent of 145 was determined to maintain a family-wise error rate of  $p < 0.01$ .

## **4.3 Results**

### **4.3.1 Behavioral data**

For the current study, only successful navigation trials were included in the subsequent analyses exploring functional connectivity between optic flow sensitive and navigation sensitive brain areas. We examined navigation performance and accuracy when navigating in both the first person perspective (FPP) and Survey perspectives. Participants reached the goal with precision (within 3 virtual units) in the FPP in 71.61% of the trials (SEM 3.81) and the

Survey perspective in 79.29% of the trials (SEM 3.24). A paired-samples t-test revealed a significant difference in accuracy between the FPP and Survey perspectives ( $t_{(13)} = 2.895, p < 0.05$ ). Participants navigated to the goal location in  $6.32 \pm 0.06$  (SD) seconds on average across all trials.

#### **4.3.2 fMRI connectivity data**

To examine functional connections during successful navigation, all results discussed are comparisons of the navigation phase against the intertrial interval (ITI) for successful trials (in which the participant navigated within three virtual units of the goal location). A complete list of significant functional connectivity differences during successful navigation from either the FPP or Survey perspective is shown in Tables 1 and 2.

##### ***4.3.2.1 Functional connections with optic flow processing regions during first person perspective navigation***

In the virtual environment, participants had to integrate optic flow motion cues to accurately monitor the spatial relationship of their current position and the goal location during navigation. Greater functional connectivity during FPP navigation than the ITI was observed between regions of the brain that process optic flow motion and brain regions previously noted in navigational studies requiring path integration, including the retrosplenial cortex, posterior parietal cortex,

hippocampus, and medial prefrontal cortex (Wolbers et al., 2007; Spiers and Maguire, 2007; Brown et al., 2010; Baumann and Mattingley, 2010; Doeller et al., 2010; Brown and Stern, 2013; Sherrill et al., 2013). For a summary of all brain regions showing significant functional connectivity with V3A, V6, and hMT+ seed regions at the whole-brain level for FPP navigation, see Tables 1, 2, and 3, respectively.

#### *V3A connectivity*

We observed significant functional connectivity between our V3A seed regions and brain regions recruited during FPP navigation. Left V3A was significantly connected with the head and body of the left and right hippocampus and the bilateral posterior parietal cortex during FPP navigation compared to the ITI (Figure 5A). Left and right V3A seed regions were both functionally connected with bilateral retrosplenial cortex and bilateral medial prefrontal cortex during FPP navigation (Figure 5A). The results suggest visual motion processing region V3A is functionally connected with the hippocampus, retrosplenial cortex, posterior parietal cortex, and medial prefrontal cortex during FPP navigation.

#### *V6 connectivity*

Our results demonstrate that the V6 seed regions are functionally connected with brain regions recruited during successful goal-directed navigation. Left and Right V6 seed regions were both significantly connected with



the head and body of the right hippocampus during FPP navigation compared to the ITI (Figure 5B). Additionally, left and right V6 seed regions were functionally connected with bilateral retrosplenial cortex and bilateral medial prefrontal cortex during successful FPP navigation (Figure 5B). Finally, the left V6 seed region was functionally connected with the bilateral posterior parietal region. These findings further support the functional interaction between optic flow processing regions, including cortical area V6, and navigationally responsive regions including the hippocampus, retrosplenial cortex, and medial prefrontal cortex.

#### *hMT+ connectivity*

During FPP navigation requiring self-motion cues from optic flow to update position in the environment, functional connections were found between the human motion complex (hMT+) and brain regions recruited for successful goal-directed navigation. Right hMT+ was functionally connected with the right head and body of the hippocampus during successful FPP navigation in which the participant successfully reached the goal location compared to the ITI (Figure 5C). Bilateral retrosplenial cortex, posterior parietal cortex, and medial prefrontal cortex were also functionally connected with the right hMT+ seed region. These results suggest optic flow processing region hMT+ is functionally connected with the hippocampus, retrosplenial cortex, and posterior parietal cortex during FPP navigation.

#### ***4.3.2.2 Functional connections with optic flow processing regions during Survey perspective navigation***

During the Survey perspective navigation phase, visual flow was minimal as the vehicle driven by our participants was the only movement simulated on the screen. From the Survey perspective, the participant was able to see a large portion of the environment and the vehicle they were controlling from a high vantage point. Therefore, tracking position in the environment via self-motion cues was not required, as it is in FPP navigation. Instead, simply processing the visual scene and making motor responses was all that was required for participants to successfully navigate to an encoded goal location. Our results demonstrate greater functional connections between visual cortical areas V3A, V6, and hMT+ and primary and supplementary motor cortices during Survey perspective navigation compared to the ITI (Figure 6). This finding was not unexpected since we contrasted the navigation phase, which required button responses to navigate, with an intertrial interval in which button responses were not performed. The results also demonstrate that the right V3A seed region was significantly connected with the body of the right hippocampus and the medial prefrontal cortex during Survey perspective navigation compared to the ITI (Figure 6A). A summary of brain regions functionally connected with V3A, V6, and hMT+ seed regions at the whole-brain level for successful navigation from the Survey perspective are shown in Tables 1, 2, and 3, respectively.

## **4.4 Discussion**

We examined functional connections between optic flow regions V3A, V6, and the human motion complex (hMT+) and navigationally responsive brain regions during first person perspective (FPP) navigation. Perception of egocentric flow motion is a critical aspect of visuospatial cognition, as humans rely on processing of visual input continuously as they navigate through their environment.

Computational models indicate that optic flow provides information about egocentric (navigator-centered) motion which influences firing patterns in spatially-tuned cells during rodent navigation (Figure 1; Raudies et al., 2012; Raudies & Hasselmo, 2012). Here, we demonstrate a functional link between optic flow regions and navigation regions in humans. Specifically, our results demonstrate a significant functional relationship between optic flow sensitive regions V6, V3A, and the human motion complex (hMT+) and areas important for FPP navigation, including the hippocampus, retrosplenial cortex, posterior parietal cortex, and medial prefrontal cortex.

### **4.4.1 The role of optic flow responsive areas in processing egocentric movement**

Visual information about one's movement in relation to the environment, known as egocentric motion, is essential to track adjustments in position and orientation during navigation. Although other cues for self-motion, such as vestibular input, proprioception, and efferent copies of motor commands, are present during

everyday movement, the primary cue for self-motion in virtual environments is optic flow. Previous retinotopic mapping and fMRI studies in humans have established a continuum of several motion-selective regions, including cortical areas V3A, V6, and hMT+ (Tootell et al., 1997; Seiffert et al., 2003; Pitzalis et al., 2006; Duffy, 2009; Cardin and Smith, 2010; Pitzalis et al., 2010). Our optic flow paradigm demonstrated activity within areas V3A, V6, and hMT+, consistent with these earlier studies. These brain regions process coherent flow motion that was not responsive to random motion similar to visual input from self-motion cues during first person spatial navigation. Cortical region V3A is highly responsive to processing objective visual motion and discarding self-induced planar retinal motion (Fischer et al., 2012). Cortical region V6 has been characterized as highly selective for coherent motion cues indicative of self-motion (Pitzalis et al., 2010) and is more responsive to egocentric motion than other types of coherent motion (Cardin and Smith, 2010). hMT+ extracts coherent motion cues selective for self-motion and has been implicated in perceiving heading direction (Peuskens et al., 2001). Thus, we predicted a functional link between these optic flow sensitive regions and brain regions recruited for FPP navigation, which depend on self-motion cues to update position and orientation.

#### **4.4.2 Optic flow processing regions are functionally connected with brain regions supporting first person perspective navigation**

Path integration, the ability to integrate perceived self-motion to update

knowledge of current position and orientation, is a fundamental mechanism of spatial navigation. Path integration tracks changes in position and orientation (Wolbers et al., 2007), provides vector knowledge of motion relative to a location (Weiner et al., 2011), and can be used to navigate in an environment towards an intended goal or remembered location (Sherrill et al., 2013; Kalia et al., 2013). Although everyday navigation often relies on landmarks, path integration is an underlying process that updates representations of position and orientation based on self-motion perceptual signals when landmarks may not be present or reliable (May and Klatzky, 2000; Foo et al., 2005). While not necessarily using path integration, per se, successful navigation in the present task required similar components, including updating position and orientation to a goal location based on self-motion cues in a landmark-free environment. Our results indicate that optic flow sensitive regions were functionally connected with brain regions recruited during navigation using path integration mechanisms. These results demonstrate significant functional connections between the retrosplenial cortex (RSC) and left and right V3A and V6 and right hMT+ seed regions during FPP navigation. Rodents with RSC lesions exhibit a deficit in path integration when visual cues are not provided, suggesting that the RSC is important for path integration when incorporating visuospatial information with positioning updates (Cooper et al., 2001; Cooper and Mizumori, 2001; Pothuizen et al., 2008; Elduayen and Save, 2014). Head direction cells have also been observed in the rodent RSC (Chen et al., 1994; Cho and Sharp, 2001). Recent human

neuroimaging studies have indicated the RSC integrates self-motion cues during navigation with route-based spatial information (Wolbers and Buchel, 2005), directs movement towards a goal location (Epstein, 2008), and is sensitive to heading direction (Baumann et al., 2010). Functional connections found here between optic flow sensitive regions and the RSC further establish a role for the RSC in updating position and orientation based on visual cues from optic flow.

In previous work, Sherrill et al. (2013) demonstrated that the posterior parietal cortex (PPC) was recruited during FPP navigation relying on self-motion processing. The current study demonstrates that the PPC has functional connections with left V3A, left V6 and right hMT+ during FPP navigation. Studies measuring single unit activity in primates (Sato et al., 2006) and hemodynamic responses in humans (Maguire et al., 1998; Rosenbaum et al., 2004; Spiers and Maguire, 2006) have suggested that the PPC plays a critical role in navigation by integrating position and self-movement information. Cells in the rodent PPC encode precise self-motion and acceleration states during free roaming in an open arena (Whitlock et al., 2012). Human neuroimaging data demonstrates that PPC was recruited during navigation to a goal suggesting a role in the coding and monitoring of response-based spatial information concerning distant locations (Spiers and Maguire, 2006). The functional connections identified here between optic flow sensitive regions and the PPC may support integration of self-motion cues and planned route actions.

Another key finding in the present study was that left V3A, left and right

V6, and right hMT+ seed regions had functional connections with the head and body of the right hippocampus during FPP navigation compared to the ITI. Functional connections between the hippocampus and optic flow regions during FPP navigation is consistent with computational models indicating that self-motion cues from optic flow might underlie coding of spatial position by grid cells and border cells in structures providing input to the hippocampus (Raudies et al., 2012; Raudies & Hasselmo, 2012). Some human lesion studies have not supported the idea that the hippocampus is necessary for path integration (Shrager et al., 2008; Kim et al., 2013), yet other neuropsychological studies found that patients with right hippocampal lesions had impairments in path integration without visual cues (Worsley et al., 2001; Philbeck et al., 2004). Additional patient studies have indicated that navigators with hippocampal lesions rely on extrahippocampal processes (context cues, object recognition) to support performance of landmark-based navigation (Kessels et al., 2011). The current study's results indicate that the hippocampus in conjunction with functional connections to optic flow sensitive regions plays a crucial role in using self-motion for FPP navigation.

Functional connections between bilateral V3A and V6 and right hMT+ seed regions and the medial prefrontal cortex were also found during successful FPP navigation compared to the ITI. Medial prefrontal involvement in the current task is consistent with its role in spatial working memory (Wolbers et al., 2007) and route navigation tasks (Spiers and Maguire, 2007). Wolbers et al. (2007)

suggested that visual path integration is linked through interplay of self-motion processing in hMT+, higher-level spatial processes in the hippocampus, and spatial working memory in the medial prefrontal cortex. In support of that claim, our results establish a functional connection between right hMT+, the right hippocampus, and the bilateral medial prefrontal cortex during FPP navigation requiring path integration mechanisms.

#### **4.4.3 Functional connections with optic flow regions and motor cortex regions during Survey perspective navigation**

When navigating in the Survey perspective, participants simply navigated the vehicle via the button box to the goal location maintained in short-term memory. During Survey perspective navigation, visual flow was minimal since the vehicle driven by our participants was the only movement on the screen. Tracking position in the environment via self-motion cues was not required as it was in FPP navigation. We found increased functional connectivity between visual cortical areas V3A, V6, and hMT+ and the primary motor cortex during Survey perspective navigation compared to the ITI. The contrast between the Survey perspective results and FPP results further strengthens our conclusion of functional interplay during FPP navigation between optic flow sensitive regions and brain regions required for navigation. Interestingly, our results demonstrated that the right V3A seed region demonstrated increased functional connectivity with the body of the right hippocampus and the right medial prefrontal cortex



during Survey perspective navigation compared to the ITI. The functional connection between right V3A, hippocampus and medial prefrontal cortex may represent a functional integration of encoded spatial information required to implement a successful route towards a goal location, even when not tied to self-motion.

#### **4.4.4 Conclusions**

A functional link between optic flow sensitive regions and navigationally responsive regions has not yet been established in animals or humans. The current study provides this functional link. Previous neuroimaging research has established that cortical areas V3A, V6, and hMT+ process optic flow. Here, we examined functional connections between these optic flow sensitive regions and brain regions known to be important for navigation. The results demonstrate that goal-directed navigation requiring path integration mechanisms involves a cooperative interaction between optic flow sensitive regions V3A, V6, and hMT+ and the hippocampus, retrosplenial, posterior parietal and medial prefrontal cortices. These functional connections suggest a dynamic interaction between self-motion processing and navigationally responsive systems to support goal-directed navigation.

#### 4.5 Chapter 4 Figures

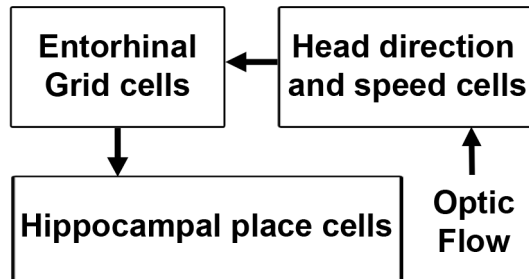
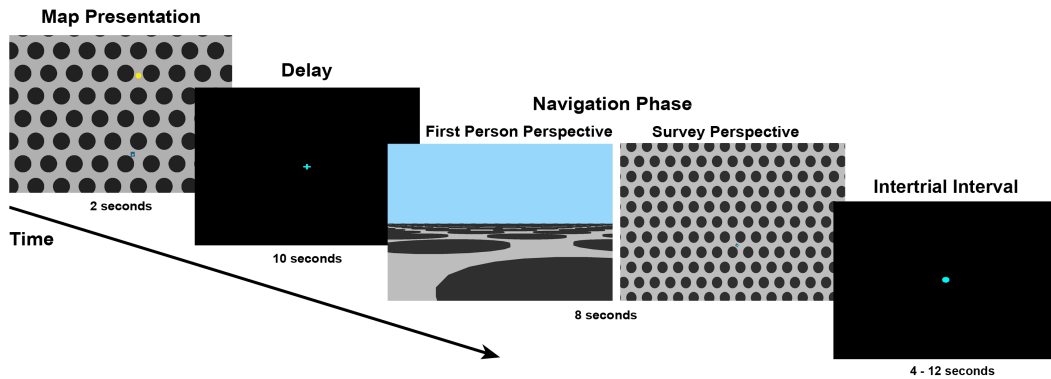


Figure 4.1

Adapted computational model. Simplified model adapted from Hasselmo (2009) depicting how optic flow input influences spatially-tuned cells. Optic flow visual information drives head direction cells to maintain the direction and speed of a trajectory. Head direction and speed cells drive grid cell responses in the entorhinal cortex that in turn update place cells in the hippocampus.



**Figure 4.2**

Navigation task paradigm. A) Survey perspective of the vehicle (blue) that was guided by participants to the goal location (yellow dot). Expanded view displays the vehicle with green arrow showing orientation in the environment. B) During the two-second map presentation, participants were shown a survey-level representation of the environment with their start location, heading direction, and goal location clearly marked. Map presentation was followed by a ten second delay, during which participants made no response. Following the delay was an eight second navigation phase requiring active navigation to the goal location in which movement occurred either in the first person perspective (FPP) or a Survey perspective.

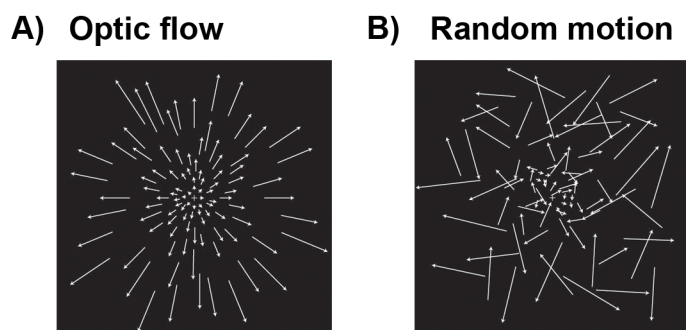


**Figure 4.3**

Optic flow stimuli depiction. The length of the arrows corresponds with dot speed; dot speed increases with greater distance from the center focus. A) Illustration of optic flow motion (“Flow”) stimuli that simulated forward and backward motion using dot fields that are expanding or contracting while rotating about a center focus. B) Illustration of non-coherent motion (“Random”) stimuli using dots moving at the same speeds as the “flow” condition, but the direction of movement is random.

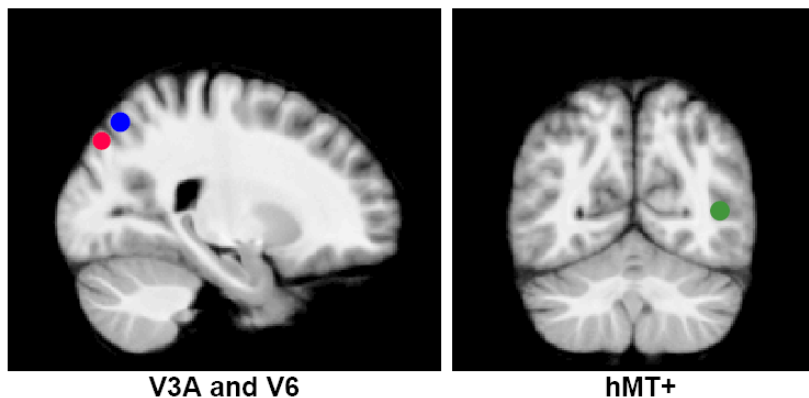


**Figure 4.4**

Connectivity seed regions. Seed region locations based on brain areas activated during the optic flow paradigm contrasting Flow and Random motion (Flow > Random). Red and blue circles indicate visual cortical areas V3A and V6 seed regions, respectively. The seed region in the right human motion complex (hMT+) is shown in green.

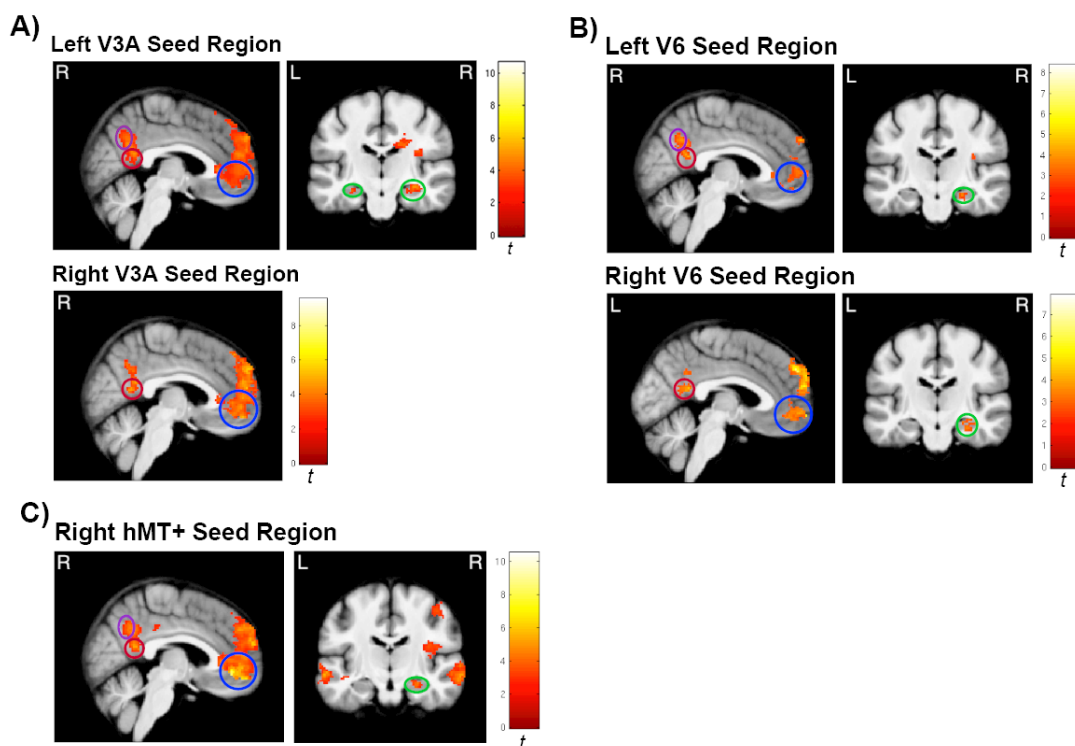


**Figure 4.5**

First person perspective (FPP) navigation: Optic flow processing regions are functionally connected with brain regions supporting FPP navigation. Functional connectivity analysis images have a statistical threshold of  $p < 0.01$  corrected for multiple comparisons with a voxel extent of 145. Green circles indicate hippocampal activations. Red circles indicate retrosplenial cortex (RSC) activations. Purple circles indicate posterior parietal cortex (PPC) activations. Blue circles indicate medial prefrontal cortex (mPFC) activations. A) Sagittal and coronal images of activations functionally connected with the left and right V3A seed regions during FPP navigation. B) Sagittal and coronal images of activations functionally connected with the left and right V6 seed regions during

FPP navigation. C) Sagittal and coronal images of activations functionally connected with the right hMT+ seed region during FPP navigation.

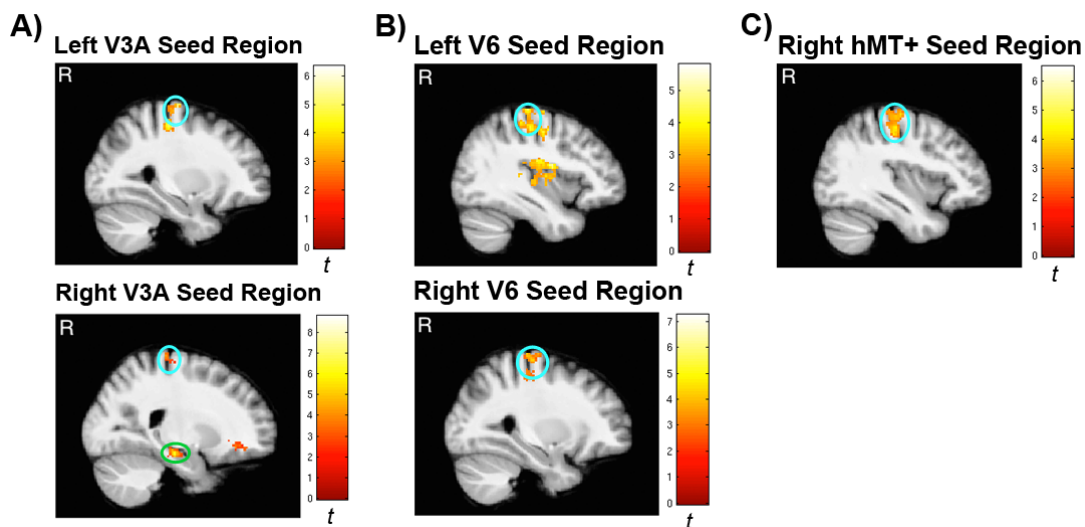


**Figure 4.6**

Survey perspective navigation: Optic flow processing regions are functionally connected with the primary motor cortex during Survey navigation. Functional connectivity analysis images have a statistical threshold of  $p < 0.01$  corrected for multiple comparisons with a voxel extent of 145. Light blue circles indicate primary motor cortex activations. Green circles indicate hippocampal activations.

A) Sagittal images of activations functionally connected with the left and right V3A seed regions during Survey perspective navigation. B) Sagittal images of activations functionally connected with the left and right V6 seed regions during Survey perspective navigation. C) Sagittal image of activations functionally connected with the right hMT+ seed region during Survey perspective navigation.



## 4.6 Chapter 4 Tables

Contrast	Seed Region	Area	Left		Right		
			T	MNI x,y,z	T	MNI x,y,z	
FPP Navigation	Left V3A	Hippocampus (Head)	4.05	-28,-12,-20	2.81	24,-8,-24	
Phase > ITI		Hippocampus (Body)	2.69	-28,-24,-14	3.92	32,-18,-16	
		Retrosplenial cortex	5.80	-2,-52,18	2.81	4,-50,14	
		Posterior parietal cortex	2.88	-2,-56,30	4.87	4,-54,30	
		Precuneus	5.49	-6,-46,34	3.14	10,-50,34	
		Superior parietal lobule	4.83	-36,-74,50			
		Angular gyrus	5.85	-54,-68,26	5.15	50,-48,28	
		Medial prefrontal cortex	4.08	-2,54,-4	4.45	4,58,6	
		Orbitofrontal gyrus	4.61	-26,36,-12	6.72	30,36,-12	
		Superior frontal gyrus (BA 9)	10.66	-10,64,26	6.38	14,56,34	
		Superior frontal gyrus (BA 6)	7.09	-10,30,52	6.28	24,40,50	
		Inferior frontal gyrus (BA 44/45)	6.63	-52,20,-4			
		Insula	4.44	-34,6,-8	5.47	32,8,-10	
		Amygdala	4.43	-16,-10,-18	3.98	24,-2,-18	
		Middle temporal gyrus	5.43	-44,14,-40	4.76	52,8,-34	
		Right V3A	Retrosplenial cortex	4.00	-4,-50,10	5.23	2,-52,16
			Precuneus	5.16	-2,-52,34	3.70	4,-56,38
			Superior parietal lobule	3.82	-34,-74,48		
			Angular gyrus	6.74	-54,-66,24	4.43	48,-50,24
			Medial prefrontal cortex	4.44	-4,52,-6	5.42	2,54,-12
	Superior frontal gyrus (BA 9)		6.29	-6,58,22	5.92	8,56,34	
	Middle temporal gyrus		6.52	-46,14,-32	8.82	52,8,-36	
Survey Navigation	Left V3A	Primary motor cortex/ Precentral gyrus			6.33	30,-16,70	
Phase > ITI		Insula			5.25	52,2,6	
		Inferior frontal gyrus			4.68	64,-6,14	
	Right V3A	Primary motor cortex/ Precentral gyrus	3.76	-12,-32,64	4.28	22,-28,72	
		Hippocampus (Body)			6.14	22,-20,-16	
		Medial prefrontal cortex			3.20	4,52,-6	
		Superior frontal gyrus (BA 4)	5.67	-34,24,54			
		Paracentral gyrus	4.33	-4,-28,58	3.51	6,-26,60	

**Table 4.1**

Brain regions functionally connected with left and right V3A seed regions during navigation from the first person perspective (FPP) and Survey perspective. MNI coordinates reflect cluster-center voxels. T-values reflect a statistical threshold of  $p < 0.01$ . Activation clusters survived cluster-threshold correction for multiple comparisons to  $p < 0.01$  with a minimum cluster size of 145.

Contrast	Seed Region	Area	Left T	MNI x,y,z	Right T	MNI x,y,z	
FPP Navigation	Left V6	Hippocampus (Head)			3.15	24,-16,-18	
Phase > ITI		Hippocampus (Body)			3.25	24,-26,-12	
		Retrosplenial cortex	4.45	-6,-52,16	2.69	6,-50,14	
		Posterior parietal cortex	4.01	-2,-64,28	4.34	6,-54,26	
		Precuneus	3.35	-4,-52,34	4.05	4,-50,32	
		Angular gyrus	6.18	-54,-66,24	5.12	52,-48,26	
		Medial prefrontal cortex	4.03	-4,56,-6	3.22	2,50,0	
		Insula			3.87	46,-10,16	
		Superior frontal gyrus (BA 9)	4.69	-12,62,24	3.98	8,56,34	
		Amygdala			3.18	18,-6,-16	
		Middle temporal gyrus			5.13	52,6,-34	
		Superior temporal gyrus			4.10	56,6,-12	
		Lateral occipital gyrus	3.25	-58,-64,12	8.39	58,-62,12	
		Right V6	Hippocampus (Head)			3.15	24,-10,-22
			Hippocampus (Body)			2.76	30,-20,-18
	Retrosplenial cortex		3.46	-2,-50,16	3.58	2,-52,18	
	Precuneus		3.23	-6,-48,34	3.14	-6,-46,34	
	Angular gyrus		5.85	-56,-64,24	5.98	52,-66,38	
	Medial prefrontal cortex		5.27	-6,62,-4	4.79	8,56,-12	
	Orbitofrontal cortex		3.77	-26,36,-12			
	Superior frontal gyrus (BA 9)		6.41	-4,54,36	4.44	8,58,32	
	Inferior frontal gyrus		5.56	-48,30,-4			
	Middle temporal gyrus		5.78	-58,0,-22	6.57	56,12,-32	
Survey Navigation	Left V6	Primary motor cortex/Precentral gyrus	5.82	-12,-30,66	5.67	14,-26,64	
Phase > ITI		Paracentral gyrus	3.84	-6,-26,66	4.35	6,-28,62	
		Superior frontal gyrus (BA 4)	5.66	-32,24,50			
		Insula	3.72	-38,-22,18	5.25	36,-2,18	
		Middle temporal gyrus			3.33	62,4,-20	
		Superior temporal gyrus			4.21	60,-6,-4	
	Right V6	Primary motor cortex/Precentral gyrus			6.88	12,-24,70	
		Insula			5.81	36,-20,14	
		Precentral gyrus			7.24	16,-26,72	
		Paracentral gyrus	4.92	-6,-26,66	4.37	6,-26,62	

**Table 4.2**

Brain regions functionally connected with left and right V6 seed regions during navigation from the first person perspective (FPP) and Survey perspective. MNI coordinates reflect cluster-center voxels. T-values reflect a statistical threshold of  $p < 0.01$ . Activation clusters survived cluster-threshold correction for multiple comparisons to  $p < 0.01$  with a minimum cluster size of 145.

Contrast	Seed Region	Area	Left		Right		
			T	MNI x,y,z	T	MNI x,y,z	
FPP Navigation	Right hMT+	Hippocampus (Head)			4.66	28,-6,-24	
Phase > ITI		Hippocampus (Body)			3.48	28,-24,-16	
		Retrosplenial cortex	3.03	-2,-54,12	5.23	4,-50,18	
		Posterior parietal cortex	4.61	-2,-64,26	3.78	4,-58,34	
		Precuneus	3.36	-4,-54,34	4.35	4,-50,36	
		Superior parietal lobule			4.48	40,-26,58	
		Angular gyrus	6.85	-46,-72,38	5.67	56,-60,30	
		Posterior cingulate gyrus	4.68	-4,-34,36	3.60	6,-30,34	
		Medial prefrontal cortex	6.50	-2,46,-4	6.16	2,48,-6	
		Orbitofrontal cortex	5.08	-34,38,-14			
		Superior frontal gyrus (BA 9)	4.40	-10,54,34	7.35	10,54,36	
		Insula			5.02	40,-10,10	
		Middle temporal gyrus	6.42	-46,14,-34	10.52	54,6,-36	
Survey Navigation		Right hMT+	Primary motor cortex/Precentral gyrus			4.05	36,-16,64
Phase > ITI			Superior parietal lobule			4.42	38,-22,48
	Paracentral gyrus		5.27	-6,-24,64	6.05	8,-26,66	
	Middle temporal gyrus				3.63	60,4,-20	

**Table 4.3**

Brain regions functionally connected with right human motion complex seed region during navigation from the first person perspective (FPP) and Survey perspective. MNI coordinates reflect cluster-center voxels. T-values reflect a statistical threshold of  $p < 0.01$ . Activation clusters survived cluster-threshold correction for multiple comparisons to  $p < 0.01$  with a minimum cluster size of 145.

**CHAPTER 5: Summary and Discussion**

## **5.1 Summary of results**

### **5.1.1 Restatement of original goals**

The three experiments discussed in this dissertation were conducted with the primary goal of examining the neural substrates underlying goal-directed navigation in humans. The first experiment, described in Chapter 2, examined navigation in a sparse, landmark-free environment. The experiment set out to examine brain regions active during map encoding and navigation from three different perspectives (first person, third person, and survey perspectives). The goal was to examine: 1) brain regions activated during successful goal-directed navigation from both the first person perspective (FPP) and the third person perspective (TPP) 2) brain regions that track proximity and time to a goal location during active navigation 3) brain regions that support the encoding of a large-scale environment required for goal-directed navigation.

The second experiment, described in Chapter 3, examined navigation in an environment in which a single landmark was added to an otherwise sparse, landmark-free environment. The goal of the second experiment was to examine: 1) brain regions that support successful goal-directed navigation with and without a landmark present in the environment 2) brain activation differences based on the absence or presence of a landmark during FPP navigation 3) brain regions that track proximity to a goal location during active navigation while utilizing an orienting landmark 4) brain regions that increase activation for larger location

computations when triangulating position between a landmark and an encoded goal.

The third experiment, described in Chapter 4, examined functional connections between brain regions sensitive to optic flow, specifically visual cortical areas V3A, V6 and hMT+, and brain regions active during goal-direction navigation.

### **5.1.2 Summary of results from Experiment 1**

The first experiment, described in Chapter 2, used functional MRI in humans to examine goal-directed navigation in an open field environment. The task was designed to require participants to encode survey-level spatial information and subsequently navigate to a goal location in either first person, third person, or survey perspectives. Critically, no distinguishing landmarks or goal location markers were present in the environment, thereby requiring participants to rely on path integration mechanisms for successful navigation. The analysis was focused on mechanisms related to successful navigation, brain activation differences during first person perspective (FPP) or third person perspective (TPP) navigation, and mechanisms tracking linear distance and time to the goal location. Successful navigation required translation of encoded survey-level map information for orientation and implementation of a planned route to the goal.

The results demonstrate that successful first and third person navigation trials recruited the anterior hippocampus more than trials when the goal location

was not successfully reached. When examining only successful trials, the retrosplenial and posterior parietal cortices were recruited for goal-directed navigation in both first person and third person perspectives. Unique to first person perspective navigation, the hippocampus was recruited to path integrate self-motion cues with location computations towards the goal location. Lastly, the results demonstrate that the hippocampus supports goal-directed navigation by actively tracking proximity to the goal throughout navigation. When utilizing path integration mechanisms in first person and third person perspective navigation, the posterior hippocampus tracks distance and time as participants approach the goal. These findings provide critical insight into the neural mechanisms by which we are able to utilize map-level representations of our environment to reach our navigational goals.

### **5.1.3 Summary of results from Experiment 2**

The second experiment, described in Chapter 3, used functional MRI to examine brain mechanisms related to navigational strategies used in an open field environment with or without the presence of an orienting landmark. A task was designed that required participants to encode survey-level spatial information and utilize these representations during navigation with or without an orienting landmark in an open field environment. On half the trials in the experiment, a single distinguishing landmark was included on the map and in the environment, which participants could use as an orientation cue. Following a delay,

participants actively navigated to the encoded goal location in either first person perspective (FPP) or Survey perspective. Critically, the goal location marker was only visible during the map presentation, but the landmark was visible in both map presentation and the navigation phase. The analysis was focused on mechanisms related to navigation, tracking Euclidean distance to the goal location, and precision based on the landmark's location in the environment.

The results demonstrate that successful first person and survey perspective navigation trials with and without a landmark recruited the anterior hippocampus more than trials when the goal location was not successfully reached. Unique to successful FPP and Survey perspective navigation trials with a landmark in the environment, the caudate nucleus was also recruited to integrate positioning calculations with location computations based on an orienting landmark. When examining only successful trials, the retrosplenial cortex, posterior parietal cortex, and parahippocampal cortex were recruited during successful FPP goal-directed navigation with a landmark present compared to successful FPP navigation trials with no landmark in the environment. The medial prefrontal cortex was recruited during successful FPP navigation with no landmark present in the environment contrasted against successful FPP navigation with a landmark present. These findings also indicate that the bilateral posterior hippocampus was modulated with participants' proximity to the goal location when triangulating position between the landmark and an encoded goal involved greater computations.



#### **5.1.4 Summary of results from Experiment 3**

The third experiment, described in Chapter 4, used a beta-series correlation methodology coupled with two fMRI tasks to examine functional interactions between optic flow responsive visual areas and brain regions required for ground-level path integration. Path integration, or the utilization of self-motion cues to track changes in orientation and location, relies heavily on the accurate perception of optic flow, the pattern of relative motion between the observer and environment. Functionally defined seed regions were selected from an optic flow simulation targeting the neural substrates of flow motion processing, specifically areas V3A, V6, and hMT+. fMRI data was collected using a navigation task in which participants utilized path integration mechanisms to successfully navigate to an encoded goal location (Experiment 1, Chapter 2). Navigation occurred in the first person perspective (FPP) or survey (Bird's eye) perspective. Patterns of activation during FPP navigation compared to the intertrial interval (ITI) indicate a functional relationship between the retrosplenial and posterior parietal cortices and V3A, V6, and hMT+ seed regions. The results also demonstrate that path integration-related connectivity exists between V3A, V6, and hMT+ seed regions and the head and body of the right hippocampus during FPP navigation. Taken together, these findings demonstrate functional connections between optic flow sensitive visual cortical areas V3A, V6, and hMT+ with areas that are involved in navigation including the retrosplenial cortex and hippocampus.

## **5.2 Discussion**

Goal-directed navigation is a fundamental process that we use in our everyday lives. Human neuroimaging research has started to provide insights into the brain regions that are recruited to support navigation. Since our world is full of landmarks, human spatial memory studies often target navigation in landmark-rich environments (Hartley et al., 2003; Brown et al., 2010; Zhang and Ekstrom, 2013). However, humans are able to successfully navigate in a landmark-free environment by continuously tracking adjustments in orientation and location using self-motion cues (Wolbers et al., 2007; Diekmann et al., 2009; Sherrill et al., 2013). This process, known as path integration, allows humans to maintain accurate self-localization and continuously update their spatial position towards a goal location. The experiments discussed in this dissertation examined goal-directed navigation that uses path integration mechanisms in environments with or without the presence of landmark cues.

### **5.2.1 Path integration signals for successful goal-directed navigation**

A spatially-tuned navigation system has been established in rodent studies of navigation. Cells within the system increase their firing rates based on different aspects of movement in space (O'Keefe and Nadal, 1978; Fyhn et al., 2004; Hafting et al., 2005; Taube et al., 1990; Sargolini et al., 2006). These findings have provided the foundation for a growing understanding of the mechanisms of spatial cognition in mammals, including humans. Studies of human navigation

have started to establish that these spatially-tuned regions may be present during human navigation and modulate activation based on navigationally driven actions (Ekstrom et al., 2003; Doeller et al., 2010; Baumann and Mattingley, 2010; Jacobs et al., 2013).

The results of this dissertation indicate that the hippocampus and regions of the parietal and prefrontal cortices support goal-directed navigation based on path integration mechanisms. In order to be successful in navigating to your goal location, participants had to orient themselves in the environment and implement a planned route to the goal. Rodent models of navigation theorize place cell representations of location drive expectations of reward for goal locations (Foster et al., 2000; Johnson and Redish, 2007). In particular, the rodent ventral hippocampus, the analog for the human anterior hippocampus, has been associated with context and reward processing (Moser and Moser, 1998; Ferbinteanu and McDonald, 2001; Fanselow and Dong, 2010; Royer et al., 2010) suggesting goal locations may be represented by the anterior hippocampus. This dissertation's results indicate that if a landmark is present or absent in an environment, the anterior hippocampus was recruited during successful navigation to a goal location. This recruitment may serve to successfully integrate orientation with a planned route. Path integration mechanisms can be used to build a metric representation of position and orientation in an environment; however, stable representations such as landmarks may calibrate these updates to reduce navigational errors that may accumulate. When an orienting landmark

is present in the environment, the caudate nucleus is recruited in addition to the anterior hippocampus during successful navigation. Since the landmark may serve as a juncture along an encoded route (Epstein and Vass, 2013) or as an egocentric cue in the environment (Baumann et al., 2010; Wegman et al., 2014), the caudate nucleus may be recruited to incorporate these types of route-based navigational strategies towards the goal location as represented by the hippocampus during successful goal-directed navigation.

### **5.2.2 The hippocampus tracks distance and time during navigation**

Spatial coding within the hippocampus is relatively novel in studies of human navigation. Results in this dissertation indicate that the human hippocampus increases in activation based on goal proximity, both when accounting for a landmark and not, and time elapsed. In environments where path integration mechanisms are crucial to navigational success, coding of distance from your current location to the goal is paramount. Previous human navigation studies found that place-goal conjunctive cells in the human hippocampus increased their firing rate when a specific goal was viewed from a specific location (Ekstrom et al., 2003). The discovery of these cells may be indicative of a hippocampal role in associating goal-related contextual inputs with place. The results from this dissertation demonstrate that the posterior hippocampus was responsive to the shortest linear distance between participants' current location and the goal location from moment-to-moment as they navigate through the

environment. Furthermore, the hippocampus has spatial coding for goal proximity regardless of if a landmark was present or absent in the environment. If a landmark is present in the environment, the results of this dissertation indicate that the hippocampus accounts for navigational accuracy to a goal relative to a visible landmark.

Recent animal models have suggested that a small portion of cells in the hippocampus may have temporally tuned patterns of activity in addition to spatially specific behavior (Pastalkova et al., 2008; MacDonald et al., 2011; Kraus et al., 2013). These “time cells” may represent a fundamental role of the hippocampus in providing an internal representation of elapsed time, supporting memory for the timing of discrete events. Since time and distance are fundamentally linked during navigation, activations in the hippocampus correlated with proximity to the goal location may, in part, represent cells sensitive to elapsed time. Results of this dissertation also indicated that activity in posterior left hippocampus, which significantly tracked distance to the goal, was also correlated with time across the FPP navigation phase. However, direct comparison of parameter estimates extracted from our distance to goal and time analyses demonstrate a significantly stronger modulation of activity by distance than time in the left hippocampus. This result suggests that during FPP navigation, tracking distance to a goal location has a significant impact on bilateral signal in the hippocampus. Taken together, results of this dissertation indicate that the hippocampus tracks distance and time during FPP navigation

and makes distance estimations between current location and a goal location relative to a landmark.

### **5.2.3 Orientation towards a goal location is supported by the parietal cortex**

Previous research suggests that the parietal cortex has a fundamental role in combining visual and motion information, both crucial processes for an allocentric-to-egocentric navigational transformation (Hasal and Nachev, 2007; Save and Poucet, 2009). Human neuroimaging studies often associate the retrosplenial cortex (RSC) and posterior parietal cortex (PPC) with landmark-based navigation (Hartley et al., 2003; Rosenbaum et al., 2004; Spiers and Maguire, 2006; Byrne et al., 2007). Results from this dissertation suggest that common recruitment of these brain regions indicates they play a more basic role in spatial mapping and orientation through path integration. Human neuroimaging studies suggest RSC integrates route-based spatial information with self-motion cues (Wolbers and Buchel, 2005) to orient and direct movement to a goal location (Epstein, 2008; Baumann et al., 2010). The nearby PPC is activated in human navigation tasks requiring in coordination of egocentric movements with allocentric information (Galati et al., 2010; Howard et al., 2014). Results from this dissertation demonstrate that the retrosplenial cortex and posterior parietal cortex were recruited for successful FPP navigation, and these regions were recruited during FPP navigation with an orienting landmark compared to trials with no landmark in the environment. When an orienting landmark is present in the

environment, these regions selectively processes egocentric heading signals based on the landmark location when successfully navigating to a goal location. The results of this dissertation indicate PPC activity may support the integration of planned route actions with the spatial relationship between current location and orientation towards a cue in the environment such as their representation of the goal location or a landmark. Orientation towards these environmental cues may be represented by the RSC.

#### **5.2.4 Optic flow processing regions are functionally connected with brain regions supporting navigation**

Path integration also relies heavily on the perception of optic flow. Visual information about our own movement, or ego-movement, in relation to the environment is an essential component to updating our self-motion cues while navigating. Computational models suggest that visual input from optic flow provides information about egocentric motion and influences firing patterns in cells that are critical for rodent navigation (Raudies et al., 2012; Raudies & Hasselmo, 2012). Self-motion cues are essential to navigators when required to track adjustments in orientation and location using path integration mechanisms. Previous retinotopic mapping and fMRI studies have established a continuum of several motion-selective regions, including visual cortical areas V3A, V6 and hMT+ (Tootell et al., 1997; Seiffert et al., 2003; Pitzalis et al., 2006; Duffy, 2009; Cardin and Smith, 2010; Pitzalis et al., 2010). Results from the optic flow task in

this dissertation demonstrated optic flow responsive activity within visual cortical areas V3A, V6, and hMT+. Navigation in the tasks discussed in this dissertation required updating location and orientation while moving towards an encoded goal location in a landmark-free environment, suggesting that path integration based on self-motion cues is involved in performing the tasks. Results discussed in this dissertation indicate that visual motion processing regions were functionally connected with path integration-related brain regions including the retrosplenial cortex, posterior parietal cortex, hippocampus, and medial prefrontal cortex, to navigate using optic flow. Path integration tracks changes in location and orientation (Wolbers et al., 2007), provides vector knowledge about locations encountered during movement (Weiner et al., 2011), and updates positioning in an environment towards an intended goal or remembered location (Sherrill et al., 2013; Kalia et al, 2013). Establishing functional connections between path integration and regions known for visual motion processing, specifically visual cortical areas V3A, V6, and hMT+, further our understanding of how neural systems interact during goal-directed navigation.

### **5.3 Conclusions**

The results of these experiments help us understand human brain mechanisms related to path integration and goal-directed navigation in an open field environment. These studies extend previous work in humans by exploring how navigation takes place in an open field environment, as opposed to a landmark-



rich environment. The experiments presented here provide evidence that the retrosplenial cortex and posterior parietal cortex are recruited during successful first person and third person navigation to a goal location based on encoded spatial representations of the environment. The hippocampus is additionally recruited during first person perspective goal-directed navigation. As landmarks are introduced into our navigational space, the caudate nucleus is recruited to incorporate route-based navigational strategies utilizing an orienting landmark for successful goal-directed navigation. Results in this dissertation indicate that visual cortical areas V3A, V6, and hMT+ are functionally connected with the retrosplenial cortex and hippocampus when processing optic flow to successfully navigate in an open field environment. Furthermore, spatial coding is represented in the hippocampus of humans in order to make us more accurate navigators to our intended goal when relying on path integration. Together, the experiments described in this dissertation have extended our understanding of brain mechanisms related to goal-directed navigation.

## BIBLIOGRAPHY

- Aguirre GK, D'Esposito M (1999). Topographical disorientation: A synthesis and taxonomy. *Brain*, 122:1613-28.
- Andersson JL, Hutton C, Ashburner J, Turner R, Friston K (2001). Modeling geometric deformations in EPI time series. *Neuroimage*, 13:903-19.
- Ashburner J (2007). A fast diffeomorphic image registration algorithm. *Neuroimage*, 38:95-113.
- Baumann O, Chan E, Mattingley JB (2010). Dissociable neural circuits for encoding and retrieval of object locations during active navigation in humans. *Neuroimage*, 49:2816-25.
- Baumann O, Mattingley JB (2010). Medial parietal cortex encodes perceived heading direction in humans. *Journal of Neuroscience*, 30:12897-901.
- Bremmer F, Kubischik M, Pekel M, Hoffmann KP, Lappe M (2010). Visual selectivity for heading in monkey area MST. *Experimental Brain Research*, 200:51-60.
- Brown TI, Ross RS, Keller JB, Hasselmo ME, Stern CE (2010). Which way was I going? Contextual retrieval supports the disambiguation of well learned overlapping navigational routes. *Journal of Neuroscience*, 30:7414-22.
- Brown TI, Ross RS, Tobyn SM, Stern CE (2012). Cooperative interactions between hippocampal and striatal systems support flexible navigation. *Neuroimage*, 60:1316-1330.
- Brown TI, Stern CE (2013). Contributions of medial temporal lobe and striatal memory systems to learning and retrieving overlapping spatial memories. *Cerebral Cortex*, Electronic publication ahead of print.
- Byrne P, Becker S, Burgess N (2007). Remembering the past and imagining the future: A neural model of spatial memory and imagery. *Psychological Review*, 114:340-375.
- Cardin V, Smith AT (2010). Sensitivity of human visual and vestibular cortical regions to egomotion-compatible visual stimulation. *Cerebral Cortex*, 20:1964-1973.
- Cardin V, Smith AT (2011). Sensitivity of human visual cortical area V6 to stereoscopic depth gradients associated with self-motion. *Journal of*

*Neurophysiology*, 106:1240-1249.

Chrastil ER (2013). Neural evidence supports a novel framework for spatial navigation. *Psychonomic Bulletin Review*, 20:208-227.

Chrastil ER, Brown TI, Aselcioglu I, Hasselmo ME, Stern CE (under review). Brain network sensitive to heading direction in humans mirrors head direction regions in rats.

Cooper BG, Manka TF, Mizumori SJ (2001). Finding your way in the dark: the retrosplenial cortex contributes to spatial memory and navigation without visual cues. *Behavioral Neuroscience*, 115:1012-28.

Cooper BG, Mizumori SJ (2001). Temporary inactivation of the retrosplenial cortex causes a transient reorganization of spatial coding in the hippocampus. *Journal of Neuroscience*, 21:3986-4001.

Deshmukh SS, Knierim JJ (2013). Influence of local objects on hippocampal representation: Landmark vectors and memory. *Hippocampus*, 23:253-67.

Doeller CF, King JA, Burgess N (2008). Parallel striatal and hippocampal systems for landmarks and boundaries in spatial memory. *Proceedings of the National Academy of Sciences USA*, 105:5915-5920.

Doeller CF, Barry C, Burgess N (2010). Evidence for grid cells in a human memory network." *Nature*, 463: 657-661.

Duffy CJ (2009). Visual motion processing in aging and Alzheimer's disease: neuronal mechanisms and behavior from monkey to man. *Annals of the New York Academy of Science*, 1170:736-44.

Dukelow SP, DeSouza JF, Culham JC, van den Berg AV, Menon RS, Vilis T (2001). Distinguishing subregions of the human MT+ complex using visual fields and pursuit eye movements. *Journal of Neurophysiology*, 86:1991-2000.

Dupret D, O'Neill J, Pleydell-Bouverie B, Csicsvari J (2010). The reorganization and reactivation of hippocampal maps predict spatial memory performance. *Nature Neuroscience*, 13:995-1002.

Durant S, Zanker JM (2012). Variation in the Local Motion Statistics of Real-Life Optic Flow Scenes. *Neural Computation*, 24:1781-805.

Ekstrom A, Kahana M, Caplan J, Fields T, Isham E, Newman E, Fried I (2003).

Cellular networks underlying human spatial navigation. *Nature*, 425:184-87.

- Ekstrom AD, Bookheimer SY (2007). Spatial and temporal episodic memory retrieval recruits dissociable functional networks in the human brain. *Learning and Memory*, 14:645-54.
- Elduayen C, Save E (2014). The retrosplenial cortex is necessary for path integration in the dark. *Behavioral Brain Research*, Electronic publication ahead of print.
- Epstein RA, Parker WE, Feiler AM (2007). Where am I now? Distinct roles for parahippocampal and retrosplenial cortices in place recognition. *Journal of Neuroscience*, 27:6141-149.
- Epstein RA, Kanwisher N (1998). A cortical representation of the local visual environment. *Nature*, 392:598-601.
- Epstein RA, Parker WE, Feiler AM (2007). Where am I now? Distinct roles for parahippocampal and retrosplenial cortices in place recognition. *Journal of Neuroscience*, 27:6141-49.
- Epstein RA (2008). Parahippocampal and retrosplenial contributions to human spatial navigation. *Trends in Cognitive Sciences*, 12:388-96.
- Epstein RA, Vass LK (2013). Neural systems for landmark-based wayfinding in humans. *Philosophical Transactions of the Royal Society*, 369: 20120533.
- Erdem UM, Hasselmo ME (2012). A goal-directed spatial navigation model using forward trajectory planning based on grid cells. *European Journal of Neuroscience*, 35:916-31.
- Erdem UM, Milford MJ, Hasselmo ME (2014). A hierarchical model of goal directed navigation selects trajectories in a visual environment. *Neurobiology of Learning and Memory*, Electronic publication ahead of print.
- Etchemendy N, Bohbot VD (2007). Spontaneous navigational strategies and performance in the virtual town. *Hippocampus*, 17:595-9.
- Fanselow MS, Dong HW (2010). Are the dorsal and ventral hippocampus functionally distinct structures? *Neuron*, 65:7-19.
- Ferbinteanu J, McDonald RJ (2001). Dorsal/ventral hippocampus, fornix, and

- conditioned place preference. *Hippocampus*, 11:187-200.
- Fischer E, Bulthoff HH, Logothetis NK, Bartels A (2012). Human areas V3A and V6 compensate for self-induced planar visual motion. *Neuron*, 73:1228-1240.
- Foo P, Warren WH, Duchon A, Tarr MJ (2005). Do humans integrate routes into a cognitive map? Map- versus landmark-based navigation of novel shortcuts. *Journal of Experimental Psychology: Learning, Memory, and Cognition*, 31:195-215.
- Foster, DJ, Morris RG, Dayan P (2000). A model of hippocampally dependent navigation, using the temporal difference learning rule. *Hippocampus*, 10:1-16.
- Fyhn M, Molden S, Witter MP, Moser EI, Moser MB (2004). Spatial representation in the entorhinal cortex. *Science*, 305:1258-64.
- Galati G, Pelle G, Berthoz A, Committeri G (2010). Multiple reference frames used by the human brain for spatial perception and memory. *Experimental Brain Research*, 206:109-20.
- Gallistel CR (1990). *The organization of learning*. Cambridge, MA: MIT Press.
- Gothard KM, Skaggs We, McNaughton BL (1996). Binding of hippocampal CA1 neural activity to multiple reference frames in a landmark-based navigation task. *Journal of Neuroscience*, 16:832-35.
- Gothard KM, Hoffman KL, Battaglia FP, McNaughton BL (2001). Dentate gyrus and CA1 ensemble activity during spatial reference frame shifts in the presence and absence of visual input. *Journal of Neuroscience*, 21:7284-92.
- Hafting T, Fyhn M, Molden S, Moser MB, Moser EI (2005). Microstructure of a spatial map in the entorhinal cortex. *Nature*, 436:801-6.
- Hartley T, Maguire EA, Spiers HJ, Burgess N (2003). The well-worn route and the path less traveled: Distinct neural bases of route following and wayfinding in humans. *Neuron*, 37:877-88.
- Hasselmo ME (2008). Temporally structured replay of neural activity in a model of entorhinal cortex, hippocampus and postsubiculum. *European Journal of Neuroscience*, 28:1301-15.

- Hasselmo ME (2009). A model of episodic memory: mental time travel along encoded trajectories using grid cells. *Neurobiology of Learning and Memory*, 92:559-73.
- Hasselmo ME, Stern CE (2014). Theta rhythm and the encoding and retrieval of space and time. *Neuroimage*, 85:656-666.
- Howard LR, Javadi Ah, Yu Y, Mill RD, Morrison LC, Knight R, Loftus MM, Staskute L, Spiers HJ (2014). The hippocampus and entorhinal cortex encode the path and Euclidean distances to goals during navigation. *Current Biology*, 24:1331-40.
- Howard MW, MacDonald CJ, Tiganj Z, Shankar KH, Du Q, Hasselmo ME, Eichenbaum H (2014). A unified mathematical framework for coding time, space, and sequences in the hippocampal region. *Journal of Neuroscience*, 34:4692-707.
- Huk AC, Dougherty RF, Heeger DJ (2002). Retinotopy and functional subdivision of human areas MT and MST. *Journal of Neuroscience*, 22:7195-205.
- Iaria G, Petrides M, Dagher A, Pike B, Bohbot VD (2003). Cognitive strategies dependent on the hippocampus and caudate nucleus in human navigation: Variability and change with practice. *Journal of Neuroscience*, 23:5945-5952.
- Igloi K, Doeller C, Berthoz A, Rondi-Reig L, Burgess N (2010). Lateralized human hippocampal activity predicts navigation based on sequence or place memory. *Proceedings of the National Academy of Sciences USA*, 107:14466-14471.
- Jacobs J, Weidemann CT, Miller JF, Solway A, Burke JF, Wei XX, Suthana N, Sperling M, Sharan AD, Fried I, Kahana MJ (2013). Direct recordings of grid-like neuronal activity in human spatial navigation. *Nature Neuroscience*, 16:1188-1190.
- Jankowski J, Scheef L, Huppe C, Boecker H (2009). Distinct striatal regions for planning and executing novel and automated movement sequences. *Neuroimage*, 44:1369-79.
- Janzen G, van Turenout M (2004). Selective neural representation of objects relevant for navigation. *Nature Neuroscience*, 7:673-77.
- Janzen G, Westeijn CG (2007). Neural representation of object location and route direction: An event-related fMRI study. *Brain Research*, 1165:116-

25.

- Johnson A, Redish AD (2007). Neural ensembles in CA3 transiently encode paths forward of the animal at a decision point. *Journal of Neuroscience*, 27:12176-89.
- Kalia AA, Schrater PR, Legge GE (2013). Combining path integration and remembered landmarks when navigating without vision. *PLoS One*, 8: e72170.
- Kessels RP, van Doormaal A, Janzen G (2011). Landmark recognition in Alzheimer's dementia: spared implicit memory for objects relevant for navigation. *PLoS One*, 6:e18611.
- Kim S, Sapiurka M, Clark RE, Squire LR (2013). Contrasting effects of path integration after hippocampal damage in humans and rats. *Proceedings of the National Academy of Sciences USA*, 110:4732-7.
- Knierim JJ, Kudrimoti HS, McNaughton BL (1995). Place cells, head direction cells, and the learning of landmark stability. *Journal of Neuroscience*, 15:1648-59.
- Knierim JJ (2002). Dynamic interactions between local surface cues, distal landmarks, and intrinsic circuitry in hippocampal place cells. *Journal of Neuroscience*, 22:6254-64.
- Knierim JJ, Rao G (2003). Distal landmarks and hippocampal place cells: Effects of relative translation versus rotation. *Hippocampus*, 13:604-17.
- Kraus BJ, Robinson RJ, White JA, Eichenbaum H, Hasselmo ME (2013). Hippocampal "time cells": Time versus path integration. *Neuron*, 78:1090-1101.
- Leutgeb S, Ragozzino K, Mizumori S (2000). Convergence of head direction and place information in the CA1 region of hippocampus. *Neuroscience*, 100:11-19.
- Logan DJ, Duffy CJ (2006). Cortical area MSTd combines visual cues to represent 3-D self-movement. *Cerebral Cortex*, 16:1494-507.
- Maldjian JA, Laurienti PJ, Kraft RA, Burdette JH (2003). An automated method for neuroanatomic and cytoarchitectonic atlas-based interrogation of fMRI data sets. *Neuroimage*, 19:1233-39.

- MacDonald CJ, Lepage KQ, Eden UT, Eichenbaum H (2011). Hippocampal “time cells” bridge the gap in memory for discontinuous events. *Neuron*, 71:737-49.
- Maguire EA, Burgess N, Donnett JG, Frackowiak RS, Frith CD, O’Keefe J (1998). Knowing where and getting there: a human navigation network. *Science*, 280:921-4.
- McNaughton BL, Barnes CA, O’Keefe J (1983). The contributions of position, direction, and velocity to single unit activity in the hippocampus of freely-moving rats. *Experimental Brain Research*, 52:41-9.
- McNaughton BL, Battaglia FP, Jensen O, Moser EI, Moser MB (2006). Path integration and the neural basis of the ‘cognitive map’. *Nature Reviews Neuroscience*, 7:663-78.
- Monchi O, Petrides M, Strafella AP, Worsley KJ, Doyon J (2006). Functional role of the basal ganglia in the planning and execution of actions. *Annals of Neurology*, 59:257-64.
- Morgan LK, Macevoy SP, Aguirre GK, Epstein RA (2011). Distances between real-world locations are represented in the human hippocampus. *Journal of Neuroscience*, 31:1238-45.
- Morris RGM (1981). Spatial localization does not require the presence of local cues. *Learning and Motivation*, 12:239-260.
- Moser MB, Moser EI (1998). Functional differentiation in the hippocampus. *Hippocampus*, 8:608-19.
- O’Keefe J, Dostrovsky J (1971). The hippocampus as a spatial map: Preliminary evidence from unit activity in the freely-moving rat. *Brain Research*, 34:171-75.
- O’Keefe J (1976). Place units in the hippocampus of the freely moving rat. *Experimental Neurology*, 51:78-109.
- O’Keefe J, Nadel L (1978). The hippocampus as a cognitive map. Oxford: Clarendon Press.
- O’Keefe J, Burgess N (2005). Dual phase and rate coding the hippocampal place cells: theoretical significance and relationship to entorhinal grid cells. *Hippocampus*, 15:853-66.



- Park S, Chun MM (2009). Different roles of the parahippocampal place area (PPA) and retrosplenial cortex (RSC) in panoramic scene perception. *Neuroimage*, 47:1747-56.
- Pastalkova E, Itskov V, Amarasingham A, Buzsáki G (2008). Internally generated cell assembly sequences in the rat hippocampus. *Science*, 321:1322-27.
- Peuskens H, Sunaert S, Dupont P, Van Hecke P, Orban GA (2001) Human brain regions involved in heading estimation. *Journal of Neuroscience*, 21:2451-2461.
- Pfeiffer BE, Foster DJ (2013). Hippocampal place-cell sequences depict future paths to remembered goals. *Nature*, 497:74-9.
- Philbeck JW, Behrmann M, Levy L, Potolicchio SJ, Caputy AJ (2004). Path integration deficits during linear locomotion after human medial temporal lobectomy. *Journal of Cognitive Neuroscience*, 16:510-20.
- Pitzalis S, Galletti C, Huang RS, Patria F, Committeri G, Galati G, Fattori P, Sereno MI (2006). Wide-field retinotopy defines human cortical visual area v6. *Journal of Neuroscience*, 26:7962-7973.
- Pitzalis S, Sereno MI, Committeri G, Fattori P, Galati G, Patria F, Galletti C (2010). Human v6: the medial motion area. *Cerebral Cortex*, 20:411-424.
- Pothuizen HH, Aggleton JP, Vann SD (2008). Do rats with retrosplenial cortex lesions lack direction? *European Journal of Neuroscience*, 28:2486-98.
- Putcha D, Ross R, Rosen M, Norton D, Cronin-Golomb A, Somers D, Stern C (2014). Functional correlates of optic flow motion processing in Parkinson's disease. *Frontiers in Integrative Neuroscience*, 8:57-72.
- Raudies F, Hasselmo ME (2012). Modeling boundary vector cell firing given optic flow as a cue. *PLoS Comput Biol*, 8:e1002553.
- Raudies F, Mingolla E, Hasselmo ME (2012). Modeling the influence of optic flow on grid cell firing in the absence of other cues. *Journal of Computational Neuroscience*, 33:475-93.
- Rissman J, Gazzaley A, D'Esposito M (2004). Measuring functional connectivity during distinct stages of a cognitive task. *Neuroimage*, 23:752-763.
- Rodriguez PF (2010). Human navigation that requires calculating heading

vectors recruits parietal cortex in a virtual and visually sparse water maze task in fMRI. *Behavioral Neuroscience*, 124:532-40.

- Rosenbaum RS, Ziegler M, Winocur G, Grady CL, Moscovitch M (2004). "I Have Often Walked Down This Street Before": fMRI Studies on the Hippocampus and Other Structures During Mental Navigation of an Old Environment. *Hippocampus*, 14:826-35.
- Ross RS, Brown TI, Stern CE (2009). The retrieval of learned sequences engages the hippocampus: Evidence from fMRI. *Hippocampus*, 19:790-9.
- Royer S, Sirota A, Patel J, Buzsáki G (2010). Distinct representations and theta dynamics in dorsal and ventral hippocampus. *Journal of Neuroscience*, 30:1777-87.
- Sargolini F., Fyhn M., Hafting T., McNaughton B., Witter M., Moser M.B., Moser E. (2006). Conjunctive representation of position, direction, and velocity in entorhinal cortex. *Science*, 312: 758-62.
- Sato N, Sakata H, Tanaka Y, Taira M (2006). Navigation-associated medial parietal neurons in monkeys. *Proceedings of the National Academy of Sciences USA*, 103:17001-06.
- Save E, Poucet B (2009). Role of the parietal cortex in long-term representation of spatial information in the rat. *Neurobiology of Learning and Memory*, 91:172-78.
- Seiffert, AE, Somers, DC, Dale, AM, Tootell, RBH (2003). Functional MRI studies of human visual motion perception: texture, luminance, attention and after-effects. *Cerebral Cortex*, 13:340–349.
- Sherrill KR, Erdem UM, Ross RS, Brown TI, Hasselmo ME, Stern CE (2013). Hippocampus and retrosplenial cortex combine path integration signals for successful navigation. *Journal of Neuroscience*, 33:19304-19313.
- Shrager Y, Kirwan CB, Squire LR (2008). Neural basis of the cognitive map: Path integration does not require the hippocampus or medial entorhinal cortex. *Proceedings of the National Academy of Sciences USA*, 105:12034-38.
- Snyder LH, Batista AP, Andersen RA (1997). Coding of intention in the posterior parietal cortex. *Nature*, 386:167-70.
- Snyder LH, Batista AP, Andersen RA (2000). Intention-related activity in the

- posterior parietal cortex: A review. *Vision Research*, 40:1433-41.
- Spiers HJ, Maguire EA (2006). Thoughts, behavior, and brain dynamics during navigation in the real world. *Neuroimage*, 31:1826-40.
- Spiers HJ, Maguire EA (2007). A Navigational Guidance System in the Human Brain. *Hippocampus*, 17:618-26.
- Steele RJ, Morris RG (1999). Delay-dependent impairment of a matching-to-place task with chronic and intrahippocampal infusion of the NMDA-antagonist D-AP5. *Hippocampus*, 9:118-36.
- Straw AD (2008). Vision egg: An open-source library for realtime visual stimulus generation. *Frontiers in Neuroinformatics*, 2:4 doi: 10.3389/neuro.11.004.2008.
- Swisher JD, Halko MA, Merabet LB, McMains SA, Somers DC (2007). Visual topography of human intraparietal sulcus. *Journal of Neuroscience*, 27:5326-5337.
- Taube JS, Muller RU, Ranch JB Jr. (1990). Head-direction cells recorded from the postsubiculum in freely moving rats. *Journal of Neuroscience*, 10:420-35.
- Taube J (1995). Head direction cells recorded in the anterior thalamic nuclei of freely moving rats. *Journal of Neuroscience*, 15:70-86.
- Taube JS (2007). The head direction signal: Origins and sensory-motor integration. *Annual Review of Neuroscience*, 30:181-207.
- Tootell RB, Mendola JD, Hadjikhani NK, Ledden PJ, Liu AK, Reppas JB, Sereno MI, Dale AM (1997). Functional analysis of V3A and related areas in human visual cortex. *Journal of Neuroscience*, 17:7060-7078.
- Vann S, Aggleton J, and Maguire E (2009). What does the retrosplenial cortex do? *Nature Reviews Neuroscience*, 10:792-802.
- Vass LK, Epstein RA (2013). Abstract representations of location and facing direction in the human brain. *Journal of Neuroscience*, 33:6133-42.
- Viard A, Doeller C, Hartley T, Bird C, Burgess N (2011). Anterior hippocampus and goal-directed spatial decision making. *Journal of Neuroscience*, 31:4613-21.

- Wandell BA, Dumoulin SO, Brewer AA (2007). Visual field maps in human cortex. *Neuron*, 56:366-383.
- Wegman J, Janzen G (2014). Encoding and retrieval of landmark-related spatial cues during navigation: An fMRI study. *Hippocampus*, 24:853-68.
- Weniger G, Siemerikus J, Schmidt-Samoa C, Mehlitz M, Baudewig J, Dechent P, Irle E (2010). The human parahippocampal cortex subserves egocentric spatial learning during navigation in a virtual maze. *Neurobiology of Learning and Memory*, 93:46-55.
- Weiner J, Berthoz A, Wolbers T (2011). Dissociable cognitive mechanisms underlying path integration. *Experimental Brain Research*, 208:61-71.
- Whitlock JR, Sutherland RJ, Witter MP, Moser MB, Moser EI (2008). Navigating from hippocampus to parietal cortex. *Proceedings of the National Academy of Sciences USA*, 105:14755-62.
- Whitlock J, Pfuhl G, Dagslott N, Moser MB, Moser EI (2012). Functional split between parietal and entorhinal cortices in the rat. *Neuron*, 73:789-802.
- Wolbers T, Buchel C (2005). Dissociable retrosplenial and hippocampal contributions to successful formation of survey representations. *Journal of Neuroscience* 25:3333-40.
- Wolbers T, Wiener JM, Mallot HA, Buchel C (2007). Differential recruitment of the hippocampus, medial prefrontal cortex, and the human motion complex during path integration in humans. *Journal of Neuroscience*, 27:9408-16.
- Worsley CL, Recce M, Spiers HJ, Marley J, Polkey CE, Morris RG (2001). Path integration following temporal lobectomy in humans. *Neuropsychologia*, 39:452-64.
- Xu J, Evensmoen HR, Lehn H, Pintzka CWS, Håberg AK (2010). Persistent posterior and transient anterior medial temporal lobe activity during navigation. *Neuroimage*, 52:1654-66.
- Zhang H, Ekstrom A (2013). Human neural systems underlying rigid and flexible forms of allocentric spatial representation. *Human Brain Mapping*, 34:1070-87.

## CURRICULUM VITAE

### KATHERINE R.M. SHERRILL

[katherinesherrill@gmail.com](mailto:katherinesherrill@gmail.com)

#### OFFICE

The Preston Laboratory  
Center for Learning and Memory  
University of Texas at Austin  
100 East 24<sup>th</sup> Street, NHB 3.340  
Austin, TX 78712

#### EDUCATION

- Fall 2010 – Fall 2014      Doctoral degree candidate (Ph.D.)  
*Boston University*, Boston, MA  
Graduate School of Arts and Sciences  
Department of Psychological and Brain Sciences  
Brain, Behavior and Cognition Program
- Qualification Exam: November 15, 2012
  - Dissertation Prospectus Hearing: January 15, 2014
  - Dissertation Defense: September 30, 2014
  - Graduation Date: January 25, 2015
- Fall 2008 – Spring 2009      Master of Arts, Psychology  
*Boston University*, Boston, MA  
Graduate School of Arts and Sciences
- Fall 2001 – Spring 2005      Bachelor of Arts, Biology, Minor in Psychology  
*Texas A&M University*, College Station, TX  
College of Science

#### Study Abroad

Summer 2004      *Université de Caen*, Caen, France

#### RESEARCH EXPERIENCE

- Spring 2015 – Present      **Postdoctoral Fellow** – University of Texas, Austin  
The Preston Laboratory  
Principal Investigator: Alison Preston, Ph.D.
- Fall 2010 – Fall 2014      **Doctoral Degree Candidate** – Boston University  
Cognitive Neuroimaging Laboratory  
Principal Investigator: Chantal Stern, D.Phil.
- Spring 2009 – Fall 2010      **Research Assistant** – Boston University  
Cognitive Neuroimaging Laboratory

Principal Investigator: Chantal Stern, D.Phil.

Fall 2008 – Spring 2009

**Directed Study** – Boston University  
Cognitive Neuroimaging Laboratory  
Principal Investigator: Chantal Stern, D.Phil.  
Advisor: Robert Ross, Ph.D.

Spring 2004

**Research Assistant** – Texas A&M University  
Social Psychology Department  
Advisor: Wendy Wood, Ph.D.

## PUBLISHED ARTICLES

- **Sherrill, K.R.**, Erdem, U.M., Ross, R.S., Brown, T.I., Hasselmo, M.E., Stern, C.E. (2013). Hippocampus and retrosplenial cortex combine path integration signals for successful navigation. *Journal of Neuroscience*, 33:19304-13.
- Ross, R.S., **Sherrill, K.R.**, C.E. Stern (2011). The hippocampus is functionally connected to the striatum and orbitofrontal cortex during context dependent decision making. *Brain Research*, 1423: 53-66.

## MANUSCRIPTS IN PREPARATION

- **Sherrill, K.R.**, Chrastil, E.R., Ross, R.S., Erdem, U.M., Hasselmo, M.E., Stern, C.E. Functional connections between optic flow areas and navigationally responsive brain regions during goal-directed navigation.
- **Sherrill, K.R.**, Chrastil, E.R., Erdem, U.M., Brown, T.I., Ross, R.S., Hasselmo, M.E., Stern, C.E. Neural correlates highlight interactions between path integration and landmark-based strategies during goal-directed navigation.
- **Sherrill, K.R.**, Chrastil, E.R., Aselcioglu, I., Erdem, U.M., Brown, T.I., Hasselmo, M.E., Stern, C.E. Structural differences in hippocampal and entorhinal cortex gray matter volume support individual differences in first-person perspective navigational ability.
- Chrastil, E.R., **Sherrill, K.R.**, Hasselmo, M.E., Stern, C.E. Hippocampus and retrosplenial cortex support encoding and maintenance of distance and orientation information used in human path integration.
- Chrastil, E.R., **Sherrill, K.R.**, Hasselmo, M.E., Stern, C.E. There and back again: Hippocampus and retrosplenial cortex track homing distance during human path integration.
- Chrastil, E.R., **Sherrill, K.R.**, Aselcioglu, I., Stern, C.E. Structural differences in gray matter volume correspond to individual differences in spatial navigation ability.
- Ross, R.S., **Sherrill, K.R.**, Stern, C.E. Prospective and retrospective retrieval of sequential associations of varying distance.

## CONFERENCE ABSTRACTS AND POSTERS PRESENTATIONS

- **Sherrill, K.R.**, Chrastil, E.R., Aselcioglu, I., Hasselmo, M.E., Stern, C.E. “Structural differences in hippocampal and entorhinal gray matter volume support individual differences in first-person navigational ability” Poster to be presented at the annual meeting of the Society for Neuroscience, Washington D.C., November, 2014.

- Chrastil, E.R., **Sherrill, K.R.**, Hasselmo, M.E., & Stern, C.E. (Nov 2014). "Tracking location during complex path integration recruits hippocampus and retrosplenial cortex." Poster to be presented at the annual meeting of the Society for Neuroscience, Washington D.C., November, 2014.
- **Sherrill, K.R.**, Chrastil, E.R., Erdem, U.M., Brown, T.I., Ross, R.S., Hasselmo, M.E., Stern, C.E. (2014). "Successful navigation in the absence or presence of an orienting landmark." Poster presented at the annual meeting of the Organization for Human Brain Mapping, Hamburg, Germany 2014.
- Chrastil, E.R., **Sherrill, K.R.**, Hasselmo, M.E., & Stern, C.E. (2014). "Tracking location during complex path integration recruits retrosplenial cortex." Poster presented at the annual meeting of the Organization for Human Brain Mapping, Hamburg, Germany 2014.
- **Sherrill, K.R.**, Chrastil, E.R., Erdem, U.M., Brown, T.I., Ross, R.S., Hasselmo, M.E., Stern, C.E. (2014). "Successful navigation in the absence or presence of an orienting landmark." Poster presented at the annual meeting of the Cognitive Neuroscience Society, Boston, MA, 2014.
- Chrastil, E.R., **Sherrill, K.R.**, Aselcioglu, I., Stern, C.E. "Structural differences in gray matter volume correspond to individual differences in spatial navigation ability." Poster presented at the annual meeting of the Cognitive Neuroscience Society, Boston, MA, 2014.
- **Sherrill, K.R.**, Ross, R.S., Brown, T.I., Erdem, U.M., Hasselmo, M.E., Stern, C.E. (2013). "Path integration and optic flow correlates of ground-level navigation." Poster presented at the annual meeting of the Society for Neuroscience, San Diego, CA, 2013.
- **Sherrill, K.R.**, Erdem, U.M., Ross, R.S., Brown, T.I., Hasselmo, M.E., Stern, C.E. (2012). The hippocampus encodes and translates route information into successful navigation from varying visual perspectives. Poster presented at the annual meeting of the Society for Neuroscience, New Orleans, LA, 2012.
- **Sherrill, K.R.**, Erdem, U.M., Ross, R.S., Brown, T.I., Hasselmo, M.E., Stern, C.E. (2012). The hippocampus encodes and translates route formation into successful navigation from varying visual perspectives. Work presented at the Office of Naval Research site visit for the Multi-University Research Initiative, Massachusetts Institute of Technology, Cambridge, MA, April 2012.
- **Sherrill, K.R.**, Ross, R.S., Stern, C.E. (2010). Functional connectivity of the hippocampus and caudate during disambiguation of non-spatial overlapping sequences. Poster presented at the biannual meeting of the Charles River Association for Memory, Massachusetts Institute of Technology, Cambridge, MA, 2010.
- **Sherrill, K.R.**, Ross, R.S., Stern, C.E. (2010). Functional connectivity of the hippocampus and caudate during disambiguation of non-spatial overlapping sequences. Poster presented at the annual meeting of the Society for Neuroscience, San Diego, CA, 2010.
- Ross, R.S., **Sherrill, K.R.**, Stern, C.E. (2010). Prospective and retrospective retrieval of sequential associations of varying distance. Poster presented at the annual meeting of the Society for Neuroscience, San Diego, CA, 2010.

### **PROGRAMMING/SCRIPTING EXPERIENCE**

- Matlab, POV-Ray, Python, E-Basic (E-Prime)

### **SOCIETY MEMBERSHIPS**

- Society for Neuroscience
- Organization for Human Brain Mapping
- Cognitive Neuroscience Society

### **SYMPOSIUM PRESENTATIONS**

- Brain, Behavior, and Cognition Presentation Day, *September 2014*
  - “Goal-directed navigation in humans”
  - Presented to the Department of Psychological and Brain Sciences, Boston University, Boston, MA
- Brain, Behavior, and Cognition Presentation Day, *September 2013*
  - “Path integration and optic flow correlates of ground-level navigation”
  - Presented to the Department of Psychological and Brain Sciences, Boston University, Boston, MA

### **UNDERGRADUATE RESEARCHER MENTOR**

- Irem Aselcioglu, Psychology, Boston University
- Greg Njus, Biomedical Engineering, Boston University
- Henry Eve, Psychology, Boston University

### **GUEST LECTURER**

- Physiological Psychology Recitation Sections, *November 2011*  
Role: Presented to Boston University undergraduates on “fMRI’s role in examining working memory”
- Weekly Seminar: “Introduction to Functional MRI”, *May – August 2011*
  - Designed and organized workshop class for the cognitive neuroscience community at the Center for Memory and Brain
  - Role: Lecturer – course on fMRI statistical methodology

### **COMMUNITY OUTREACH**

- Summer Pathways Outreach in Science and Engineering Program, *July 2011 & 2013*
  - Role: Organized “Neuroscience Presentation” component for female high-school students from Massachusetts.
  - Presentation title: “MRI and Memory”